The ENGINEERS' DIGEST

REVIEW OF ENGINEERING PROGRESS ABROAD

VOL. IX. No. 11 NOVEMBER, 1948

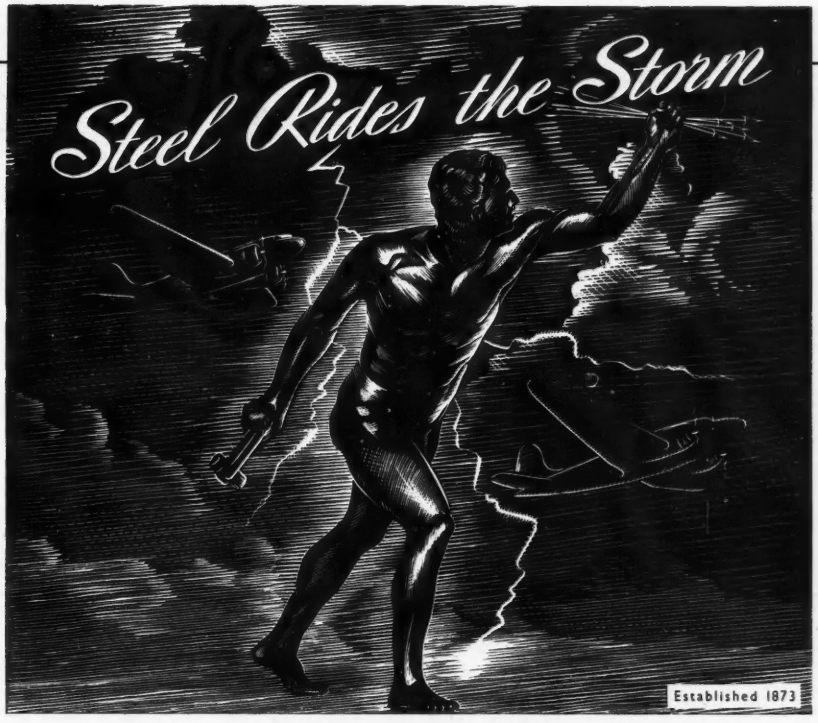

ALLOY & SPECIAL CARBON STEELS

Manufacturers of BARS · SHEETS · PLATES · WIRE RODS

TRADE MARKS

Hallamsteel

THE HALLAMSHIRE STEEL & FILE CO. LTD. SHEFFIELD 3 ENGLAND

Telephone: Sheffield 24304 (7 lines) Telegrams: Hallamsteel, Sheffield

Downtons/24/D.

THE ENGINEERS' DIGEST

Published Monthly by Engineers' Digest Ltd., 120 Wigmore Street, London, W.1. **Tel.: WELBECK 9357**

ANNUAL SUBSCRIPTION OF 12 NUMBERS, £2 2s. :: **SINGLE COPIES, 4s. 6d.**

ADVISORY COMMITTEE

J. F. ALCOCK, B.A., M.I.Mech.E.
R. W. ALLOTT, M.A., A.R.Ae.S.
E. ALTON, D.Eng., A.M.Inst.B.E.
R. W. AYERS, M.I.W.
Col. J. BOWDEN, M.Inst.C.E., M.I.Mech.E.
H. H. BROUGHTON, M.I.Mech.E.
F. BUCKINGHAM, B.Sc., A.M.Inst.C.E., A.M.I.Mech.E., A.M.I.E.E.
T. H. BURNHAM, B.Sc. (Lond.), A.M.I.Mech.E.
J. S. CASWELL, M.Sc., M.I.Mech.E.
G. C. SAFFERY COOPER.
J. DICK, Ph.D., B.Sc., A.M.I.Mech.E.
D. FIFE, M.I.Mech.E.
G. E. FOXWELL, D.Sc. (Lond.), F.Inst.P., F.Inst.F., M.Inst.Gas.E.
R. GRIFFITHS, M.Sc.
H. HEYWOOD, D.Sc., Ph.D., M.I.Mech.E.
O. HURST, M.Inst.N.A.
Capt. J. S. IRVING, M.I.Mech.E., M.I.A.E., A.F.R.Ae.S., M.S.A.E.
F. C. JOHANSEN, M.Sc. (Eng.), M.I.Mech.E., F.R.Ae.S., M.I.Loco.E.
W. J. KEARTON, D.Eng., M.I.Mech.E., A.M.Inst.N.A.
Prof. W. KERR, Ph.D., M.I.Mech.E.
G. V. LOMONOSOFF, Dr.Ing., M.I.Mech.E.
B. J. LYMER, M.I.Mech.E.
D. T. MACIVOR, M.I.Mech.E., M.Cons.E.
W. O. MANNING, F.R.Ae.S.
R. B. MATTHEWS, Wh.Ex., A.M.Inst.C.E., M.I.E.E., F.R.Ae.S.
Prof. A. L. MELLANBY, D.Sc., LL.D., M.I.Mech.E.
J. H. R. RATCLIFFE, B.Sc. (Eng., Hons.), M.I.Mech.E.
Col. C. W. D. ROWE.
W. A. SCOBLE, D.Sc., A.R.C.Sc., M.I.Mech.E.
P. W. SEEWER, D.E. (Zurich), M.Int.C.E., M.I.Mech.E.
Prof. S. PARKER SMITH, D.Sc., M.I.E.E., A.M.Inst.C.E.
C. E. H. VERITY, A.M.Inst.C.F., A.M.I.E.E., A.M.I.Mech.E.
E. G. WALKER, F.C.G.I., B.Sc. (Eng.), M.Inst.C.E., M.I.Mech.E., M.A.Soc.C.E.
Major F. L. WATSON, M.I.C.E., M.I.Mech.E.
G. WATSON, M.Inst.C.E., M.I.Mech.E.
R. J. McL. WHIBLEY, A.M.I.Mech.E.
C. H. WOODFIELD, M.I.Mech.E., M.I.Struct.E.
T. WRIGHT, Ph.D., M.Sc.
M. L. YATES, Ph.D., M.Sc.Tech., M.A.(Com.), M.I.Mech.E.

ADVISORY COMMITTEE OF THE AMERICAN EDITION

Chairman · DR. ALEXANDER KLEMIN, New York University.

R. S. ARCHER, Climax Molybdenum Company.
Prof. O. W. BOSTON, University of Michigan.
Dr. W. H. CARRIER, Carrier Corporation.
R. W. CARSON, Instrument Specialties Co., Inc.
Dr. L. W. CHUBB, Westinghouse Electric Corp.
A. E. RICHARD DE JONGE, Babcock & Wilcox Co.
Dr. O. S. DUFFENDACK, North American Phillips Co.
HANS ERNST, Cincinnati Milling Machine Co.
R. D. EVANS, The Goodyear Tire & Rubber Co.
CHRISTIAN E. GROSSER, Standard Machinery Co.
GEORGE F. HABACH, Worthington Pump & Machinery Corp.
Dr. VICTOR O. HOMERBERG, The Nitralloy Corp.
HERBERT R. ISENBURGER, St. John X-ray Service.
J. B. JOHNSON, A.A.F., Wright Field.
CHARLES M. JONES, John A. Roebling's Sons Co.
H. MANDEL, The Wickman Corp.
J. C. MATHES, Dow Chemical Co.
H. W. MCQUAID, Republic Steel Corp.
R. F. MILLER, Carnegie-Illinois Steel Corp.
Professor L. F. MOODY, Princeton University.
Professor H. F. MOORE, University of Illinois.
LAWRENCE OTTINGER, United States Plywood Corp.
C. E. PRITCHARD, Republic Steel Corp.
JOHN SANDS, International Nickel Co.
JAMES G. SAWYER, Buffalo Turbine Corp.
Dr. A. O. SCHMIDT, Kearney & Trecker Corp.
L. K. SILLCOX, New York Air Brake Co.
ALBERT F. SPERRY, President, Instrument Society of America.
R. DAVID THOMAS, JR., Arcos Corp.
GEORGE A. TINNERMAN, Tinnerman Products, Inc.

"Cronite"
REGD. TRADE MARK
The HIGH TEMPERATURE ALLOY
SALT, LEAD AND CYANIDE VESSELS
CARBURIZING BOXES AND POTS
ROTARY RETORTS & PROPELLING WORMS
FURNACE HEARTHS AND FITTINGS
ENAMELLING PERRITS AND SUPPORTS
GLASS-BLOWING NOZZLES
PYROMETER PROTECTION SHEATHS
CASTINGS FOR USE AT 700°/1200° C.
The CRONITE FOUNDRY Co. LTD
LAWRENCE RD · TOTTENHAM · LONDON. N15
PHONE · STAMFORD HILL 4237

The New ECCLES

4-WHEELED GENERAL PURPOSE TRUCK

The demand for a truck that will carry a bulky load requiring a large platform area has been met by this New Eccles G.P. Truck. Requires less effort, costs nothing to run, is silent, strong, and light in weight. Full lock enables Truck to be turned in minimum of space. Write for details of this and the complete range of Eccles Factory Trucks.

ECCLES (BIRMINGHAM) LTD.
81 Hazelwell Lane, Stirchley, Birmingham, 30
Telephone: Kings Norton 1181 (P.B.X.)
London: Grafton House, 3 Golden Sq., W.1
Telephone: Gerrard 8853.

Your enquiries welcomed for Light Engineering, Quantity, Milling, Capstan Work, Small Assembling, etc.

A TRUCK for every TRADE

For Optimum Hardness and Strength

Nitrided NITRALLOY STEEL

Particulars from:

NITRALLOY LIMITED
25, TAPTONVILLE ROAD. SHEFFIELD 10

Telephone: 60689 Sheffield
Telegrams: Nitralloy Sheffield

KEEP AHEAD WITH "PROLITE." The experience of 40 years of Metallurgy is behind the "PROLITE" range of products—Cemented Tungsten Carbide in its many forms, as tools, dies and wear-resisting parts. The raw materials from which "PROLITE" is made are the products of the parent company, Murex Ltd., Rainham, Essex—the largest works of its kind in the world—and at every stage of its evolution from the Ore to the finished product "PROLITE" is under close laboratory control, extensive research laboratories being continuously employed in seeking for still further improvements and in probing for new applications. *SPECIFY "PROLITE."*

PROTOLITE LIMITED
(A Subsidiary Company of Murex Ltd., Rainham, Essex)
Central House, Upper Woburn Place, London, W.C.1

MAKE SHORTER WORK OF IT WITH OXY-ACETYLENE FLAME HARDENING

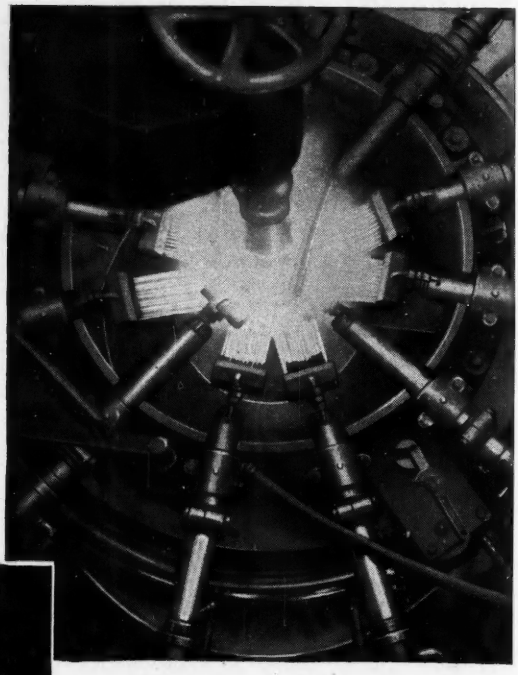

Illustration by courtesy of Head Wrightson & Co. Ltd.

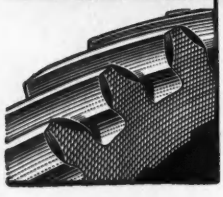

Hardening once required a whole series of operations—but the Shorter Flame Hardening Process reduces the number. By heating just that part of an article which needs to be hard for maximum wear resistance, and immediately quenching the heated area with a jet of water, the B.O.C. Shorter Flame Hardening machines enable gear teeth, for example, to be treated in one pass of the oxy-acetylene flame. The top illustration shows a roll hardening machine in operation. The roll is rotated vertically, and the flame and quenching heads of the machine travel along its length. The inset shows the areas hardened on the teeth of a typical gear—the roots of the teeth and the core of the gear remain tough and ductile—the flanks of the teeth are hardened in just the right place. For full technical data, write for Booklet TIB/13.

THE BRITISH OXYGEN COMPANY LIMITED

LONDON AND BRANCHES

IN THIS ISSUE

THE classical theory of strength of materials cannot satisfactorily explain fatigue at high stress concentrations, and earlier efforts to find a general theory for the dynamic capacity of rolling bearings have been unsuccessful. Attempts to increase the theoretical understanding of this problem have failed because of lack of agreement with experimental results. Despite the fact that thousands of bearings have been run to fatigue failure, experimental investigations have not been able completely to determine the dependence upon bearing design details of the various coefficients entering into empirical formulae. In the article "Dynamic Capacity of Rolling Bearings," the first instalment of which is published on page 369 in this issue, the foundation is laid for a statistical theory of fatigue, i.e., the basic dynamic capacity is related to the probability that the bearing will endure a given load. The authors also refer to Hertz's theory of contact between rolling bodies, and correlate theoretical results to the values obtained experimentally. Formulae and tables are given to allow for assessing the life of bearings as well as the maximum permissible bearing loads.

* * *

When no steps are taken, in electric arc welding, to protect the molten metal against the attack of oxygen and nitrogen present in the air, very poor quality welds are obtained. The article on page 375 deals with the action of oxygen and nitrogen on steel and their solubility in liquid as well as solid iron is examined. The harmful and useful effects of these elements are discussed; the harmful effects to which reference is made are the resultant porosity and the adverse influence upon mechanical strength, whilst the favourable effects are promotion of heat transfer and metal transfer across the arc. This leads to a discussion of the part played by the reaction between oxygen and carbon.

* * *

The heat treatment of high-speed cutting tools has been the subject of numerous publications and discussions since F. W. Taylor's famous investigations half a century ago. Therefore, one can hardly expect to be presented with new aspects of this problem or with facts and data which have not previously been made known. Advanced practices have only been altered slightly, and recent changes are in the nature of refinements rather than radical departures from established practice. Yet we have no hesitation in publishing "The Practical Heat Treatment of High-Speed Steel Cutting Tools" on page 386, for this article, in our opinion, is very valuable in that the subject is treated both from a scientific and practical point of view. Not only are the conclusions presented in a clear and convincing way, but they are also given in a form which allows the best use to be made of our present knowledge of the metallurgy of high-speed steel.

* * *

Nickel-plated plastic offers almost unlimited possibilities to the designer and can be produced at low cost by a process developed by the Camin Laboratories in New York. Another process, electro-forming, allows nickel to be deposited on ground steel mandrils which constitute the inside dimension of the shape to be formed. When the desired thickness is obtained, the mandril can be withdrawn without damaging the plated structure. It is claimed that complicated shapes can thus be made on a production basis (as many as 40,000 finished pieces per machine per week) which it should be difficult to produce economically by other manufacturing methods. The two processes are reviewed on page 390.

* * *

Whilst the theory of the new hydrodynamic bearing "Hydrosphere" was brought to our readers' notice last month, the article is concluded in this issue, on page 372, with a discussion of the test results obtained. It is evident from these test results that the bearing is fully hydrodynamic in operation, the minimum coefficient of friction obtained being 0·005 at a load of 550 psi and a speed of 1,400 rpm. It seems that the bearing possesses a number of characteristics which should make it interesting for practical applications.

* * *

It rarely happens that the highly perfected technique of flow metering is improved by new methods presenting such ingenuity and simplicity as to warrant a deviation from standard practice. Yet a great number of articles can be found in literature which indicate the constant endeavour to find ways and means for an extension of the measuring range of flow meters, which is limited by the square-law relationship between mass flow and pressure loss. The physical laws involved are simple and so well understood that any improvement likely to be successful must depend on inventive ingenuity. This is clearly demonstrated by the great number of patent applications relating to this subject. Limitations set by the square law are appreciated both by the engineer and the salesman; the latter, in attempting to sell a flow meter, will invariably claim the pressure loss to be low and almost constant for all flow rates, while the engineer would question the word "almost." An article describing actual experience involving a comparatively simple modification to a normal Venturi tube is published on page 378. Very satisfactory constancy of pressure loss as well as an extension of the measuring range are obtained with this device.

The Ray Transformer

By R. WIDERÖE (From *Schweizer Archiv*, Vol. 13, No. 8, August, 1947, pp. 225-232, and No. 10, October, 1947 pp. 299-311 : 14 illustrations.)

Concluded from September Issue.

For larger values of Δt, if the injection efficiency is calculated from eq. (52), the exponential curve can be replaced by a suitable tangent and calculated with a correspondingly larger time constant T_1. In this case

$$T_1 = \frac{1}{\frac{\partial}{\partial t}\left[1 - \exp(-\Delta t/T)\right]_{t=t_1}} = T e^{\Delta t_1/T} \quad (58$$

Eq. (56) also gives

$$\rho_e = \sqrt{\frac{1}{3\,a\,R_g}\left(1 - \frac{R_0\,B_0}{R_g\,B_g}\right)\left(1 - e^{-\Delta t/T}\right)} \quad (59)$$

With the aid of these equations and of the curves in Fig. 8, the injection efficiency and the charging capacity of the potential groove can easily be calculated as functions of the time Δt_1. As illustrated by Fig. 9, the injection efficiency in the given example reaches a maximum value of about 52 per cent. The charging capacity of the potential groove $d\Delta V_{stab}/dt$ also has a maximum. The charging time should not exceed 2·5 to 3 times T; it can be made so short (about 1/10th of t_a) that the equilibrium orbit, that is, the ρ_e curve, will be very rapidly displaced towards the interior. The injection efficiency will then be considerably higher, even in the case of a source of electrons placed within the potential groove. The efficiency can be readily calculated from eqs. (43), (44) and (45) and by means of the curves of Fig. 9.

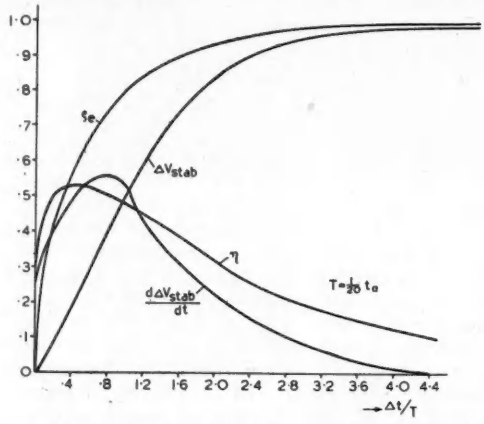

Fig. 9. Variation of the potential groove and of the injection efficiency with the use of a rapidly decreasing auxiliary field.

In order to extract the electrons after they have been accelerated to the required potential, the electron beam of the virtual conductor can be altered in various ways so that the electrons will either be projected against an anticathode or target, or ejected from the tube. This can be obtained, for instance, by varying the guiding field so that it will have a different value from that given by eq. (10). If, therefore, the guiding field is weakened by a superimposed auxiliary field ΔB, the radius of the non-material conductor will increase gradually to that of the boundary orbit, and thereafter expand very rapidly. In the case of an increase of the superimposed auxiliary field proportional to time:

$$\Delta B = \Delta B_m\,[1 - \exp(-\Delta t/T)] \cong \Delta B_m\,\Delta t/R$$

and with considerations similar to those used to derive eq. (56) we obtain

$$\ddot{\rho} = \frac{e^2}{m^2} R_g\,B_g\,(3\,a\,R_g\,B_g\,\rho^2 + (\Delta B_m\,\Delta t/T)) \quad (61)$$

This equation shows that the electrons will effectively follow the Painlevé curves of Fig. 7 during the ejection process, but in this case in the opposite direction. An electron going through this process without any superimposed oscillations of appreciable amplitude, will therefore be moving outwards approximately following the curve e of Fig. 7. The trajectory is at first parabolic and after crossing the boundary orbit it leads the electrons so rapidly out of the tube that one could almost speak of an explosion of the non-material conductor. The additional weakening of the guiding field can be obtained in various ways, for instance with an iron saturation of the magnetic paths of flux (Steenbeck, Kerst), by a phase displacement between the guiding and the induction field (Wideröe), or by superimposed magnetic fields which are periodically generated by an auxiliary winding (Kerst, Gund). The last method appears to be particularly favourable when a rapid ejection of the electrons is required. It can easily be shown that the switch-in power for the periodic guiding pulses will be at a minimum when the additional field ΔB_m is twice as great as the minimum value ($R_g\,B_g - R_0\,B_0$)/R_g. A time constant T of about 0·1 m sec can fairly easily be obtained; and as a rule the ejection process will thus only take a very small fraction of the total acceleration time.

If, instead of slowing down the electrons in the tube to create gamma rays, it is desired to lead them out of the tube in the form of a concentric beam, then it will be necessary to set up deflecting electrodes in the immediate vicinity of the boundary orbit (Kollath and Wideröe). To prevent losses due to an excessive proportion of electrons striking the edge of the deflecting electrodes, this electrode should be made extremely thin (thin wire). As the deflection of an electrode of this type will be very small, the final deflection of the electrons out of the tube can be obtained by means of a second pair of deflecting plates.

3. STABILIZATION WITH MAGNETIC LENSES

Eq. (38) shows that the stabilizing forces of the guiding field reach their lowest value at the beginning of the acceleration, just when the opposing space-charge forces are greatest (see eq. (41a)). As a result, the charge and the mean current intensity of the transformer will be comparatively small. This applies particularly to large-size ray transformers, since Q_{max} is proportional to $1/R_0$ according to eq. (41).

The charging capacity can be increased by introducing additional stabilizing forces obtained by means of electrical or magnetic lenses (Wideröe, 1943). With additional stabilization of this type, comparatively large stabilizing forces can be generated, particularly at low electron voltages, and the effectiveness of the guiding field is improved with a considerable increase in the power output of the transformer.

The electric lenses can consist, for instance, of a continuous series of annular electrodes mounted in the toroidal tube (see Fig. 10) and charged at alternatively positive and negative potentials. The electrons are alternatively accelerated and decelerated by the fields

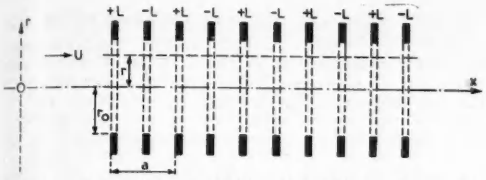

Fig. 10. **Generation of additional stabilizing forces by means of electric lenses.**

of these lenses, and their velocity in the longitudinal direction is modulated by the period of these lenses. At the same time, the electrons are influenced in the radial direction, and as they are under the influence of repulsive forces for a longer period owing to the arrangement of the lenses, the result is an inwardly directed stabilizing force. The stabilizing forces of a "lens street" of this type show a very rapid (exponential) decrease with increasing distance of the electrons from the lenses. Because of the comparatively low voltage between the lens electrodes (about 20-40 kilovolts), the increase in power of the transformer which can be obtained with electrical lenses is limited. Magnetic lenses enable much greater increases in power to be obtained, and in the following the investigation will, therefore, be confined to magnetic lenses.

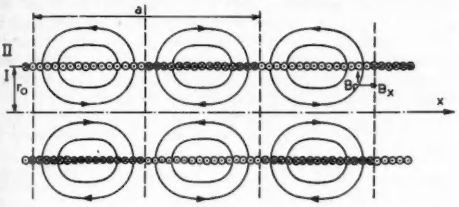

Fig. 11. **Additional stabilization by mean of magnetic lenses.**

Fig. 11 shows an electromagnetic lens street. The lens fields are constituted by a series of coils with alternatively opposite magnetization, which are wound round the entire periphery of the toroidal tube. Both longitudinal and radial field components are obtained. The radial components, in conjunction with the basic longitudinal motion of the electrons, generate Lorentz forces which give rise to azimuthal oscillations of the electrons (i.e. oscillations parallel to the flow of electrons through the coil winding). This azimuthal motion generates, together with the longitudinal field component, an inward stabilizing force which is nearly twice as great as the outward centrifugal force of the oscillating electrons, hence the resultant stabilizing force will be about half as great as the radial field component in the inward direction.

The magnetic field of a "magnetic lens street" of this type will now be calculated, assuming for the simplest case that the magnetic excitation follows a sine-curve distribution along the periphery of the tube, so that

$$d\mathfrak{F}/dx = \theta \sin kx \quad .. \quad .. \quad (62)$$

where $k = 2\pi/a$ is the lens period, and a = double interval between two coils. If A_ψ is the vector potential of the magnetic field of the coils, then Laplace's equation for the space inside the coils is

$$\Delta A_\psi = \frac{\partial^2 A_\psi}{\partial r^2} + \frac{1}{r}\frac{\partial A_\psi}{\partial r} + \frac{1}{r^2}\frac{\partial^2 A_\psi}{\partial \psi^2} + \frac{\partial^2 A_\psi}{\partial x^2} = 0 \quad (63)$$

and the corresponding Poisson equation for the space outside the coils will be

$$\Delta A_\psi = \mu_0 i_\psi \; (i_\psi = \text{vorticity} = \text{curl}\, H_\psi) \quad .. \quad (64)$$

As A_ψ is a vector, it can be represented by

$$A_\psi = A_\psi e^{i\psi} \quad .. \quad .. \quad .. \quad (65)$$

so that in eqs. (63) and (64) we have

$$\frac{1}{r^2}\frac{\partial^2 A_\psi}{\partial \psi^2} = -\frac{A_\psi}{r^2} \quad .. \quad .. \quad (66)$$

These partial differential equations can be converted into two ordinary simultaneous differential equations by the usual substitution $A_\psi = A_{\psi r} A_{\psi x}$. Eq. (63) then gives

$$\frac{d^2 A_{\psi r}}{dr^2} + \frac{1}{r}\frac{d A_{\psi r}}{dr} - \left(k^2 + \frac{1}{r^2}\right) A_{\psi r} = 0 \quad (63a)$$

and

$$\frac{d^2 A_{\psi x}}{dx^2} + k^2 A_{\psi x} = 0 \quad .. \quad (63b)$$

The solution of eq. (63) is therefore a product of cylindrical and trigonometrical functions, and as the electron beam current flowing through the lens coils has been assumed to have a sinusoidal distribution, the solution of eq. (63) will be

$$A_\psi = \alpha\,(-i)\, I_1\,(ikr) \sin kx \quad .. \quad .. \quad (67)$$

where I_1 is the Bessel function of the first order. For the solution of eq. (64), since the vector potential must vanish at infinity, we choose the corresponding Hankel functions of the first order, so that

$$A_\psi = [\beta H_1^{(1)}\,(ikr) + \gamma H_1^{(1)}\,(ilr)] \sin kx \quad .. \quad (68)$$

The constants α, β and γ of these solutions must be chosen in such a way that they will satisfy the boundary conditions of eqs. (63) and (64) and give, when $r = r_0$ (assuming the winding is infinitely thin), the same value for A_ψ as for $\partial A_\psi/\partial r$, for the space inside and outside the coils. The integration constants are

$$\alpha = \frac{1}{2}\pi r_0 \mu_0 \theta H_1^{(1)}\,(ikr_0),\ \beta = \frac{1}{2}\pi r_0 \mu_0 \theta I_1\,(ikr),$$
$$\gamma H_1^{(1)}\,(ilr) = 0 \quad .. \quad .. \quad (67b)$$

and the results, which can easily be verified, are as follows:—

Inside the coils

$$A_\psi = \frac{\pi}{2} r_0 \mu_0 \theta\, H_1^{(1)}\,(ikr_0)\,(-i)\, I_1\,(ikr) \sin kx \quad .. \quad (67a)$$

Outside the coils

$$A = \frac{\pi}{2} r_0 \mu_0 \theta\,(-i)\, I_1\,(ikr_0)\, H_1^{(1)}\,(ikr) \sin kx \quad .. \quad (68a)$$

With the relation $B = \text{curl}\, A$ we obtain for the components of the magnetic field inside the coils :

$$B_x = \frac{1}{r}\frac{\partial\,(rA_\psi)}{\partial r} = \frac{\pi^2 r_0 \mu_0 \theta}{a} H_1^{(1)}\,(ikr_0)\, I_0\,(ikr) \sin kx \quad (69)$$

$$B_r = -\frac{\partial A_\psi}{\partial x} = -\frac{\pi^2 r_0 \mu_0 \theta}{a} H_1^{(1)}\,(ikr_0)\,(-i) \times I_1\,(ikr) \cos kx \quad (69a)$$

From eq. (69a) the azimuthal velocity of the electrons is obtained:

$$v_{az} = \int_0^t \frac{e v_x B_r}{m}\, dt = \int_0^x \frac{e}{m} B_r\, dx = -\frac{e}{m} A_\psi$$
$$= -\frac{e}{m}\alpha\,(-i)\, I_1\,(ikr) \sin kx \quad (70)$$

This velocity generates, in conjunction with the longitudinal field component, a radial Lorentz force

$$P_{rad} = -ev_{az} B_z = \frac{e^2}{m} \alpha^2 k (-i) I_1(ikr) I_0(ikr) \times \sin^2 kx \ldots \quad (71)$$

If we subtract the centrifugal force mv_{az}^2/r, we obtain for the resultant stabilizing force

$$P_{stab} = \frac{e^2 \alpha^2 k}{m} \left[(-i) I_1(ikr) I_0(ikr) + \frac{1}{kr} I_1^2(ikr) \right] \sin^2 kx \quad \ldots \quad (72)$$

and the mean stabilizing force is

$$\overline{P}_{stab} = \frac{e^2 \pi^3 r_0^2 \mu_0^2 \theta^2}{4ma} \left[H_1^{(1)}(ikr_0) \right]^2 \times \left[(-i) I_1(ikr) I_0(ikr) + \frac{1}{kr} I_1^2(ikr) \right] \quad (72a)$$

At the distance $r = r_1$, this force will be capable of stabilizing a space charge Q :

$$Q = \frac{U + \epsilon}{\epsilon} \frac{\epsilon_0 \pi^2 R_0 r_1^2 \mu_0^2 \theta^2 c^2}{2\epsilon} G_M(r_1, r_0, a) \quad (73)$$

where $G_M = \frac{2\pi^2 r_1}{\alpha} \left[H_1^{(1)}(ikr_1) \right]^2 \times \left[(-i) I_1(ikr_1) I_0(ikr_1) + \frac{1}{kr_1} I_1(ikr_1) \right] \times \left[\frac{r_0 H_1^{(1)}(ikr_0)}{r_1 H_1^{(1)}(ikr_1)} \right]^2$

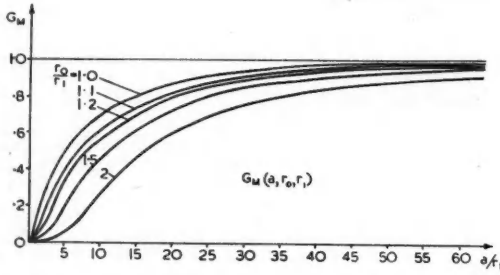

Fig. 12. Geometry factor for magnetic lenses as a function of the relative lens length a/r_1.

Fig. 12 shows the variation of the "geometry factor" G_M with the relative lens length (a/r_1) and the relative coil radius (r_0/r_1). It is evident from these curves that the coils should be as long as possible. However, the electrons under the influence of the periodically variable stabilization force (eq. (72)) also perform radial oscillations which will not reach excessive amplitudes provided the lens length is not greater than, say, 10-20 cm. The maximum amplitude of the radial oscillations is given by

$$\left(\frac{\Delta r}{r_1} \right)_m = \frac{\mu_0^2 \theta^2 c^2 G_M}{128 \pi^2 (U^2 + 2U\epsilon)} a^2 \quad \ldots \quad (74)$$

and under these conditions, the radial oscillations will still be less than 10 per cent of r_1. The azimuthal oscillations increase with the lens length; when $\theta = 300$ amp. turns/cm, $a/r_1 = 20$, $r_0/r_1 = 2$ and $r_1 = 1$ cm, the maximum azimuthal amplitude of oscillation will be about 45°. The maximum amplitude of the azimuthal oscillation is

$$\psi_{max} = \frac{a\mu_0 \theta c}{4\pi \sqrt{U^2 + 2U\epsilon}} \left[\pi \frac{r_0}{r_1} H_1^{(1)}(ikr_0) \times (-i) I_1(ikr_1) \right] \quad (75)$$

The increase of the space charge due to the magnetic lenses (with the same radius r_1) can be calculated by comparing eq. (73) with the previous eq. (41) for the maximum space charge. The following values are obtained for various tube radii R_0, assuming $U_a = 30$ Kv, $K = 1/2$, $\theta = 300$ amp. turns/cm, and $G_M = 1/2$:

R_0	=	14	28	70 cm
$Q_{lens}/Q_{guide\ field}$	=	11	44	275
$\bar{i}_{lens}$	=	4	8	20 μA

These results show that the magnetic lenses considerably increase the power output of the transformer.

As the Lorentz forces due to the magnetic lenses can supply no energy to the electrons, the kinetic energy required for the azimuthal velocity must be taken from the longitudinal velocity. The magnetic lens street thus produces a periodic modulation of the longitudinal velocity, and this modulation must not exceed a certain value, so that (as first mentioned by E. A. Hylleraas) the excitation of the lens coils cannot be increased beyond certain limits. If v_z is the non-modulated, and v_z' the modulated longitudinal velocity, then in the non-relativistic region we have

$$v_z = \sqrt{v_z'^2 + v_{az_m}^2 \sin^2 kx} \quad \ldots \quad \ldots \quad (76)$$

hence $v'_z/v_z = 1 - \frac{1}{4} \left(\frac{v_{az_m}}{v_z} \right)^2 (1 - \cos 2kx)$ (76a)

When $v_{az_m}/v_z = 1/2$, the longitudinal velocity has a modulation of approximately ± 6·25 per cent, and its mean value is also reduced by this same percentage. A decrease of this order is unimportant and can easily be compensated for by a corresponding increase of the initial velocity. The complete Hamiltonian expression for azimuthally oscillating electrons which also perform superimposed r and z axis perturbation oscillations, is obtained in a form similar to that of eq. (18b):

$$H = e(U + u) = c \sqrt{m_0^2 c^2 + p_r^2 + p_z^2 + e^2 A\psi^2 + \left(\frac{p\varphi_0}{R_0} + eA_\varphi \right)^2} - m_0 c^2 \quad (78)$$

The additional voltage u corresponds to the momentums p_r and p_z of the superimposed disturbance oscillations, plus the momentum $eA_\psi = (mv_{az})$, plus the initial momentum $p_{\varphi 0}/R_0$ in the longitudinal direction. At first, when $B = 0$, the additional voltage u has the initial value $u_0 = \epsilon [v_r^2 + v_z^2 + v_{az}^2 + v_0^2]/(2c^2)$, and u increases slowly as the voltage U rises, without affecting the working of the transformer. To determine the corresponding lens excitation θ_m, we obtain with eq. (70):

$$V_{az} = \frac{e\pi}{2m} r_0 \mu_0 \theta_m (-i) I_1(ikr_1) H_1^{(1)}(ikr_0) = \frac{v_z}{2} = \frac{c}{2} \sqrt{\frac{2U_a}{\epsilon}} \quad (77)$$

whence $\theta_m = \sqrt{2U_a \epsilon}/[\pi c \mu_0 r_0 (-i) I_1(ikr_1) H_1^{(1)}(ikr_0)]$

For the case $U = 10$ kV, $r_0 = 2$ cm, $r_1 = 1$ cm, and $a = 20$ cm, for instance, we have $\theta_m = 344$ amp. turns/cm. It thus appears that the maximum excita-

tion of the lenses will be somewhat higher, taking modulation into account, than the excitation previously assumed at 300 amp. turns/cm on the basis of thermal considerations.

The conditions existing during the introduction of electrons into the magnetic lens street will now be investigated. Generally, the source of electrons will be situated within the field of forces of the lens, to avoid the extremely difficult problem of injecting electrons from the outside of the tube. The conditions are then as a whole similar to those occurring with stabilization by a guiding magnetic field. The stabilizing forces of the mean field of the lenses constitute a potential groove, and as these forces increase nearly in proportion to the radius r_1, the potential groove will be parabolic in the first approximation. The electrons will be able to oscillate in this potential groove about the axis of the magnetic lenses. As long as the charge in the tube is small, the wave length of these oscillations will be

$$\lambda = 4\pi\sqrt{2\,(U^2 + 2\,U\epsilon)/G_M/(\mu_0\, c\theta)} \quad .. \quad (79)$$

Owing to the periodic variation of the lens forces the electron motion will be determined more accurately by the differential equation :

$$\ddot{r} = \frac{\dot{U}}{U+\epsilon}\,\dot{r} + \left(\frac{\mu_0\ \theta\ c}{U+\epsilon}\right)\frac{G_M}{8}(1 - \cos k\, v_z\, t)\ r = 0 \quad (80)$$

The solution of this differential equation leads to Mathieux functions. If, however, the wavelength λ of the fundamental oscillation is slightly greater than the lens period a, then it will be possible to approximate the Mathieux oscillations by the fundamental oscillation λ and two superimposed harmonics with frequencies $\left(\frac{2\lambda}{a} + 1\right)$ and $\left(\frac{2\lambda}{a} - 1\right)$ times the fundamental frequency and the amplitudes $a^2/[8\lambda\ (\lambda \pm a)]$. The fluctuation of the maximum oscillatory amplitude is thus $\pm\ a^2/[4(\lambda^2 - a^2)]$; for instance when $\lambda = 2a$, the fluctuation is $\pm$ 8·25 per cent. It will be seen from eq. (74) that this lens length would correspond to a radial velocity with a relative amplitude $(\Delta r/r)_m = \pm$ 6·25 per cent for a fully charged tube.

The action integral of the electron oscillations becomes

$$\oint p_r\, dr = e\pi\, r_m{}^2\, \mu_0\, \theta\sqrt{G_M/8} \quad .. \quad .. \quad (81)$$

and is, therefore, independent of the electron voltage U for the empty potential groove. When the groove contains charges, the dynamic attraction forces, which increase with rising velocity, will increase the stabilizing forces and thereby contribute to reduce the amplitude of the oscillations. To introduce electrons into the potential groove, we must, therefore, proceed in the same way as in filling the potential groove of the magnetic guiding field; the groove must consequently be expanded starting from a small value, during the injection process, and the charging ratio of the groove will thus remain constant.

The potential groove of the lens field can be varied in two different ways: either by rapidly varying the excitation current of the lenses, or as already previously described, by superimposing a rapidly varying auxiliary field upon the magnetic guiding field. The first process gives rise to considerable technical difficulties owing to the eddy currents in the guide poles, which are not easily avoided; therefore, only the second process will be considered.

The auxiliary guiding field ΔB_z is the cause of an additional radial force acting on the electrons in the R direction. For an azimuthally oscillating electron, the additional force can be resolved into two components, the first acting perpendicularly to v_{az} and increasing the radius r_1 of the azimuthal oscillation, while the second component acts in the direction of v_{az} (or $-v_{az}$) and also affects the azimuthal oscillation.

Under the influence of the second component, the amplitude and velocity of the azimuthal oscillations will vary, and free superimposed azimuthal oscillations can also occur. These free oscillations can be avoided by an appropriate choice of initial conditions. However, the increase of the azimuthal velocity during the lens period is extremely important. As already stated, the centrifugal force of the oscillation is about half as great as the Lorentz force acting on the electrons, and an increase of azimuthal velocity by a factor α will therefore reduce the resultant stabilizing force by a factor $\alpha\,(2 - \alpha)$.

If P_{az_m} is the maximum azimuthal force of the lens field, and P_z is the radial additional force, then the differential equation for azimuthal motion of the electrons will be

$$z'' = [P_{az_m} \cos kx - P_z \sin (z/r_1)]/(mv_z{}^2) \quad (83)$$

or $$z'' \cong [P_{az_m} \cos kx - z\, P_z/r_1]/(mv_z{}^2) \quad .. \quad (83a)$$

and its solution is

$$z = \frac{P_{az_m} \cos kx}{k^2 mv_z{}^2 - (P_z/r_1)} + z\, F \cos\sqrt{P_z/r_1 x}\ .. \quad (84)$$

Then $\alpha = k^2/[k^2 - (P_z/r_1\, mv_z{}^2)]$ .. .. (84a).

We have therefore

$\alpha =$	1	1·2	1·5	2	2·5	3
$2\,\alpha - \alpha^2 =$	1	0·96	0·75	0	−1·25	−3

and from this it is apparent that with the aid of an

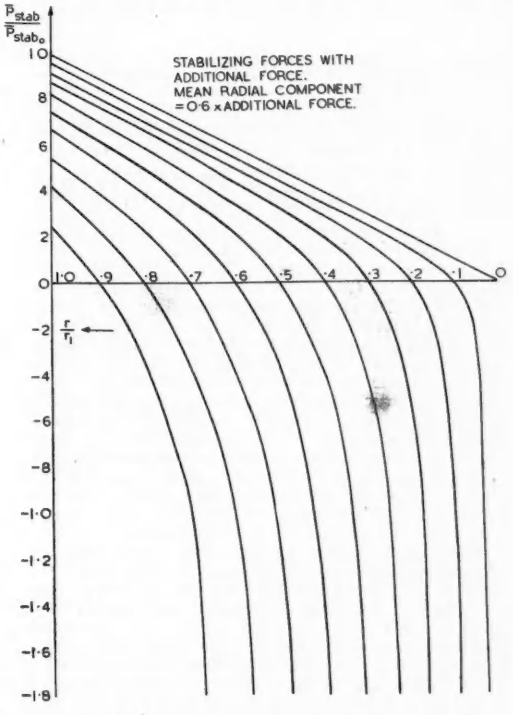

Fig. 13. **Variation of the mean value of the magnetic lens forces by an additional radial force.**

additional radial field it will be possible to vary the stabilizing force of the magnetic lenses as desired. Fig. 13 shows the variation of the lines of force of the lens field under the influence of an additional radial force. The potential groove is displaced outwards, and in this way the zero value of the potential groove can be shifted by means of the additional field ΔB_s to the position occupied by the source of electrons and then gradually brought back, during the injection of electrons, to the centre of the tube by reducing the additional field. The trajectories of the electrons become extremely complicated with this process and can hardly be calculated. A rough estimation shows, however, that the injection efficiency will not be very high, so that it will be necessary to introduce very considerable current intensities (roughly 80-100 mA per μA of mean current intensity) into the tube.

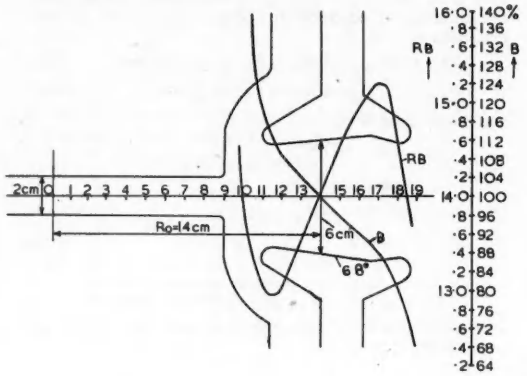

Fig. 14. Induction poles and guiding poles with field pattern for a ray transformer of 15 Megavolts.

4. EXPERIMENTAL INVESTIGATIONS WITH A 15-Mv TRANSFORMER

A test transformer for 15 Mv and 50 cycles/sec was constructed at Hamburg, and the guiding poles, the flux density of the guiding field, and the *RB* curve which also corresponds approximately to the course of the stabilization forces, are shown in Fig. 14. The electron source was placed in the vicinity of the outer boundary orbit (R_0 = 17·2 cm). The tapered iron expansions of the guiding poles (see Fig. 14) became saturated before the flux reached its maximum value, and caused the equilibrium orbit to expand from a normal radius R_0 of about 14 cm to a radius exceeding 17·2 cm. The electrons were accelerated to a high voltage and struck therefore, at the end of the accelerating period, the inner parts of the electron injector, and in decelerating generated hard gamma rays. In order that most of the electrons may impinge upon the anticathode, the injector must, as already explained, be situated very close to the boundary orbit. This was confirmed experimentally, and it was found that a slight displacement of the electron injector by a few millimetres out of the most favourable position reduced the gamma radiation considerably. Unfortunately, the tests with this transformer had to be prematurely interrupted. The most important result was the comparatively powerful radiation output of this transformer in spite of the relatively low voltage per revolution of about 17 volts for 10 kilovolts (so that $\Delta U/U = 1{\cdot}7 \times 10^{-3}$). According to Kerst's earlier views, such a low value for the voltage per revolution should have corresponded to a decrease of the radii of the orbits of only a few hundredths of a millimetre per revolution, and this would not enable practically any gamma radiation to be generated.

The greatest radiation intensity measured was about 0·02 roentgens/sec at a distance of 1 metre from the anticathode, corresponding to the radiation of approximately 100 gr of radium. The radiation intensity at 1 meter distance from the anticathode being given by

$$\mathcal{J} = \frac{U_m\, i_{\text{mean}}}{2150\ \text{cm}^2}\ \frac{1}{2}\ 0{\cdot}07 \times 3400\ \frac{\text{r cm}^2}{\text{sec W}}$$

and for U_m = 13 Mv, this gives $i_{\text{mean}} = 1{\cdot}4\,\mathcal{J}\ \frac{\mu\text{A}}{\text{r/sec}}$

If the efficiency of radiation generation is assumed to be approximately 7 per cent using a molybdenum anticathode, and also assuming that half the generated radiation is located ithin a solid angle of 30 deg., then the measured radiation intensity of 0·02 r/sec corresponds to a mean current intensity of about 0·028 mA.

This corresponds to only about 10 per cent of the charge of a space-charge cylinder with a radius r_1 of 1·5 cm, and this shows (although the calculation naturally contains many uncertain factors) that it would still probably be possible to raise the output of the transformer considerably.

The radiation output decreased, as expected, considerably with a deterioration of the degree of vacuum. The intensity of radiation dropped to between $^1/_3$th and $^1/_7$th of its previous value when the pressure in the accelerator tube was raised from 2 to 10 $\times$ 10^{-6} mm Hg. It is easily understandable that the degree of vacuum will play an even more important role if the frequency and the voltage per revolution are lower, or the acceleration path is longer. The electrode needles used were all of experimental design which could still be greatly improved. The most favourable results were obtained with an oxide cathode subjected to short excitation pulses. The investigation was undertaken with the aid of Dr. R. Kollath and B. Touschek, the latter having contributed a considerable portion of the theoretical work, and the construction and development of the 15 Mv radiation transformer were carried out with the collaboration of C. Flegel, G. Krohn, A. Kuntke, Dr. Müller, Reiniger, and G. Schumann.

BIBLIOGRAPHY.

(1) J. SLEPIAN : *U.S. Pat.* No. 1,645,304, March 1, 1922.
(2) R. WIDERÖE : *Arch. f. Elektrotechnik*, Vol. 21, 1928, p. 387.
(3) G. BREIT, O. DAHL, M. A. TUVE ; *Carnegie Inst. Year Book*, 27, 1927-1928, p. 209.
(4) E. T. S. WALTON : *Proc. Cambr. Phil. Soc.*, Vol. 25, 1929, p. 469.
(5) R. RÜDENBERG and M. STEENBECK : *D.R.P.* 656,378, April 1, 1933.
(6) M. STEENBECK : *D.R.P.* 698,867, March 7, 1935.
(7) M. STEENBECK : *Naturwissenschaften*, 1943, H. 19/20, p. 234.
(8) D. W. KERST : *Phys. Rev.*, Vol. 58, 1940, p. 41 ; Vol. 59, 1941, p. 110 ; Vol. 60, 1941, p. 47.
(9) D. W. KERST and K. SERBER : *Phys. Rev.*, Vol. 60, 1941, p. 53.
(10) D. W. KERST : *Electronics*, Feb., 1942, pp. 22-23.
(11) W. F. WESTENDORP, and E. E. CHARLTON : *J. Appl. Phys.*, Vol. 16, 1945, No. 10, p. 581.
(12) O. WERNHOLM : *Teknisk Tids.*, March 2, 1946, No. 9.
(13) W. F. WESTENDORP : *J. Appl. Phys.*, Vol. 16, Nov. 1945, pp. 657-659.
(14) D. W. KERST : *Phys. Rev.*, Nov. 1-15, 1945, p. 233.
(15) D. W. KERST : *Nature*, Vol. 157, Jan. 26, 1946, No. 3978, pp. 90-95.
(16) H. F. KAISER : *J. Appl. Phys.*, Jan., 1947.
(17) D. IWANENKO and I. POMERANCHUCK : *Phys. Rev.*, Vol. 65, 1944, p. 343 ; *J. Phys.*, 1940, Vol. 2, p. 65.
(18) C. BALDWIN and H. W. KOCH : *Phys. Rev.*, Vol. 67 1/2, 1945, pp. 1-11.
(19) L. I. SCHIFF : *Rev. Sc. Instr.*, Jan., 1946, Vol. 17, pp. 6-14.
(20) R. WIDERÖE : *Norwegian Pat. applicn.* No. 84,507, Jan. 31, 1946.
(21) R. WIDERÖE : *D.R.P. applicn.* No. W.113,763, Sept. 3, 1943.
(22) W. F. WESTENDORP : *J. Appl. Phys.*, Nov., 1945, Vol. 16, p. 657.
(23) R. WIDERÖE : *D.R.P. applicn.*, No. W.113,740, Sept. 1, 1943.
(24) HEITLER : *The quantum theory of radiation*, Oxford, 1936, p. 21.
(25) R. KOLLATH and R. WIDERÖE : *Phys. Rev.*, Vol. 71, 1947, No. 6, p. 376.

New Method of Measuring the Coefficient of Friction*

By V. G. GHEORGHIU. (From *Bulletin de l'Ecole Polytechnique de Jassy*, Vol. 2, No. 2, July/December, 1947, pp. 200-206, 1 illustration.)

IN the following a test rig and test method devised by the Ecole Polytechnique de Jassy are described, which have been developed in order to determine the coefficient of friction between two sliding faces. With this method, two friction values are measured simultaneously, i.e., one coefficient of friction is determined by means of another. The test rig (Fig. 1) consists of a rigid frame *ABCD* having a horizontal base plate *BC* and two uprights *AB* and *DC*. An assembly of two cylinders of radius *R* can slide or roll on *BC*. These cylinders contact, at *E*, a plate *GH* made of the material to be investigated. Between these two cylinders is placed a smaller cylinder of radius *r* which rests on the other material to be tested, i.e. *LM*. Part *LM* is attached to a frame which, by means of rigid bar *IJ* and wing nut Q_1, is so held in a slot in upright *AB* that part *LM* extends horizontally. The movable system is loaded if a tensile force F′ is exerted in the vertical direction on bar *IJ* by means of wing-nut Q_2. This force is read off on dynamometer D_1. The force *F* is, therefore, given by:—

$$F = F'\,a/b \quad .. \quad .. \quad .. \quad (1)$$

The direction of this force goes through axis *O* and supporting point *E*.

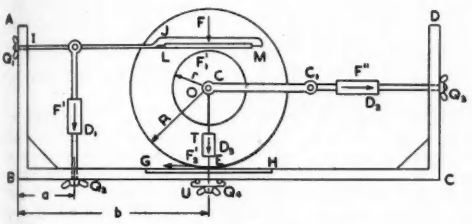

Fig. 1

A second force *F″* is exerted by wing nut Q_3 and transmitted via link CC_1 to a ball bearing carrying the cylinder shaft. This force can be read off on dynamometer D_2. If the forces due to bearing friction are negligible compared with the forces F_1' and F_2' caused by the force *F* at the friction faces *LM* and *GH*, we obtain the following two relations, f_1 and f_2 being the coefficients of friction at the outset of the motion and *P* the weight of the movable system

$$F_1' = f_1 F \quad .. \quad .. \quad .. \quad (2)$$

$$F_2' = f_2 (F + P) \quad .. \quad .. \quad (3)$$

If the force *F″* increases, the movable system rolls either clockwise or anticlockwise according to whether the torque $F_1' r$ is smaller or larger than the torque $F_2' R$. If the radii *r* and *R* of the cylinders are so selected that

$$F_1' r = F_2' R \quad .. \quad .. \quad .. \quad (4)$$

then the system acted upon by force *F″* slides without simultaneous rotation. In this case

$$f_1 F r = f_2 (F + P) R \quad .. \quad (5)$$

If force *P* is neglected with respect to *F*, we obtain

$$f_1 r = f_2 R \quad .. \quad .. \quad .. \quad (6)$$

Therefore, if one coefficient of friction is known, the other can be determined by means of eqs. (5) and (6). If both coefficients of friction have to be found, the torque equations yield

$$f_1 R (R + r) = F'' R \quad .. \quad .. \quad (7)$$

$$f_2 (F + P)(R + r) = F'' r \quad .. \quad (8)$$

$$f_1 F/R = f_2 (F + P)/r = F''/(R + r) \quad .. \quad (9)$$

From this it follows that

$$f_1 = \frac{F'' R}{F (R + r)} \quad .. \quad .. \quad (10)$$

and

$$f_2 = \frac{F'' r}{(F + P)(R + r)} \quad .. \quad .. \quad (11)$$

If *P* is neglected again in comparison with *F*, we obtain

$$f_2 = \frac{F'' r}{F (R + r)} \quad .. \quad .. \quad (12)$$

Writing eq. (5) in the form

$$(f_1 r - f_2 R) F = f_2 R P \quad .. \quad .. \quad (13)$$

shows that it is not necessary to change *R* or *r* to prevent sliding of the system without rotating about its axis. Moreover, *F* can be regulated by adjusting force *F′* so as to satisfy eq. (13). We thus obtain

$$F = F' \frac{a}{b} = \frac{f_2 R P}{f_1 r - f_2 R} = \frac{P}{f_1 r/(f_2 R) - 1} \quad (14)$$

and

$$F' = \frac{P b}{[f_1 r/(f_2 R) - 1]\, a} \quad .. \quad .. \quad (15)$$

The quotient $f_1 r/f_2 R$ must be always greater than one. In other words, $f_1 r > f_2 R$, or

$$f_1/f_2 > R/r \quad .. \quad .. \quad (16)$$

In practice, this condition can be fulfilled by a suitable choice of the nature of surfaces to be investigated and, if necessary, by adjusting the radii *R* and *r*.

In order to permit of greater variations of the weight *P*, the system can be made hollow and filled with mercury or other heavy liquid. In this way, a series of tests can be conducted, with different weights *P*, to establish the coefficients of friction of the same materials.

In order to be able to vary force *F* within wide limits, the system can be supplemented by a force *T* acting in a direction perpendicular to the axis of the system. This force *T* can be produced by wing-nut Q_4 which presses against a small carriage *U* abutting, with balls or rollers, against the frame *BC* from below. When operating the movable system by means of the force *F″*, this carriage is moved in a horizontal direction. The rolling friction can be neglected if the wheels and the supporting surface of the frame are made of a hard and smooth material. We obtain the following equations :—

$$f_1 = \frac{F'' R}{F (R + r)} \quad .. \quad .. \quad .. \quad .. \quad (17)$$

$$f_2 = \frac{F'' r}{(F + P + T)(R + r)} \quad .. \quad .. \quad (18)$$

$$F = \frac{P + T}{f_1 r/(f_2 R) - 1} = F' \frac{a}{b} \quad .. \quad .. \quad (19)$$

*Abstract by courtesy of Industrial Diamond Information Bureau, 32-34 Holborn Viaduct, London, E.C.1.

$$F' = \frac{(P + T)\,b}{\left(\frac{f_1 r}{f_2 R} - 1\right) a} \quad .. \quad .. \quad .. \quad (20)$$

It is thus shown that for any two materials and for given values of a, b, R and r, definite values of F' and F'' can be obtained for arbitrary values of T if the movable system slides without rolling.

If the movable system only consists of a single cylinder of radius R, i.e., if $r = R$, we obtain the following relations:—

$$f_1 = \frac{F''}{2F} \quad .. \quad .. \quad .. \quad (21)$$

$$f_2 = \frac{F''}{2(F + P + T)} \quad .. \quad .. \quad (22)$$

$$F = \frac{P + T}{\frac{f_1}{f_2} - 1} = F' \frac{a}{b} \quad .. \quad (23)$$

$$F' = \frac{(P + T)\,b}{\left(\frac{f_1}{f_2} - 1\right) a} \quad .. \quad .. \quad (24)$$

In this case it is necessary that f_2 be smaller than f_1 to obtain positive values for the forces F and F'.

RUSSIA

New Type of Portable Temperature Regulator for Electro-Furnaces

By Y. S. GINSBURG. (From *Kotloturbostroyenie*, No. 4, 1947, pp. 29-30, 1 illustration).

The automatic temperature regulator shown has been developed to supersede potentiometer, magnetic and galvanometer-type regulators. It has proved more robust, requires less maintenance and regulates within finer limits, namely, $\pm$ 2·5° C up to a temperature of 1000° C. Its principle of operation is based on the difference in elongation between the porcelain rod 4 and the steel tube 1.

The regulator operates in the following manner:— The regulator tube is inserted into an aperture of the furnace. Rheostat 19 is adjusted to permit the furnace temperature to rise 50-100° C above that required. Rheostat 20 is designed to allow a current through the furnace winding which is 50 per cent of the maximum. Disk 17 is now set to the required temperature and the main supply switch is closed. When the required temperature is reached, lever 10 is turned by the action of spring 11 due to different elongations of the rod and tube, and contact 15 touches the cam, thus closing the circuit of solenoid 26. The solenoid operates the mercury switch opening the main furnace circuit. The winding 18 is now fed through rheostat 20, which reduces the current by 50 per cent. Consequently, the furnace temperature falls, the steel tube 1 contracts, and the porcelain rod turns lever 10 against the action of the spring, opening the solenoid circuit, and restoring the original state.

Thermo-couple 12 is fitted in order to obtain accurate temperature readings.

If the furnace is to operate without supervision over long periods (more than 2-3 hours) it is advisable to provide an overload relay in order to avoid overheating should the mercury switch fail. This function is carried out by the spring contacts 14 and 15. If the temperature rises by more than 5° C above that set on the disk, rod 4 will press on lever 10 until spring 15 is bent to such an extent that it touches spring 14. This closes the circuit of solenoid 22, thus separating the contacts 27 and 28 and completely breaking the main furnace circuit.

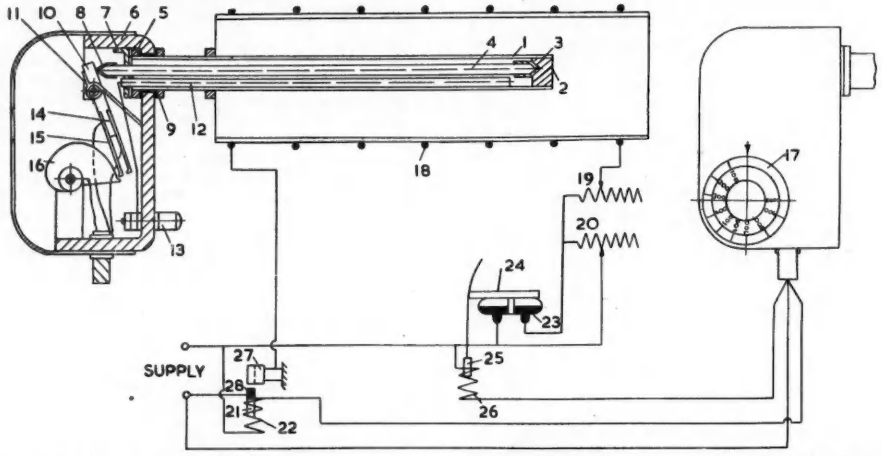

1 —Heat-resistant sheet steel tube (thickness 1-1·5 mm)
2.—Bush welded to (1)
3, 8.—Metal caps
4.—Porcelain rod
5.—Nut
6.—Bracket
7.—Guide
9.—Mica heat-insulation
10.—Lever
11.—Spring
12.—Thermo-couple
13.—Contacts for (12)
14, 15.—Spring contacts
16.—Archimedean spiral cam
17.—Regulating disk
18.—Furnace winding
19, 20.—Rheostats
21, 22, 27, 28.—Solenoid with fixed and moving contacts
23.—Mercury switch
24.—Lever
25.—Armature
26.—Solenoid

The Dynamic Capacity of Rolling Bearings

By G. LUNDBERG and A. PALMGREN. (From *Acta Polytechnica*, Mechanical Engineering Series, Vol. 1, No. 3, Issue 7, 1947, 50 pages, 22 illustrations.)

INTRODUCTION

THE calculation of the dynamic capacity of rolling bearings has always been based on formulas containing empirical coefficients. It has not been possible to bring the theoretical calculations, based on Hertz's theory of stress distribution of bodies in contact, in agreement with experimental results. Furthermore, this theory did not cover the most dangerous case of fatigue stress when bodies roll relatively to each other.

Hertz's theory is based on the assumptions that the contact area is small compared with the dimensions of the bodies, and that frictional forces in the contact areas can be neglected. For ball bearings these conditions are only approximately true. For line contact, the validity limit of the theory is exceeded whenever edge pressure occurs. Furthermore, the assumption of a homogeneous material is not justifiable under heavy stress concentrations. In actual materials, the material strength is different from one volume element to another, and the overall strength depends on the magnitude of the stressed volume.

In this report a statistical formula for the life of bearings is developed, and the foundations are given for a unified theory of the dynamic capacity of rolling bearings. Hertz's theory is extended to determine the dependence of the basic dynamic capacity on the conformity between rolling elements and bearing rings, and the shear stress is calculated in a plane parallel to the direction of rolling. By a suitable choice of exponents, which may be regarded as material coefficients, satisfactory agreement has been obtained between theoretical and experimental results.

1. DETERMINATION OF SHEAR STRESS AMPLITUDE

A study of the changes in the materials of bearing rings, occurring under rolling loads, shows that fatigue cracks start from certain weak points, for instance slag inclusions, which give rise to strong local stress concentrations in the surrounding material. Slippage occurs in the material before the fatigue crack develops, and changes the material in the neighbourhood of the weak point. As a result of the rolling process slag inclusions usually take a flat shape, and the fatigue cracks start therefore in planes parallel to the direction of rolling. With sharp cornered slag inclusions which sometimes occur the fatigue cracks often extend in a 45 deg. direction.

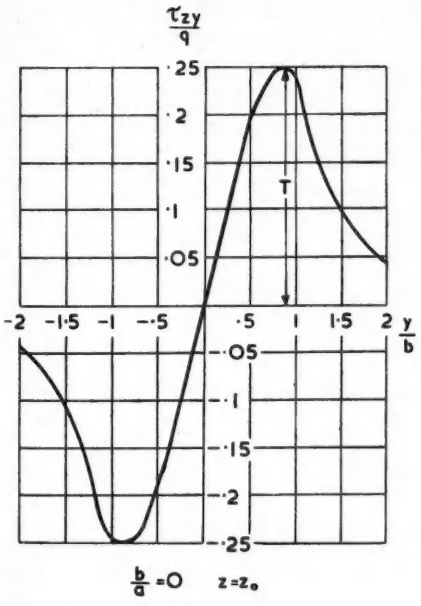

Fig. 1.

Since fatigue cracks usually start at a certain depth below the surface in planes parallel to the direction of rolling, special attention should be given to the shear stress amplitude occurring in these planes and reaching a maximum value at a certain depth below the surface. This investigation will be limited to a study of the shear stresses which occur in these planes, and to cross-sections situated in the plane of symmetry of the roller path.

A system of rectangular co-ordinates will be used, with its origin at the centre of the contact area, the positive z-axis coinciding with the interior normal of the body considered, the y-axis with the direction of rolling, and the x-axis with the direction perpendicular to these, x, y and z forming a right-hand screw system. Then, according to Hertz's theory, the shear stress τ in the plane of symmetry of the roller path ($x = 0$), expressed as a function of the potential U is

$$\tau_{yz} = 2z\,\partial^2 U/(\partial y\,\partial z) \quad .. \quad .. \quad (1)$$

$$\text{with} \quad U = \frac{3Q}{16\pi}\int_{s_0}^{\infty}\left[1 - \frac{y^2}{b^2+s} - \frac{z^2}{s}\right]\frac{ds}{R(s)}$$

where Q = rolling body load, and

$$R(s) = \sqrt{(a^2+s)(b^2+s)s} \quad .. \quad (2)$$

while s_0 is the largest root of the equation

$$\frac{y^2}{b^2+s_0} + \frac{z^2}{y_0} = 1 \quad .. \quad .. \quad (3)$$

a and b being the major and minor half-axes of the pressure ellipse, and s an auxiliary quantity.

From eqs. (1) and (3), by differentiation

$$\left.\begin{aligned} \tau_{zy} &= \frac{3Qz^2}{4\pi s_0 R(s_0)}\,\frac{\partial s_0}{\partial y} \\ \partial s_0/\partial y &= 2ys_0/[2s_0 + b^2 - y^2 - z^2] \end{aligned}\right\} \quad (4)$$

The solution can be expressed in parametric form by the introduction of two auxiliary angles φ and γ, so that

$$\left.\begin{aligned} \tau_{zy} &= \frac{3Q}{2\pi}\,\frac{\cos^2\varphi\sin\varphi\sin\gamma}{a^2\tan^2\gamma + b^2\cos^2\varphi} \\ y &= \sqrt{b^2 + a^2\tan^2\gamma}\,\sin\varphi \\ z &= a\tan\gamma\cos\varphi \\ s_0 &= a^2\tan^2\gamma \end{aligned}\right\} \quad .. \quad (5)$$

Fig. 1 shows the variation of the shear stress with y at the depth z_0 where it reaches its maximum value. When the contact point rolls along the raceway, the shear stress in a horizontal cross-section at a given depth alternates between $+\tau_0$ and $-\tau_0$, where $\tau_0 = |\tau_{zy\,\max}|$.

The amplitude of τ_0 is determined from $\partial\tau_{zy}/\partial\varphi = 0$

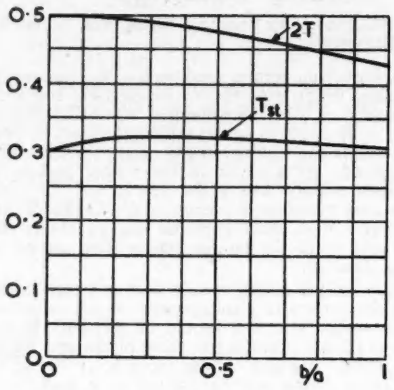

Fig. 2.

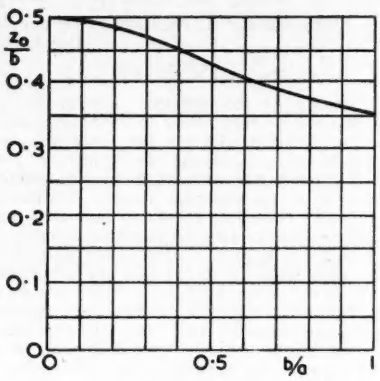

Fig. 3.

and $\partial\tau_{zy}/\partial\gamma = 0$. For the point of maximum shear stress:

$$\left.\begin{aligned} &\tan^2\varphi = t, \quad \tan^2\gamma = t-1, \\ \text{and} \quad &(b/a)^2 = (t^2-1)(2t-1). \end{aligned}\right\} \quad .. \quad (6)$$

The position of this maximum point is determined by $z = z_0 = \zeta b$, and $y = \pm\eta b$, where

$$\left.\begin{aligned} \zeta &= \frac{1}{(t+1)\sqrt{2t-1}}, \\ \eta &= \frac{t}{t+1}\sqrt{\frac{2t+1}{2t-1}} \end{aligned}\right\} \quad .. \quad .. \quad (7)$$

and its magnitude is found from

$$\tau_0 = Tq,\ T = \sqrt{2t-1}/[2t(t+1)],$$

where q = maximum Hertz pressure within the contact area.

During the passing of one rolling body, the shear stress τ_{zy} varies between $+Tq$ and $-Tq$. Thus, the determining factor for material fatigue is $2\tau_0$. Fig. 2 shows the variation of $2T$ with the shape of the pressure surface, and gives also for comparison the relative shear stress $T_{st} = \tau_{st}/q$ which is decisive for static loading. From this figure it is evident that T_{st} should not be used for an estimation of the fatigue strength.

Fig. 3 gives the depth z_0 at which the shear stress amplitude is greatest for different values of b/a. Investigations show that the greatest number of fatigue cracks occurs at this depth. Table I gives corresponding values of t, b/a, T, and ζ.

TABLE I.

t	b/a	T	ζ
1	0	0·2500	0·5000
1·02	0·2050	0·2475	0·4854
1·05	0·3358	0·2436	0·4651
1·1	0·5020	0·2371	0·4347
1·2	0·7849	0·2241	0·3842
1·2808	1	0·2139	0·3509

2. STATISTICAL METHOD FOR THE TREATMENT OF FATIGUE PROBLEMS

The strong stress concentrations in the neighbourhood of weak points (microscopic cavities, etc.) in the material, can cause local plastic flow of the material, in spite of the fact that they do not affect the macroscopic stress distribution and therefore need not be considered in determining macroscopic stress magnitudes. The internal stresses at the weak points are, however, proportional to the macroscopic stresses, and also depend to a certain extent on the shape of the weak points. The dispersion in material fatigue strength should be regarded as a material characteristic, and is related to the dispersion in the number of weak points.

For a statistical treatment of fatigue problems it should be borne in mind that the material changes gradually under repeated loads. Plastic flow appears around the weak points of the material, which increase gradually in size until, finally, a microscopic crack forms which slowly reaches macroscopic magnitude. At this advanced stage of fatigue, the macroscopic stress distribution is disturbed, and a continuation of the destructive process would rapidly lead to rupture.

Let $\lambda\,(n)$ be a function giving the condition of the material at a depth z after n loadings, and $d\lambda\,(n)$ the change in condition after dn loads. The probability that a crack may occur in the volume element ΔV under observation at a depth z under the surface, for a change $d\lambda$ in the condition of the material is

$$\mathbf{F}\,(\lambda\,(n))\,d\lambda\,(n)\Delta V.$$

Let $S\,(n)$ denote the probability that the volume element considered will withstand n loading cycles or more. The size of ΔV may be regarded as a measure of the number of weak points which can lead to the incidence of fatigue failure.

The probability that the volume element ΔV will endure $n + dn$ load cycles is the product of the probabilities that it will endure n load cycles and that the material will endure the change of condition $d\lambda\,(n)$, hence

$$\Delta S\,(n+dn) = \Delta S\,(n)\,[1 - \mathbf{F}\,(\lambda\,(n))\,d\lambda\,(n)\,\Delta V]. \quad (8)$$

When $dn \to 0$, we have

$$\lim_{dn\to 0} \frac{1}{dn}[\Delta S\,(n+dn) - \Delta S\,(n)] = \frac{d\Delta S\,(n)}{dn} \quad (9)$$

then eqs. (8) and (9) give

$$\frac{1}{dn}\frac{d\Delta S(n)}{\Delta S\,(n)} = -\,\mathbf{F}\,(\lambda\,(n))\frac{d\lambda\,(n)}{dn}\Delta V \quad .. \quad (10)$$

Integration between 0 and N, considering that $\Delta S\,(0) = 1$ yields

$$\log\frac{1}{\Delta S(N)} = \Delta V\int_0^N \mathbf{F}\,(\lambda(n))\frac{d\lambda(n)}{dn}\,dn, \quad .. \quad (11$$

$$= \Delta V G\,(\lambda\,(N)),$$

where G is the integral in the above expression.

The probability that the entire volume will endure is obtained by multiplication of the probabilities that the different parts will endure N load cycles:

$$S\,(N) = \Delta_1\,S\,(N)\,\Delta_2\,S\,(N). \quad .. \quad .. \quad (12)$$

Therefore $$\log \frac{1}{S(N)} = \Sigma G(\lambda(N))\,\Delta V$$

and with $\Delta V \to 0$

$$\log \frac{1}{S(N)} = \int_V G(\lambda(N))\,dV \quad .. \quad (13)$$

the integration being performed over the entire volume.

Changes in the material condition at a depth z for the N-th load, as long as the fatigue failure is of microscopic size, can be regarded as mainly dependent on the macroscopic stress amplitude $\tau(N)$, which is most dangerous as regards fatigue, and on the condition of the material, $\lambda(N)$, in the element dV. Changes in condition may also depend on the depth z, below the surface, of the element dV considered. For a small number of load cycles dN, the changes in condition $d\lambda(N)$ of the material can thus be written

$$d\lambda(N)/dN = \mathcal{J}[\lambda(N), \tau(N), z]. \quad .. \quad (14)$$

The probability that the material in the volume V will endure N or more load cycles is thus uniquely determined from eqs. (12) and (13) when the functions G and $\mathcal{J}$ are known. Various statistical methods can now be used, one of these being to introduce power functions for G and $\mathcal{J}$:

$$\left.\begin{aligned} G[\lambda(N)] &= \kappa[\lambda(N)]^g \\ \mathcal{J}[\lambda(N), \tau(N), z] &= \lambda(N)^{-j}\ K[\tau(N), z] \end{aligned}\right\} \quad .. \quad (15)$$

the constants κ, g and j depending on the material; then, since $d\lambda/dN = \mathcal{J}$:

$$\lambda^j\,d\lambda = K[\tau(N), z] \quad .. \quad .. \quad (16)$$

For $N = 0$, $S(0) = 1$, and thus $\lambda(0) = 0$ for all volume elements. The integration of eq. (16), between the limits 0 and N, yields

$$\lambda(N) = \left[\frac{g}{e}\int_0^N K\,[\tau\,(N),\ z]\ dN\right]^{e/g} \quad .. \quad (17)$$

where $e = g/(j+1)$, and therefore,

$$\log \frac{1}{S(N)} = \kappa\left(\frac{g}{e}\right)^e \int_V \left[\int_0^N dN\,K[\tau(N), z]\right]^e dV \quad (18)$$

which may be applied for the statistical treatment of various fatigue problems.

For highly concentrated loads, as in rolling bearings, the calculation can be simplified as a result of the observation that only the conditions in the neighbourhood of the point where the maximum fatigue stress amplitude occurs are decisive for the risk of fatigue. Assuming that the amplitude τ is independent of N, we have, from eq. (18), the proportionality

$$\log \frac{1}{S(N)} \propto N^e \int_V K^e(\tau, z)\,dV \quad .. \quad (19)$$

Introducing the approximation $\tau = \tau_0 f(x/a, z/z_0)$, where z_0 is the position of the maximum fatigue stress amplitude τ_0, and denoting the length of the raceway by l, we have

$$\int_V K^e(\tau, z)\,dV = \int_0^l \int_0^\infty \int_0^\infty K^e(\tau, z)\,dx dy dz \quad .. \quad (20)$$

or using the new variables of integration

$$u = x/a,\ v = z/z_0$$

$$\left.\begin{aligned} \int_V K^e(\tau, z)\,dV &= a\,z_0\,l\,\Theta(\tau_0, z_0) \quad .. \quad .. \\ \Theta(\tau_0, z_0) &= \int_0^\infty \int_0^\infty K^e[\tau_0 f(u, v), z_0 v]\,du\,dv \end{aligned}\right\} \quad (21)$$

From eqs. (19) and (21), if τ_0 is independent of N

$$\log \frac{1}{S(N)} \propto N^e\,\Theta(\tau_0, z_0)\,a\,z_0\,l \quad .. \quad .. \quad (22)$$

For practical applications, if τ_0 is dependent on N, in calculating the probability that the material will endure N cycles, eq. (18) can be replaced by

$$\log \frac{1}{S(N)} \propto l\left[\int_0^N [\Theta(\tau_0, z_0)\ az_0]^{1/e}\ dN\right]^e \quad (23)$$

and the function Θ is replaced by a power function

$$\Theta(\tau_0, z_0) = \tau_0^c\,z_0^{-h} \quad .. \quad .. \quad .. \quad (24)$$

3. LIFE FORMULA FOR ROLLING BEARINGS

It is a known fact that the more concentrated the stress is, the greater is the endurance. Neuber and Föppl-Huber sought the explanation of the dependence of fatigue strength on volume in the crystalline nature of the material and the dispersion in material strength. Frequent examples have shown that many cracks do not reach the surface, so that Weibull's assumption that the first crack always leads to a break is not valid for fatigue in rolling bearings. However, in accordance with Weibull's theory, it can be assumed that (1) the probability of a fatigue break occurring depends on the depth z_0 at which the most dangerous stress develops, and (2) the logarithm of the probability of the material enduring is proportional to the magnitude of the stressed volume (probability following a multiplicative law). Hence the life formula for the probability S that the material will endure for N million stress cycles may be written as

$$\log \frac{1}{S} = F(\tau_0, N, z_0)\,V \propto \tau_0^c\,N^e\,z_0^{-h}\,V \quad .. \quad (25)$$

where τ_0 is the decisive stress amplitude. The volume V is representative of the stress concentration, and proportional to a, z_0 and l:

$$V \propto a\,z_0\,l \quad .. \quad .. \quad .. \quad (26)$$

The relations (25) and (26) then give

$$\log \frac{1}{S} \propto \tau_0^c\,N^e\,a\,l\,z_0^{1-h} \quad .. \quad .. \quad (27)$$

For point contact, according to Hertz, the maximum pressure q in the area of contact is

$$q = 3Q/(2\pi ab) \quad .. \quad .. \quad (28)$$

From (7), (27) and (28), we have

$$\log \frac{1}{S} \propto T^c\,a\,l\,(\xi b)^{1-h}\,N^e\,(Q/ab)^c \quad .. \quad .. \quad (29)$$

The Hertzian expressions for the semi-axes of the pressure ellipse will now be introduced:

$$a = \mu\lambda,\ b = \nu\lambda, \text{ and } E_0 = m^2\,E/(m^2 - 1) \quad .. \quad (30)$$

where $\lambda = \sqrt[3]{3Q/(E_0\,\Sigma\rho)}$, ρ = the curvatures of the bodies in contact, while E = modulus of elasticity, $1/m$ = Poisson's ratio, μ and ν = auxiliary quantities introduced by Hertz. The formulae are valid for similar materials in both bodies. From eqs. (30) we have

$$ab^2 = \mu\nu^2\lambda^3 \quad .. \quad .. \quad .. \quad .. \quad (31)$$

(To be continued)

The Hydrosphere—A New Hydrodynamic Bearing

By M. C. SHAW and C. D. STRANG, Jr. (From *Journal of Applied Mechanics*, Vol. 15, No. 2, June, 1948, pp 137-145, 16 illustrations.)

(*Concluded from October issue.*)

APPARATUS AND PROCEDURE

The simple small-scale bearing-testing machine used (see Fig. 8), was constructed around an ordinary bench-type drill press, the journal being mounted in a conventional Jacobs chuck. Load was applied by movement of the drill-press spindle, and a platform was used to measure the applied thrust load.

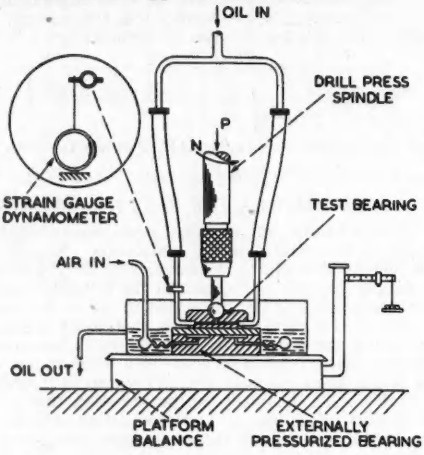

Fig. 8. **Bearing test apparatus.**

An externally pressurized air bearing provided a frictionless support for the test bearing (Fig. 9). Compressed air from a manifold was introduced to four recessed areas in the lower member through individual pneumatic resistances, which maintained the plates parallel under an eccentric load by increasing the pressure in the recessed regions under the most heavily loaded portion of the bearing and simultaneously decreasing pressure in the less heavily loaded recessed areas. Frictional torque was accurately measured by means of a temperature-compensated dynamometer ring, with wire-resistance strain gauges on the outer and inner surfaces of the ring connected to adjacent arms of a Wheatstone bridge circuit. As the air bearing is restrained from moving, it will introduce no friction torque, and hence the torque measured by the dynamometer represents that due to the test bearing only. Oil was introduced through flexible neoprene tubes in order to minimize extraneous torque. The range of operating conditions obtainable with this bearing-testing machine is given below.

Variable	Range.
speed (rpm)	700-4500
thrust load (lb)	0-400
friction torque (oz-in)	0·07-30·0
oil-inlet temp. (deg F) ..	80-150
oil supply pressure (psi) ..	0-50

Many tests were made on bearings of 24S-T aluminium, which, being a poor bearing metal, accentuates the effects of changes in mechanical design and gives easily reproducible results. The spherical seat in the bearing surface was machined with a ball end mill, and then cold-pressed with a steel ball. The oil grooves, approximately $\frac{1}{32}$-in wide × $\frac{1}{32}$-in deep, were introduced by hand with a scraper, and finished by lapping with Bon Ami powder against a steel ball

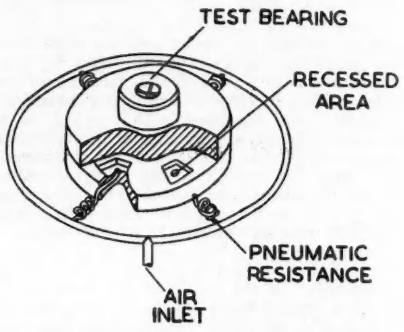

Fig. 9. **Externally pressurized bearing.**

until a perfect seat was obtained. All tests were made on 180 deg bearings unless otherwise noted.

Tests were also run on a lead-tin bearing with four symmetrically spaced radial oil grooves extending to the edge of the bearing; the 50-50 lead-tin alloy 0·020-in thick used to line this bearing had characteristics similar to those of commercial white metal and was used because of its availability.

Each bearing was run-in until reproducible friction values were obtained under high load. Frictional torque was then determined for progressively increasing loads, sufficient time being allowed between readings for temperature equilibrium to be established. Oil-inlet and bearing temperatures were determined by means of thermocouples. Oil-heating and temperature-control apparatus were used in some tests to determine the influence of oil viscosity on the bearing operating characteristics.

RESULTS AND DISCUSSION

For a given hydrodynamic bearing the friction coefficient varies inversely with the dimensionless product $\mu N/P$, while the friction coefficient varies directly with $\mu N/P$ for non-hydrodynamic bearings, where μ = viscosity (reyns. = lb sec/sq in), N = journal speed (rpm), and P = load acting on the bearing per unit projected area (psi). From the shape of the test curve in Fig. 10, it is evident that the bearing is fully hydrodynamic above $\mu N/P = 0{\cdot}9 \times 10^{-8}$, the minimum coefficient of friction being 0·005 at a load of 550 psi and a speed of 1400 rpm. The viscosity of the kerosene lubricant, supplied at ambient temperature, was practically constant at $0{\cdot}21 \times 10^{-6}$ for all test points. A further 0·750-in

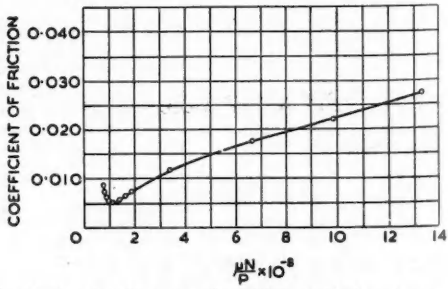

Fig. 10. **Friction curve for 0·75-in dia Hydrosphere.**

diameter lucite unit with four grooves was also tested, using a steel journal, and by means of indirect lighting the oil film was clearly visible at loads up to 600 psi.

To ascertain the effective region of the bearing surface, the bottom portion of a 0·375-in diameter 180-deg aluminium bearing was gradually cut away. The load-carrying capacity of the bearing was not appreciably affected until the entire lower half was completely removed, and the load capacity then decreased rapidly. In further tests on an identical aluminium bearing, the upper portion of the surface was gradually removed by facing off the bearing block; and with the slightest removal of metal from the upper region of the surface an appreciable decrease in load capacity was evident. Excessive lapping of the bearing caused a slight bell-mouth condition to develop at the upper edge, similarly reducing the load capacity. These tests confirmed the theory that negative pressure tended to be developed in the lower half of the bearing.

The load capacity of the hydrosphere is much more sensitive to the removal of metal in the vicinity of ϕ = 90-deg (point A in Fig. 1) than at ϕ = 45-deg, and this is due not so much to the fact that a surface developing positive pressure is removed, but rather that the effective pressure seal normally present is altered when even a little metal is removed from that region.

The minimum value of $\mu N/P$ before the onset of boundary lubrication was found to be much lower with 50-50 lead-tin alloy than with 24S-T aluminium. The tests showed that a highly-loaded hydrosphere should be provided with a very thin layer of a soft low-shear-strength material such as tin-base babbitt, deposited uniformly on a harder-base material such as bronze or steel.

Whereas with a slider or journal bearing a single

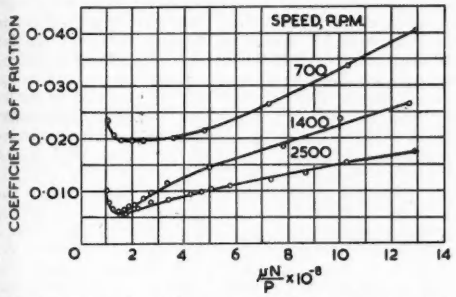

Fig. 11. **Effect of speed upon the μ N/P curve using 0·75-in dia 50-50 tin-lead bearing.**

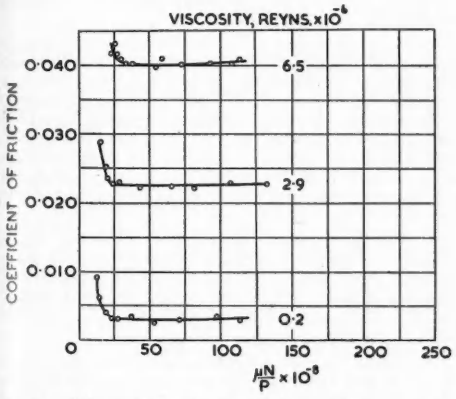

Fig. 12. **Effect of viscosity upon the μ N/P curve using 0·375-in dia 24S-T aluminium bearing.**

curve is obtained when the friction coefficient is plotted against the non-dimensional quantity $\mu N/P$ regardless of the individual values of the parameters μ, N and P, the hydrosphere gives different curves for various values of the parameters (Figs. 11 and 12). The fact that the performance of the hydrosphere is improved significantly as speed is increased (Fig. 11) has prompted the suggestion that the centrifugal inertia force acting on the oil particles is sometimes of importance. It can, however, be shown that its component in the s–direction is negligible compared with the pressure and shear forces occurring for all practical values of Reynolds' number; for this reason inertia force in the s–direction has been ignored in the analysis leading to eqs. (14) and (18). As shown by Kingsbury, the centrifugal inertia force due to the n–direction will become sufficient, when the speed of the bearing is increased, to alter the flow from the bearing and hence to influence the variable α, so that it may be an important parameter. Eqs. (14) and (18) show that sin α need decrease in the s–direction by only the same order of magnitude as the film thickness of a Kingsbury or Michell bearing to be equally effective in causing pressure to be developed in the oil film.

A dimensional analysis for a hydrodynamic bearing shows that the coefficient of friction f is a function of the Reynolds' number $\mathbf{R} = \rho ND^2/\mu$ and of the ratio $\mu N/P$:

$$f = f(\mu N/P, \mathbf{R}), \quad .. \quad .. \quad .. \quad (21)$$

where D = diameter of the journal (sphere), ρ = mass density of the lubricant, μ = viscosity, N = journal speed, P = unit load, and this should account for the multiplicity of friction curves obtained with different values of N and μ.

A series of tests was made with an aluminium bearing to ascertain the optimum number of radial grooves in a hydrosphere. Without grooves there was immediate incipient failure, indicating little or no load capacity. Tests with the same bearing with 1, 2, 4, and 8 symmetrically spaced radial grooves (see Fig. 13), indicated that the optimum number of grooves lies between 4 and 8, and this is expected to hold good on the basis of similitude for bearings of all sizes.

The hydrosphere without grooves will not operate satisfactorily because at least one radial groove is required for the oil to be carried into the bearing against the outward pressure gradient by the shear force along the moving spherical surface. The streamline pattern and the temperature rise are altered as the number of grooves is changed, hence from eq. (18) it is to be expected that an optimum number of grooves exists for a given bearing. Curved grooves spiraling from the centre outwards may prove more advantageous than straight radial grooves, but this possibility has not yet been investigated.

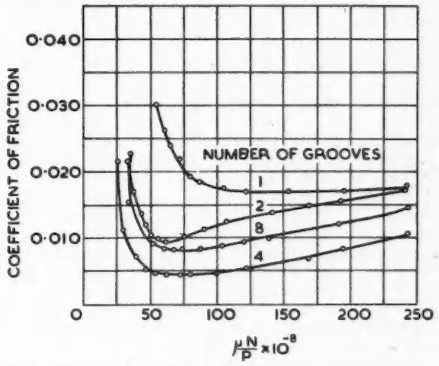

Fig. 13. **Effect of number of radial oil grooves upon the μ N/P curve for 0·375-in dia 24S-T aluminium bearing.**

The oil grooves also enable the oil to circulate through the bearing and thus carry away the heat developed by viscous shear. As with a crescent-shaped oil film in the hydrosphere the flow from the equatorial region is practically prevented, the grooves must extend to the outer periphery of the bearing to provide an exit for the oil.

The negative pressure tending to develop in the lower half of the hydrosphere is equivalent to an external positive pressure, in causing the oil to flow into the grooves from the main oil supply. This ability of the hydrosphere to supply its own pumping capacity is a factor of safety in the event of a failure in the lubrication system, and the hydrosphere can operate under high load for extended periods of time after the pressure oil feed to the bearing is interrupted. Operation of the hydrosphere was found to be unaffected by considerable misalignment (of 2 degrees or more) of the journal.

A comparison of bearing temperatures under pure thrust and combined radial and thrust loads showed that less friction was developed with a combined load than when the same thrust load was present alone. Bearing temperature measurements showed that the thrust-load capacity of the bearing is unaffected by radial loads ranging up to at least 50 per cent of the thrust load capacity.

The crescent-shaped film allows appreciable flow within the hydrosphere for the establishment of pressure, but a minimum of flow from the bearing. The seal which exists at the equator of the hydrosphere effectively limits the " end leakage." The flow from the equatorial region is negligible, and hence the operating temperature may be adjusted by merely proportioning the grooves to provide sufficient flow to carry away the heat generated. The oil-supply pressure can also be used to alter the flow of cooling oil, since bearing operation is insensitive to oil-inlet pressure.

The hydrosphere requires a pair of perfectly mating spherical surfaces, and the precision obtainable by pressing and lapping of the fitted spherical surfaces far exceeds that obtainable by the use of machine tools and ordinary measuring instruments.

Owing to its small effective radius, which gives rise to a low friction torque, the hydrosphere is of particular interest for high-speed applications, and it is expected that the stabilizing influence of the thin-film equatorial region of the bearing will prevent the occurrence of the high-speed self-excited vibration known as " shaft whirl."

Surge Phenomena in Transformers

By B. HELLER, J. HLAVKA and A. VEVERKA. (From *Elektrotechnicky Obzor, Czechoslovakia,* Vol. 37 No. 6, March, 1948, pp. 93-115, 61 illustrations.)

THE initial distribution of the potential is theoretically and experimentally investigated for various types of windings used in transformers with earthed and insulated terminals. Particularly interesting are the conditions during surges within the layers of the winding and inside the turns of each layer, especially in the first one, where large variations of voltage can arise, causing high electrostatic stresses in the winding. The results obtained for layers can be applied in determining the voltage conditions within individual coils. Formulae are derived for the effective capacitance and initial potential gradient. The theoretical results were verified by experiments, which were carried out by using condenser models for various types of windings. Various possible ways of improving the initial distribution of voltage mainly for layer windings, are also discussed.

Furthermore, the transient phenomena produced as a result of the difference between the initial voltage distribution and the voltage in the steady state are investigated.

1. *Determination of the resultant field for various types of windings.* The relation of the coefficient of mutual induction of two turns is analyzed with respect to their spacing for windings in air, with an iron core and with short circuited windings on an iron core. It is found in all cases that the relation can be expressed by an exponential function with a suitably chosen parameter λ.

2. *Free oscillations of a single layer winding.* By knowing the mutual effect of all turns, the differential equations characterizing the problem can be solved by the method of standing waves. A formula given in the article correlates the time-frequency of free oscillations with their frequency in space and includes as special cases all formulas hitherto published in the technical literature. The exact solution of the integro-differential equations in cases where the terminal of the winding is earthed or insulated shows that the voltage along the axis of the winding can be expressed by the sum of trigonometric and hyperbolic functions. At the same time it appears that the wavelengths for windings with an earthed terminal closely approach multiples of π. Previous solutions have always given exact multiples of π as the values of these wavelengths. In the case where the terminal of the winding is insulated the fundamental wavelength may vary within wide limits, so that the value of $n\,\pi/2$ commonly used may result in considerable errors.

3. *Free oscillations of a double-layer winding.* Here, the frequency formula taking into account varying numbers of turns in both layers is developed. Because of the difficulties associated with the solution of the system of integro-differential equations, the corresponding system of simultaneous differential equations is solved instead by means of harmonic functions. In this case we can solve the special problem of windings with one terminal of both layers earthed and the other terminal free. The solution leads to two sets of wavelengths, one consisting of even multiples and the other of odd multiples of $\pi/2$. In all the cases under consideration, the amplitudes of the free oscillations are determined, on one hand, by Fourier analysis and the difference between the initial and the final voltage distributions, and, on the other, by the expressions obtained for the free vibrations and by then comparing the corresponding coefficients. At the same time, it is found that with the terminal of the winding earthed and a small value of λ, and with the terminal of the winding insulated and a large value of λ, the deviations from the approximate solution are negligible. Large errors may arise where the terminals are insulated and λ is small.

4. *Free oscillations of a coil.* The results obtained in the case of layer windings are applied to cylindrical coil windings by replacing the coil by a layer winding, the constants of which are derived from the constants of the former. The free oscillations within individual coils, especially within the first coil, are investigated. The natural oscillations of coils due to their own high frequencies are rapidly damped and are quite negligible as compared with the free oscillations of the whole winding.

5. *Permissible electrical stresses.* As the voltage is known at any time at any point of the winding, the stress curve can be drawn. When this is compared with the impulse characteristics, as obtained experimentally, the required surge protection data will be known.

6. Finally the authors calculate the surges in a 100-kV transformer firstly where the windings have an insulated terminal and secondly, where regulating taps are provided.

The part played by Oxygen and Nitrogen in Arc-Welding

By J. D. Fast. (From *Philips Technical Review*, Vol. 10, No. 1, July, 1948, pp. 26-34, 4 illustrations.)

In order to obtain welds with satisfactory mechanical properties it is essential to protect the metal against the attack of oxygen and nitrogen while being transferred from the electrode to the workpiece.

In principle, the simplest way to provide such protection is to carry out the welding in a gas which is absolutely free of components which react with iron. Welding in hydrogen, for instance, has become well-known ; use is thereby made of the large quantity of heat released by the re-combination of the atomic hydrogen formed in the arc. This method, however, is rather expensive and, consequently, is used only in special cases. The same applies to welding in helium and argon.

More economical protection is obtained by coating the electrodes with substances which, during the welding process keep the oxygen and nitrogen away from the metal, either by the development of large quantities of other gases (organic substances) or by the formation of a sealing slag on the metal (mineral substances). Frequently, a combination of both these processes is applied.

To study more closely the effect of oxygen and nitrogen on iron and steel we shall concentrate our attention particularly upon questions of importance in the technique of welding, viz :—

(a) The solubility of oxygen and nitrogen in liquid iron between its melting point and boiling point.

(b) The solubility of oxygen and nitrogen in solid iron, particularly alpha iron.

(c) The chemical reaction between oxygen and carbon dissolved in liquid iron; this reaction is apt to cause porosity in the welds and, still more important, provides the propelling force for the transfer of the metal from the electrode to the workpiece.

THE IRON-OXYGEN SYSTEM

Solubility of Oxygen in Liquid and in Solid Iron

If liquid iron is attacked by oxygen and the pressure of the oxygen exceeds a certain value, then all the metal will be gradually transformed into liquid oxide. This can be read from the partial constitutional diagram of the iron-oxygen system (Fig. 1).

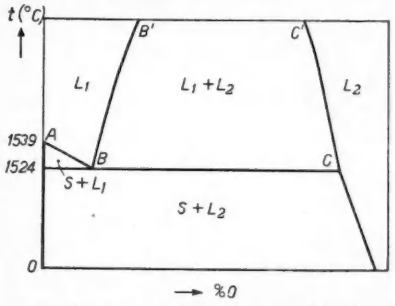

Fig. 1. **Part of the constitutional diagram of the iron-oxygen system.**

Let us suppose that while maintaining a constant temperature, say, 1600° C, we cause the oxygen pressure above the liquid iron to rise gradually from zero. The state of saturation, indicated in the diagram by the solubility curve *BB'*, will then be reached at a very low oxygen pressure. At 1600° C this pressure is about 10^{-2} atm. As soon as the state of saturation has been reached, then, in addition to the liquid metallic phase, a liquid oxide phase begins to form, the composition of which is given by the position of the line *CC'*. According to Gibbs' phase rule, the pressure should remain constant until all the metal has been transformed into this oxide phase.

If at the constant temperature of 1600° C the pressure of the oxygen is caused to rise further, then the liquid oxide, the composition of which on the line *CC'* was not far removed from the stoichiometric composition FeO, gradually absorbs more oxygen. Finally, at a pressure of one atmosphere, an oxygen content is reached which is already greater than that corresponding to the formula Fe_3O_4.

In electric arc welding with bare electrodes, the reaction time is so short that not all the metal is transformed into oxide, as is required by the thermodynamic equilibrium, but only a partial oxidation takes place. Immediately underneath the electrode a molten mass is formed, consisting of a metallic phase containing oxygen and covered by a thin layer of liquid oxide. At the interface the compositions of these two phases will be as represented by the lines *BB'* and *CC'* in Fig. 1. The average composition of the metallic phase, however, will be given by points a little to the left of *BB'* and that of the oxide phase by points a little to the right of *CC'*.

The position of the line *BB'*, i.e., the solubility of oxygen (or FeO) in liquid iron as a function of the temperature is of particular importance. For the temperature range between 1800° K and 2083° K this solubility has been accurately determined by Chipman and Fetters[1].

It is highly important to know the solubility also at higher temperatures, for there are indications that, while passing from the electrode to the workpiece, the metal is in many cases heated to the boiling point of iron.

By means of a few simple hypotheses regarding the thermal effect and the change in entropy taking place when liquid Fe is homogeneously mixed with liquid FeO, the following relation between solubility and temperature can be deduced :—

$$T = \frac{C}{R} \frac{1-2x}{\log_e \frac{1-x}{x}} \quad \ldots \quad \ldots \quad \ldots \quad (1)$$

where T is the absolute temperature and x the solubility

[1] J. Chipman and K. L. Fetters, Trans. Am. Soc. Metals **29**, 953-967, 1941.

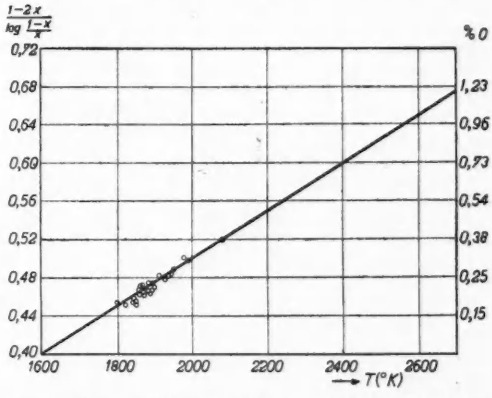

Fig. 2. **The expansion $(1 - 2x)/\log[(1 - x)/x]$ as a function of the absolute temperature.**

of FeO expressed as a molecular fraction, i.e., the number of molecules of FeO in the saturated solution divided by the total number of molecules. R is the gas constant and C a constant which has to be determined experimentally.

Formula (1) indicates that when plotting $(1 - 2x)/\log(1 - x)/x]$ as a function of T, we should obtain a straight line through the origin. As shown in Fig. 2, Chipman's and Fetters' measurements satisfy this requirement quite well. From the slope of the straight line the constant C in eq. (1) is found to be

$$C = 18\,300 \text{ cal.}$$

The satisfactory agreement between theory and experiment encourages us to use eq. (1) also for calculating the solubility at higher temperatures. These (calculated) solubilities can be read directly from Fig. 2.

Absorption of Oxygen when Welding with Bare Electrodes

Since the boiling point of iron lies at about 2750° K, it may be expected that when welding with bare electrodes the molten metal will always contain less than 1·2 per cent oxygen.

Losana[2], who used bare electrodes of different diameters and made of different kinds of steel, found that both the oxygen and the nitrogen content of the deposited metal increased as the thickness of the electrode decreased. Not in one single experiment was the oxygen content found to be lower than 0·140 per cent, or higher than 0·953 per cent. The results of these experiments, therefore, are not in contradiction with Fig. 2.

As an example taken from a series of experiments by Losana, Table I gives the C, Mn, Si, P, S, O and N contents of the metal deposited from electrodes containing 0·10 per cent C, 0·89 per cent Mn, 0·17 per cent Si, 0·015 per cent P and 0·021 per cent S (the balance being Fe).

TABLE I. COMPOSITION OF THE METAL DEPOSITED IN SOME OF LOSANA'S EXPERIMENTS[2].

Wire dia. mm	C %	Mn %	Si %	P %	S %	O %	N %
1	?	?	?	?	?	0·720	0·218
2	0·026	0·054	0·039	0·010	0·019	0·550	0·180
4	0·048	0·070	0·053	0·014	0·021	0·302	0·130
6	0·068	0·124	0·058	0·014	0·022	0·140	0·105

The drop in the oxygen content with increasing diameter of the electrode wire is probably related to the fact that the thicker the wire, the larger are the droplets of metal transferred from the electrode to the workpiece. It may be that, consequently, the temperature of the metal crossing the arc is lower when thicker rods are used. Moreover, we have to take into account the fact that there is no time for the equilibrium of dissolution and the chemical equilibria fully to adjust themselves.

THE REACTION BETWEEN OXYGEN AND CARBON IN ELECTRIC ARC WELDING

To a liquid iron phase containing small quantities of C and FeO (or O) in solution, in the state of equilibrium, there belongs a gas phase consisting of a mixture of CO and CO_2. The following reactions can take place between the components in the two phases

$$[FeO] + [C] \rightleftarrows [Fe] + CO \quad .. \quad .. \quad (2)$$

$$2[FeO] + [C] \rightleftarrows 2[Fe] + CO_2 \quad .. \quad .. \quad (3)$$

$$[FeO] + CO \rightleftarrows [Fe] + CO_2 \quad .. \quad .. \quad (4)$$

$$[C] + CO_2 \rightleftarrows 2\,CO \quad .. \quad .. \quad .. \quad (5)$$

the brackets indicating the components of the homogeneous liquid phase.

With the aid of thermodynamics and experimental data taken from literature, it is possible to calculate the positions of these equilibria as functions of the temperature of the steel. Table II gives the equilibrium pressures of CO and CO_2 which should correspond to the C and O contents of the deposited metal given in Table I.

TABLE II. CALCULATED EQUILIBRIUM PRESSURES OF CO AND CO_2 (IN ATMOSPHERES) CORRESPONDING TO THE C AND O CONTENTS IN TABLE I.

% C	% O	2300° K		2700° K	
		f_{CO}	p_{CO_2}	p_{CO}	p_{CO_2}
0·026	0·550	10·4	1·23	14·3	0·75
0·048	0·302	11·3	0·79	15·3	0·47
0·068	0·140	7·7	0·26	10·3	0·15

In the calculations which led to the pressures given in Table II, extrapolations were employed which may have caused errors of 10 per cent in the results. This, however, does not detract from the conclusion that, when welding with bare electrodes, conditions are far removed from the state of chemical equilibrium.

This failure to reach states of equilibrium will prove to be of essential importance also when dealing with coated electrodes.

THE IRON-NITROGEN SYSTEM

Dissociation Pressure of Iron Nitride

In the case of nitrogen it is found that, at high temperatures, the state of saturation both for liquid and for solid iron is reached only at N_2-pressures far above the partial pressure of nitrogen in air. Consequently, it has not yet been possible to reach the saturation concentrations for liquid iron. It has, however, been possible to determine the concentrations corresponding to a nitrogen pressure of 1 atm.

For alpha-iron it was possible to reach the condition of saturation by causing, instead of N_2, mixtures of NH_3 and H_2 to react with iron. As soon as the limit of solubility is exceeded a new phase is formed (the nitride Fe_4N), the dissociation pressures of which, at various temperatures, naturally correspond to the equilibrium pressures of the saturated solutions of nitrogen in iron. These dissociation pressures can be calculated and will enable us to compute an upper limit for the solubility of nitrogen in alpha-iron. We shall also see (Table III) that more direct determinations of the position of the solubility line AC diagrammatically represented in Fig. 3 give widely divergent values.

The explanation of why NH_3 is so much more active than N_2 lies in the fact that the equilibrium

$$8\,Fe + 2\,NH_3 \rightleftarrows 2\,Fe_4N + 3\,H_2 \quad .. \quad .. \quad (6)$$

is reached comparatively quickly, whereas the reactions

$$N_2 + 3\,H_2 \rightleftarrows 2\,NH_3 \quad .. \quad .. \quad .. \quad (7)$$

and

$$2\,Fe_4N \rightleftarrows 8\,Fe + N_2 \quad .. \quad .. \quad .. \quad (8)$$

take place but very slowly. If, for instance, NH_3 is heated to 500° C for a long time, it dissociates almost entirely into hydrogen and nitrogen, since the stoichiometric gas mixture in the state of equilibrium at 500° C and 1 atm contains only 0·12 per cent NH_3 by volume. However, when iron is heated to 500° C in a stream of $NH_3 + H_2$, the velocity of the gas can easily be chosen such that the percentage of NH_3 drops only very little. The iron then reacts with a mixture of NH_3 and H_2, which corresponds to very high nitrogen pressures in the state of equilibrium. The constant of the reaction (7)

$$K_{NH_3} = \frac{p^2_{NH_3}}{p_{N_2} p^3_{H_2}} \quad .. \quad .. \quad .. \quad (9)$$

at 500° C amounts to $1{\cdot}5 \times 10^{-5}$.

When mixtures of NH_3 and H_2 of varying com-

[2])L. Losana, Metallurgia Italiana **26**, 391-403, 1934.

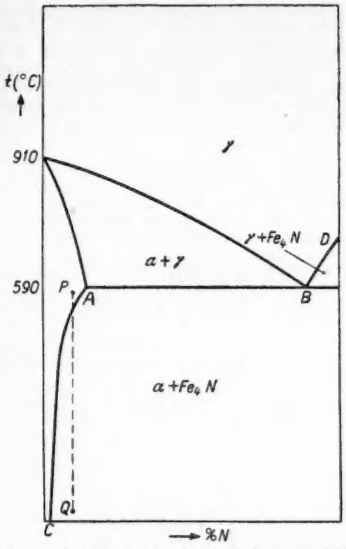

Fig. 3. **Part of the constitutional diagram of the iron-nitrogen system.**

position are passed over iron at 500°C, the formation of Fe_4N begins as soon as the NH_3 content rises above 20 per cent by volume. The reaction takes place in the opposite direction as soon as the NH_3 content falls below 20 per cent.

From the experimental data available the following relation between the dissociation pressure of Fe_4N (in equilibrium with Fe) and the absolute temperature can be deduced:

$$\log p = -\frac{1760}{T} + 5{\cdot}99 \quad .. \quad .. \quad (10)$$

According to this formula, the dissociation pressure at 20° C is already about 1 atm. The Fe_4N needles in steel, so well known in metallography, should, therefore, dissociate spontaneously; the fact that they continue to exist is due only to the inertia of this dissociation.

Solubility of Nitrogen in Solid Iron

In order to be able to speak about the solubility at a certain nitrogen pressure without causing confusion, we shall, from now onwards, call the (true) solubility as indicated in the constitutional diagram of Fig. 3 by the lines *CA* and *BD* the " maximum solubility."

Reliable data in regard to the solubility of nitrogen in solid iron are only available for a pressure of 1 atm. They are given by Sieverts and his collaborators[3]) and are represented by Fig. 4.

According to Sieverts the solubility in alpha-iron is 0·002 per cent by weight at 890° C and 0·0004 per cent by weight at 750° C. At these relatively low temperatures, equilibrium is established so slowly that the values given are less reliable than those for gamma and delta-iron. Now the iron atoms in alpha as well as in delta-iron form a body-centred cubic lattice, and it is, therefore, to be expected that one continuous curve can be drawn through the points of alpha and delta-iron. This does indeed prove to be the case (see dotted line in Fig. 4) and it makes the points for alpha-iron more reliable. According to Fig. 4, the solubility in the gamma-phase, stable between 910° C and 1400° C, and

[3]) A. Sieverts G. Zapf and H. Moritz, Z. physik. Chem. A **183**, 19-37, 1938.

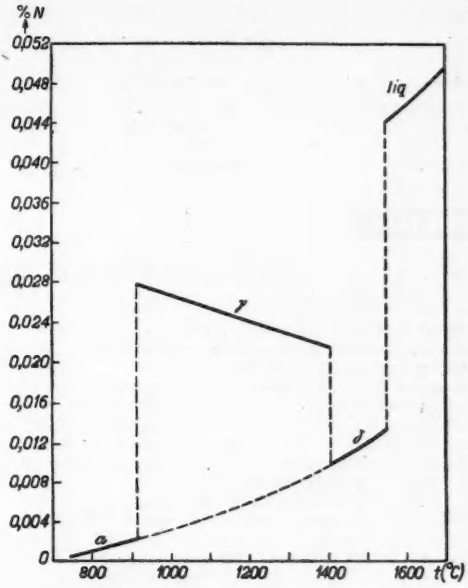

Fig. 4. **Solubility of nitrogen in iron at 1 atm nitrogen pressure as a function of the temperature.**

the solubility in liquid iron are much greater than that in alpha (delta)-iron.

The concentration of a bi-atomic gas in a metal is, in general, approximately proportional to the square root of the pressure. As the temperature coefficient of the solubility in alpha-iron is positive the given solubility of 0·0004 per cent N at 750° C is certainly an upper limit for the solubility (still at 1 atm) at temperatures lower than 750° C. For the solubility C (in per cent by weight N) at some other pressure we have

$$C < 0{\cdot}0004\sqrt{P_{N_2}} \quad .. \quad .. \quad (11)$$

An upper limit of maximum solubility is then immediately found by substitut ng for p_{N_2} the dissociation pressure of Fe_4N as calculated from (10). If it is desired to avoid this pressure, which only arises as a secondary quantity, then we may directly combine the formulae (9) and (11) and write

TABLE III. VALUES OF THE UPPER LIMIT OF MAXIMUM SOLUBILITY OF NITROGEN IN ALPHA IRON CALCULATED FOR VARIOUS TEMPERATURES, AND THE EXPERIMENTAL VALUES OF MAXIMUM SOLUBILITY FOUND BY VARIOUS INVESTIGATORS.

Temp. (in °C)	Maximum solubility (in per cent by weight)			
	calculated (upper limit)	measured		
590	0·040	0·5[4])	0·42[5])	0·13[6])
550	0·035			0·05[6])
500	0·030			
450	0·025		0·32[5])	
400	0·020			0·02[7])
300	0·010			0·01[7])
200	0·005			0·005[7])
100	0·002			0·001[7])
20	0·0004			

[4]) A. Fry, Stahl und Eisen **43**, 1271-1279, 1923.

[5]) O. Eisenhout and E. Kaupp, Z. Elektrochem. **36**, 392-404, 1930.

[6]) D. Séférian, Etude de la formation des nitrures de fer par fusion et du systeme fer-azote. Paris, 1935.

[7]) W. Kôster, Arch. Eisenhüttenwes. **3**, 637-658, 1930.

$$C_{max} < \frac{0{\cdot}0004\, p_{NH_3}}{\sqrt{K_{NH_3}\, p_{H_2}^3}}, \quad .. \quad .. \quad (12)$$

where p_{NH_3} and p_{H_2} are the partial pressures of NH_3 and H_2 in the gas mixture of 1 atm, at which the maximum solubility is reached and the formation of Fe_4H begins.

Thus, we find the values given in column 2 of Table III for the upper limit of maximum solubility.

The values of maximum solubility found experimentally by various research workers do not by any means agree with each other, as may be seen from column 3 of this table. Remarkably enough, our calculated values correspond almost completely with Köster's experimental values[7]). Even the lowest values taken from literature are, therefore, probably to be regarded as an upper limit.

(To be continued.)

GERMANY

A Flow Meter for Gases and Liquids

By R. Bosselmann. (From *Die Technik*, Vol. 2, No. 12, December, 1947, pp. 551-552, 4 illustrations.)

Owing to the quadratic relationship between mass flow and pressure loss, the measuring range of Venturi-type meters is limited, because measuring errors increase as flow quantities decrease. At 25 per cent of the full mass flow, the pressure difference and, consequently, the force actuating the pointer mechanism are only 6·25 per cent, so that, therefore, the accuracy of measurement suffers considerably even at a point at some distance from zero.

This drawback was always in evidence at the power station of the Osram Company in Berlin, where steam generation was about 30 tons per day-shift in winter and only 4 to 7 tons per night-shift in summer.

To avoid a switch-over twice daily to different instruments, the instrument shown in Fig. 1 has been developed. It comprises a short Venturi-tube with measuring points p_1 and p_2. Inside the tube, a pear-shaped float is carried by two ball-bearing sleeves l_1 and l_2. The float is acted upon by the flow pressure as well as by the tension spring f and it will, therefore, maintain equilibrium between these two forces by changing its position, and, in consequence, the area of the annular flow passages will also vary. When the float is in the zero position, the tension spring is unloaded and the throat of the tube is closed. The other extreme position is shown by a dotted line in Fig. 1. The area of the passage resulting from this position, at maximum flow, is even smaller than that at the throat. Thus, there is only one increase and decrease in the flow-speed as is also the case with the usual type of Venturi tube.

Curve *a* in Fig. 2 shows the pressure distribution as measured at points p_1 and p_2, and curve *b* represents the actual total pressure loss in the Venturi-tube. The quadratic curve *c* and the straight line *d* show to what extent the goal aimed at has been achieved. It is an easy matter to transform curve *a* into curve *d*

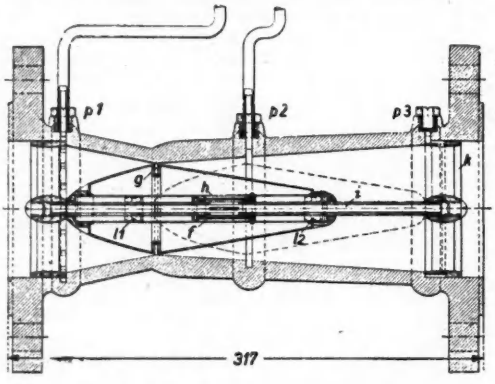

Fig. 1. **Cross-sectional view of modified Venturi tube.**

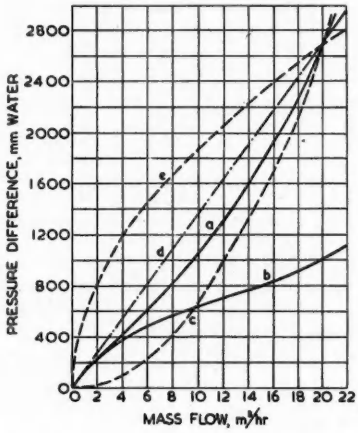

Fig. 2. **Mass flow as a function of the pressure difference.**

by the provision of two cams in the recording device.

When taking readings at the two stationary points p_1 and p_2, the pressure difference at full flow can only be obtained accurately if the pressure is at a minimum at point p_2. To enhance the accuracy of the device still further, readings should be taken at the maximum float diameter. For this purpose, the float, at its maximum diameter, was provided with a circular groove *g*, whence the pressure was transmitted through four slots *h* into the supporting tube *i*, and finally through the six guide vanes *k* to the measuring point p_3. The pressure curve *e*, obtained by taking the difference in readings at p_1 and p_3, lies above line *d*, and one third of the maximum pressure difference is already obtained at 10 per cent of the full mass flow (Fig. 2). This curve is symmetrical to the quadratic curve *c* (power $\frac{1}{2}$) with respect to line *d* and can be expressed by the formula $H = C\sqrt{Q}$, where H is the pressure difference in mm of water and Q the mass flow in m³/hr. C is a constant (in the present case $C = 597{\cdot}1$).

Two types of differential pressure transmitters used in conjunction with this modified Venturi-tube are also described and illustrated in the original paper. Both function without the use of mercury; one, suitable for gauge pressures up to 18 atmospheres, embodies metallic bellows with inset rings in the outer folds, and the other, for gauge pressures from 25 to about 130 atm, employs metallic plates distanced by thin sheet metal rings.

The use of this relatively cheap but important device is recommended even for small-scale boiler plant.

Design and Industrial Applications of the Shunt-Commutator Motor

By M. MELONE. (From *L'Elettrotecnica* Vol. 35, No. 4bis, April, 1948, pp. 166-182, 34 illustrations.)

(*Continued from October Issue.*)

4. THE CIRCLE DIAGRAM

In the circle diagram of Fig. 13 the horizontal component of the current vector represents the reactive current, and the vertical component is the active current. The circle is divided into two parts by the axis of the abscissae, the upper half representing the machine functioning as a motor and the lower half representing it functioning as a generator.

4. (a). *Asynchronous position of the Brushes.*
This corresponds to circle C_3 in Fig. 13. The motor then works in the same way as an ordinary asynchronous motor, the brushes being situated on the same commutator segment, so that the regulator winding is in short-circuit. Under no-load conditions, the current I_0 absorbed from the grid has a phase angle φ_0 with regard to the voltage vector; the small active component covers the mechanical losses of the machine, and the reactive component $I\mu$ serves for magnetizing the laminated circuit. The diagram is based upon the assumption of zero losses, so that only $I\mu$ need be considered. At zero load, slip is practically zero and the rotor rotates at nearly synchronous speed. With increased loads the current vector is shifted around the circle, and the vector I_{m3} corresponds to full load at point M_3. If the primary current is increased beyond this point, slip will increase until it is equal to unity or 100 per cent at point K, which is the short-circuit point at which the motor will stop. If the motor speed is increased above synchronous speed, slip becomes negative; the current vector shifts to the lower half of the circle, and the machine functions as a generator.

4. (b). *Brushes Adjusted to Positions Above and Below Synchronous Speed.*

Moving both brushes symmetrically away from the asynchronous position, the centre of the circle will be shifted upwards when the speed is increased, and downwards when speed is reduced. In Fig. 13, the circle C_5 corresponds to maximum speed, and circle C_1 to minimum rpm. At higher speeds there is an increase in the maximum torque and a decrease in the phase angle, so that the power factor will become nearly equal to unity, while the power factor and the maximum torque will decrease at reduced speeds.

4. (c). *Non-Symmetrical Displacement of the Brushes.*

When the brushes are both shifted in the same direction, the phase variation obtained will serve to improve the power factor at lower running speeds. For medium and high-power motors, this is achieved by displacing the brushes asymmetrically through an angle δ of, for instance, 10 electrical degrees (see Fig. 5d). The portion of the circle corresponding to super-synchronous conditions will then remain practically unchanged, while the portion for sub-synchronous speeds will be favourably altered. The geometrical locus is, thus, no longer a circle, but it has been found as a result of tests that the first part of the circle between I_0 and I_k can be used in practice for an indirect determination of the motor characteristics between $^1/_4$ load and full load.

5. SPEED REGULATION RATIO

In theory, the speed ranges on either side of the synchronous speed are equal, and are determined by

$$n_{min} = (1 - \beta)\, n_0 \qquad .. \qquad .. \qquad (9)$$

and

$$n_{max} = (1 + \beta)\, n_0 \qquad .. \qquad .. \qquad (10)$$

with

$$\beta = (k - 1)/(k + 1),$$

where k represents the regulation ratio between maximum and minimum speed. Actually, particularly as a result of the slip, the range of adjustment is shifted towards the lower speeds, although the total range is practically unchanged. Previously, motors with regulation ratios of 1 : 2 or 1 :3 were required, but in recent years the normal designs are for regulation ratios as high as 1 : 8, with corresponding increases in the size of the commutator, the number of brushes, and the overall dimensions of the machine.

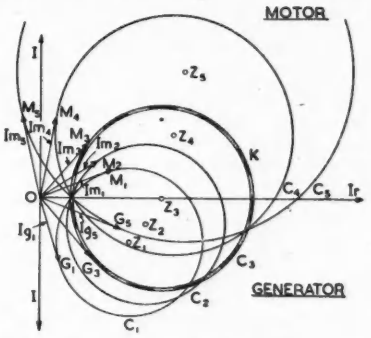

Fig. 13. Circle diagram for five brush positions.

If low motor speeds are only required over short periods for auxiliary operations, the motor can be designed with the effective normal regulating ratio, and a slip resistance is provided at the secondary, which will enable the minimum speed to be obtained, as in the case of a normal asynchronous motor, without resorting to the shunt characteristic for this auxiliary operation. If stability of speed is also required for auxiliary operation, the commutator motor can be designed for the full regulating ratio of, say, 1 : 50, this being, however, an expensive solution. Alternatively, it can be coupled rigidly to a normal auxiliary synchronous motor, with transmission gearing if required. In special cases, the commutator motor may be fed with a low frequency by means of a frequency changer. The most suitable solution, however, based on eq. (4), will be to alter the ratio of the turns of the regulator and the secondary winding. This principle is used in the Brown Boveri system (Italian Patent No. 327,321), shown in Fig. 14.

In this arrangement, the secondary winding (a six-phase winding in Fig. 14) is made up of two branches, $S_1' - S_6'$ and $S_1'' - S_6''$, with a phase angle γ. In the figure, the commutator is represented by two concentric circles, while the switches $U_1 - U_6$ are two-way switches mechanically combined into a single unit.

For normal functioning, the two branches of the winding are series-connected with the switches pointing in the counter-clockwise direction, so that for the first phase, for instance, the circuit will comprise switch a_1; paths S_1' and S_1'', and switch b_1. The brushes a_1, b_1 in the figure are shown phase-displaced by 120

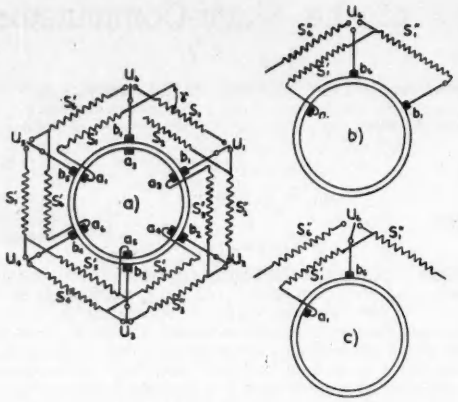

Fig. 14. **Secondary winding with series-parallel switches for extending regulation below the minimum position.**

degrees and are, therefore, near the minimum-speed position, since the remaining 60 degrees do not have much effect in further reducing the motor speed, as can be seen by referring to curve α of Fig. 11.

In the diagram, the conductor connecting S_1' and S_6'' has the same voltage as the brush b_6; by turning the switch U_6 in the clockwise direction, the portion S_1'' of the winding is cut out (Fig. 14*c*), and the circuit then consists of brush a_1, path S_1', and brush b_6, and this does not change the motor speed. This reduces the angle between the two brushes a_1 and b_6 to 60 electrical degrees, and any further brush displacement will result in a further decrease in speed. In any case, the reduction of the secondary turns will increase the current flowing through this circuit. The motor will then only be able to operate for slow-speed auxiliary processes at reduced load, or at normal loads for a short period, and the objective stated at the beginning of this section is thus achieved.

6. COMMUTATION

The value of the voltage per turn for which good commutation is obtained is determined experimentally. The commutation problem is complicated by the fact that in the commutating conductor there is not only the dynamic e.m.f. due to self-induction, but also a static e.m.f. known as the transformer voltage.

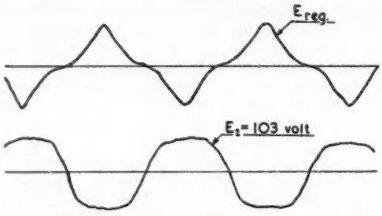

Fig. 15. **Oscillograms of transformer voltage of commutation, and of secondary voltage with motor stopped.**

The transformer voltage e_t is due to the stator field, and is independent of the rotor motion. It is determined by

$$e_t = 4{\cdot}44\, w f_a f\, \Phi \times 10^{-8} \quad .. \quad .. \quad (11)$$

where w = number of turns, f_a = winding factor, f = frequency, and Φ = flux. Measurements are made with the rotor stopped, and Fig. 15 shows the waveform of the transformer voltage between two consecutive laminations. The lower curve in this figure shows the voltage induced in the corresponding secondary winding. In the rotor-fed motor, the transformer voltage is induced at network frequency and is, therefore, independent of the rotor speed; in the stator-fed motor, it depends on the slip frequency. Both types of machines can be regarded as equivalent with regard to the transformer voltage considered within the normal regulating range, but behaviour during starting is different. In the motor-fed machine, the transformer voltage remains the maximum regulating voltage, even when the motor is stopped, whereas it becomes considerably higher in the stator-fed motor, so that the latter type is less favourable when frequent starting is necessary over fairly short periods.

The e.m.f. due to self-induction, generated as a result of the variation and reversal of the current in the turn, is proportional to the linear current density of the winding connected to the commutator, and is different for the two types of supply systems of the shunt-commutator motor. In the stator-fed motor, the commutation winding is dimensioned for the full power of the motor. In the rotor-fed motor the commutator is connected to the small regulating winding, which is designed only for the slip power, and the primary winding is entirely outside the commutation process. In the rotor-fed system, the e.m.f. of self-induction can be made even smaller, with a corresponding improvement in commutation, by increasing the number of phases of the secondary winding. Actually this amounts to increasing the number of brush-holders and decreasing the current, without, however, increasing the total cross-section of the brushes.

7. POWER PER POLE

In accordance with eq. (11), the flux per pole is determined by

$$\Phi = 10^{-8}\, e_t/(4{\cdot}44\, w f_a f) \quad .. \quad .. \quad (12)$$

For a pre-determined value of the voltage e_t at the laminations, and if $w = 1$ turn between two consecutive laminations, the flux Φ can therefore only be increased by decreasing the total winding factor f_a. This reduction, however, will not give values considerably below unity, for various reasons depending on the quality of the commutation. It follows that the limiting value for the flux will also limit the power per pole. This can reach approximately 15 kW for a regulating ratio of 1 : 2, and it is thus possible to construct a shunt-commutator motor with 12 poles delivering 180 kW at maximum speed. Further development work is in progress with a view to raising this limit, in order to produce motors running at higher speeds and at a lower cost for the same total power requirements.

7. (a). *Lap-type Regulator Winding with 2 Parallel Paths.*

This winding tends to increase the power per pole. For the same transformer voltage, with the lap-type winding with two paths in parallel ($a = 2p$) it should theoretically be possible to double the flux and, hence, the power output.

Specially designed systems are, however, required to maintain the quality of the commutation. Schrage, working with Brown Boveri, has solved the problem in a comparatively simple manner (see Italian Pat. No. 344,091) by employing two parallel circuits for the regulator winding (Figs. 16 and 17). In Fig. 16 the turn a of the regulator winding is connected to lamination 3 through two turns c and d of the auxiliary winding, which has a much smaller pitch, and which is also connected to laminations 1, 2 and 3. In the example considered, each turn of the auxiliary winding includes one-third of the pole pitch, while the turns of the main winding include the entire pole pitch; thus, the induced voltages are in the ratio of 1 : 2.

The auxiliary winding is connected to all the commutator bars. With the two windings arranged in this

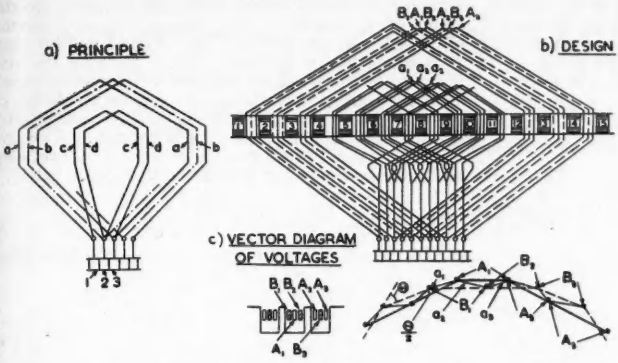

Fig. 16. **Two-path lap winding.**

manner, one turn of the main winding can be connected in parallel with two auxiliary turns which are series-connected. Thus, the function of the turns c and d is to divide in two the voltage of turn a. The circuit of the regulator winding under consideration is, therefore, not only connected to the commutator bars 1, 3, 5, etc., but also to the even-numbered ones 2, 4, 6, etc., via the auxiliary winding. The same reasoning applies to the other path of the regulator winding.

A typical example with two paths in parallel is that of Fig. 16b, with $n = a/p = 2$, $k = 3$, $Q = 12$, $\theta = 15°$, $y_r = 11$, $y_a = 4$, $f_{ar} = 0{\cdot}991$, $f_{aa} = 0{\cdot}5$, where n = number of parallel paths, k = number of commutator bars per slot; Q = number of slots per pole, y_r = pitch of regulator winding, y_a = pitch of auxiliary winding, f_{ar} = regulator winding factor, f_{aa} = auxiliary winding factor, p = number of pole pairs, θ = electrical angle of the slot.

The voltages are given in the diagram of Fig. 16c, with the angle θ drawn greater than 15° in order to increase the clarity of the diagram. In this figure, the voltages A_1, A_2, A_3, etc., are the series voltages of the circuit represented by solid lines, while B_1, B_2, B_3, etc., are those of the circuit shown by dotted lines. The finer lines joining the two polygons represent the voltages of the commutator bars in the same sequence.

Since the voltage per turn of the auxiliary winding must be equal to the voltage between two consecutive commutator bars a_1, a_2, etc., the pitch values of the winding must be chosen in such a way that, theoretically,

$$f_{ar}/f_{aa} = 2\cos(\theta/2) \quad .. \quad .. \quad (14)$$

and this condition is satisfied in the example given: $0{\cdot}991/0{\cdot}5 = 2\cos(15°/2) = 2 \times 0{\cdot}991$.

7. (b). *Lap Winding with Three or More Parallel Paths.*

In order to increase the flux per pole and consequently the power output, the regulating winding can be designed with three or more parallel paths (Italian Patent No. 399,362) along the lines already described. Fig. 17 gives an example of a winding of this type, with $n = a/p = 3$, $k = 2$, $Q = 15$, $\theta = 12°$, $y_r = 11$, $y_a = 3$, $f_{ar} = 0{\cdot}912$, $f_{aa} = 0{\cdot}309$, the three parallel circuits being denoted by the letters A, B, and C. The voltage diagram is given in Fig. 17b, in which a_1, a_2, etc., are the voltages of the corresponding turns of the auxiliary winding.

The pitch values of the windings in the above example must be so chosen that the ratio between the winding factors will be

$$f_{ar}/f_{aa} = 1 + 2\cos\theta \quad .. \quad .. \quad (14)$$

this condition being fulfilled in the case considered, since $0{\cdot}914/0{\cdot}309 = 1 + 2\cos 12° = 1 + 2 \times 0{\cdot}978 = 2{\cdot}956$.

The auxiliary winding is in parallel with the regulating winding, and the secondary current, therefore, flows through it, so that its turns, although small, should be regarded as active conductors. This winding, besides serving to divide the voltage, may also have the effect of indirectly improving the commutation, by damping the harmonics which nearly always exist in the induced voltage of the regulator winding.

The use of the multiple-path lap windings enables the voltage per pole to be raised to about 35 kW for a regulation ratio of 1 : 2, and with 14 poles the power output is, therefore, approximately 500 kW. Above this power, and where the limits of the speed control range are not too wide, the normal asynchronous motor can be used in conjunction with a regulator group, for instance, a Scherbius motor.

8. CONSTRUCTIONAL FEATURES

For a rational magnetic utilization of the rotor, the rotor assembly can be designed as shown in Fig. 18. Most of the space is taken up by the primary winding

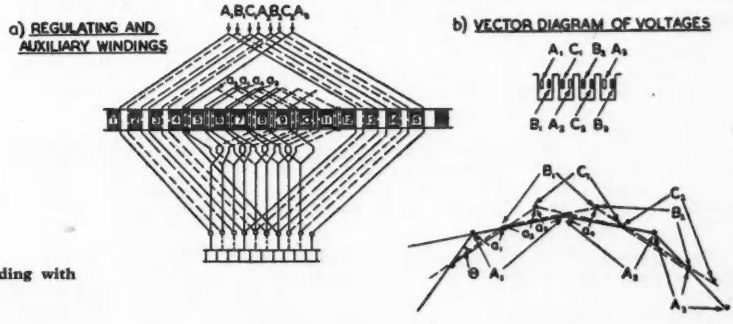

Fig. 17. **Lap-type regulator winding with three parallel paths.**

P connected to the supply network, and above the primary is the second rotor winding, which is the regulator winding R. In the figure the stator with the corresponding secondary winding S is also shown; this does not differ from a normal winding for a polyphase alternating current.

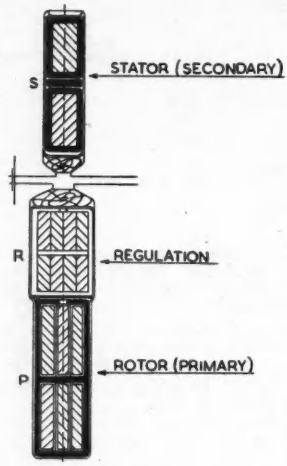

Fig. 18. **Rotor and stator design of a commutator motor.**

8. (a). *Brush Control.*

The brush carriers are adjustable in opposite directions. For small motors, and also for medium-power motors which have to rotate optionally in both directions, the brush displacement is symmetrical, the two brush-carriers being controlled by a control shaft and a counter-shaft, so that they are shifted symmetrically away from the common position. Minimum speed is obtained with zero shift, and maximum speed with a 180 degree shift to position K. For symmetrical displacement, the gearwheels Z_1 and Z_2 in Fig. 19 have the same number of teeth, while gearwheels with slightly different numbers of teeth are used for asymmetrical displacement in compensated medium or high-power machines. In this case, the two brush-carriers are displaced through different angles, and the direction of rotation of the motor must remain unchanged.

Generally, the asymmetrical control is obtained by displacing the brush-carrying arms in the opposite direction to the direction of rotation of the motor, through an angle δ equal to approximately 10 electrical degrees, as shown in Fig. 19. When the brushes are shifted, the angle δ decreases, until it becomes zero in the maximum speed position. In this case it is also possible to reverse the direction of rotation of the motor, because when the two phases of the supply are changed, the number of teeth of the corresponding gearwheels is reversed as well.

For rapid reversal of the direction of rotation with the motor stopped, a simple reversing arrangement is used, consisting of a pair of gearwheels Z_1 and Z_2 mounted on the control shaft and counter-shaft, respectively, the change of direction being obtained by reversing the gear ratio. With this arrangement the compensated motor is not fully reversible as when the system is arranged for symmetrical displacement.

8. (b). *Electrical Brush Control.*

The brush adjustment is electrically controlled by means of a small 30-watt motor with a very high starting torque. This motor is rigidly coupled to a reduction gear with a high step-down ratio, which is built integral with the motor, the entire unit being mounted on the casing of the machine. The change from one extreme brush position to the other is achieved in less than 40 seconds. A stop switch, when reaching the end position, automatically disconnects the small motor from the supply network and also blocks the switch of the main motor, so that stopping is only possible with the brushes in the minimum-speed position. A remote control system for starting, accelerating, decelerating and stopping the motor can also be arranged.

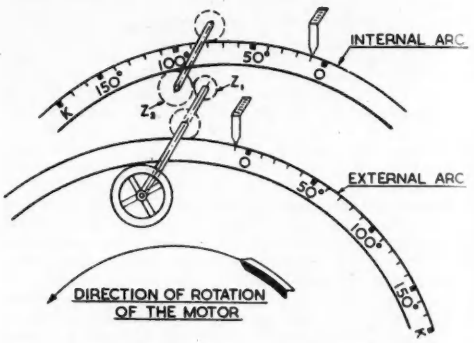

Fig. 19. **Brush control for asymetrical displacement.**

8. (c). *Utilization.*

The machine is generally designed as a protected type, and is available with automatic cooling and ventilation ducts, or as a flame-proof motor. It can be used for the operation of textile, paper, spinning, and cable-making machines, oil well boring and extracting machines, lathes, rotary furnaces and various types of machine tools. Although the shunt-commutator motor has been primarily designed to provide mechanical power, it can also be utilized because of its internal electrical characteristics and can act as a frequency and voltage converter.

BIBLIOGRAPHY

SCHRAGE, H. K.: A new three-phase commutator motor with shunt control obtained by brush displacement. "*E.T.Z.*", 1914, p. 89.
PARIS, M.: The rotor-fed three-phase shunt-commutator machine. "*L'Elettrotecnica*," 1934, p. 186.
TEDESCHI, F.: Three-phase commutator motor with adjustable speed and shunt characteristic. "*Rivista Marelli*," 1933, p. 83.
VANNOTTI, R.: The Schrage-Brown-Boveri three-phase shunt-commutator system. "*Rassegna Tecnica TIBB*," 1936, p. 3.
NÜRNBERG, W.: Stator and rotor-fed three-phase shunt-type motors with current converters. "*E.T.Z.*", 1941, p. 817.
FOCACCIA, B.: Applicazionie elettriche. (Electrical applications). Vallardi, Publishers, Milan.
ARNOLD, A.: The circle diagram of the three-phase shunt-commutator motor. "*J. Inst. El. Engrs*," London, 1926, p. 1139.
SAWALISCHIN, K.: Experimental and theoretical circle diagrams of polyphase commutator machines. General converter designs. "*E. u. M.*", 1931, p. 101.
SCHOMBOURGER: Diagram of the polyphase commutator motor with a shunt characteristic and speed control by brush displacement. "*Rev. Gén. Electricité*," 1932, p. 639.
STIX. The operating diagram of the rotor-fed three-phase commutator motor. "*Archiv f. El.*", 1938, p. 187.
SCHACKNIELSEN: The circle diagram of the rotor-fed three-phase commutator motor, "*Archiv für El.*," 1938, p. 187.
BRABEC: Current diagram and study of the electromagnetic torque of the rotor-fed three-phase commutator motor with shunt characteristic. "*Rev. Gén. El.*", 1938, p. 291.
SCHRAGE, H. K.: Multiple-path lap windings for three-phase commutator machines. "*Bull. S.E.V.*", 1943, p. 138.
MELONE, M.: Flame-proof electrical machines. "*L'Elettrotecnica*," 1945, p. 137.
PUVANO, A.: The control of oil well boring machines by means of shunt-commutator motors. "*Rassegna Tecn. TIBB.*", 1938, p. 30.
HARZ, H.: Asynchronous single-armature converters. (Schrage motor used as voltage and frequency converter). "*E.u.M.*", 1943, p. 191.

DESIGN AND WORKSHOP

A Digest of articles of interest to Works Managers, Planning and Production Engineers, Superintendents, Jig and Tool Designers, Inspectors, Time Study Engineers, and all those concerned with the practical aspects of Engineering.

Hot-Pressing and Hot-Forging Light Alloys

By M. CHARTRON. (From *Revue de l'Aluminium, France*, Vol. 25, Nos. 141 and 143, pp. 37-43, and 113-122, 27 illustrations).

(*Concluded from October issue*).

E. Use of Mechanical Presses

Mechanical presses are also used for die pressing and usually are quickly and easily handled. The flywheel energy is imparted fully, or in part, to the pressing, according to the resistance of the material. The pressures can, therefore, be very high indeed, and although safety measures are provided in the machine, it is not normally possible to utilize these presses to full capacity for continuous service. They are, therefore, best when used for the series production of small and medium forgings. Mechanical presses are fed either with rough-forged pieces or with disks cut from bars of convenient length and cross-section. Rough pre-forged pieces can be given a metal flow structure which will impart to the finished piece the optimum physical properties. Complete forging of simple pieces in one heat and one die is also possible, and with carefully chosen tool arrangements, it is more economical, although the amount of material used is slightly greater and the die is occupied for a longer time, since pre-forging in it requires a repetition of comparatively light blows.

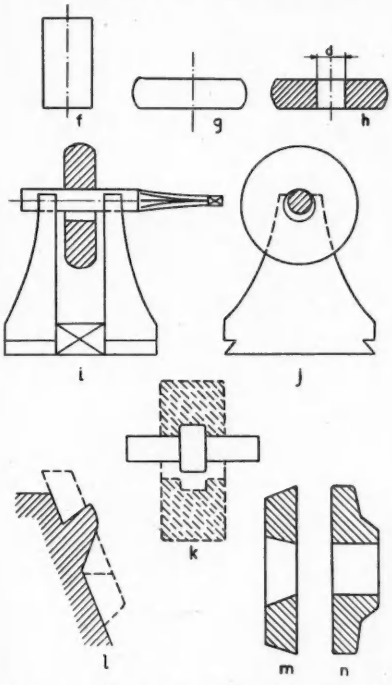

Fig 7. **Stages of forging a ring on trestle and anvil beak.** *f* = billet cut from bar, *g* = pre-forged disk, *h* = pierced disk, *i*, *j* = forging of ring by rotating on trestle, *k* = recessing of bore on mandril, *l* = flaring of hole on anvil beak, *m*, *n* = forms which can be forged on anvil beak.

V. PRACTICAL EXAMPLES

A. Disks

Disks are forged by flattening pieces cut from bar. If the height of the pieces before forging is more than three times the diameter, there is a risk of buckling and

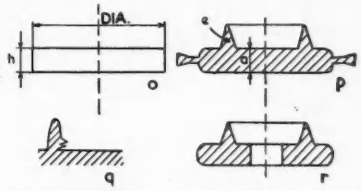

Fig. 8. **Drop forging of disk with single annular projection.** *o* = pre-forged disk, *p* = drop forging. If thickness *a* is still too large, *e* must be machined down before further drop forging, so that excess metal can flow into remaining cavity. Otherwise, cracks result as at *q*. With drop forging *r*, excess metal may be made to flow into bore cavity.

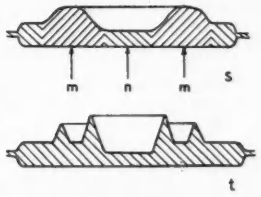

Fig. 9. **Drop forging with two annular projections.** *S* = disk pre-forged between dies. Volumes *m* and *n* must be very accurately determined and produced. *t* = finished drop forging.

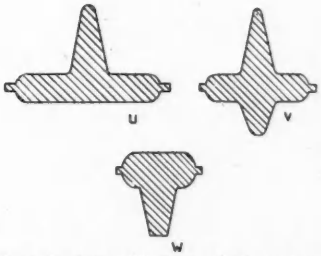

Fig. 10. **Drop forgings with large displacement of metal.**

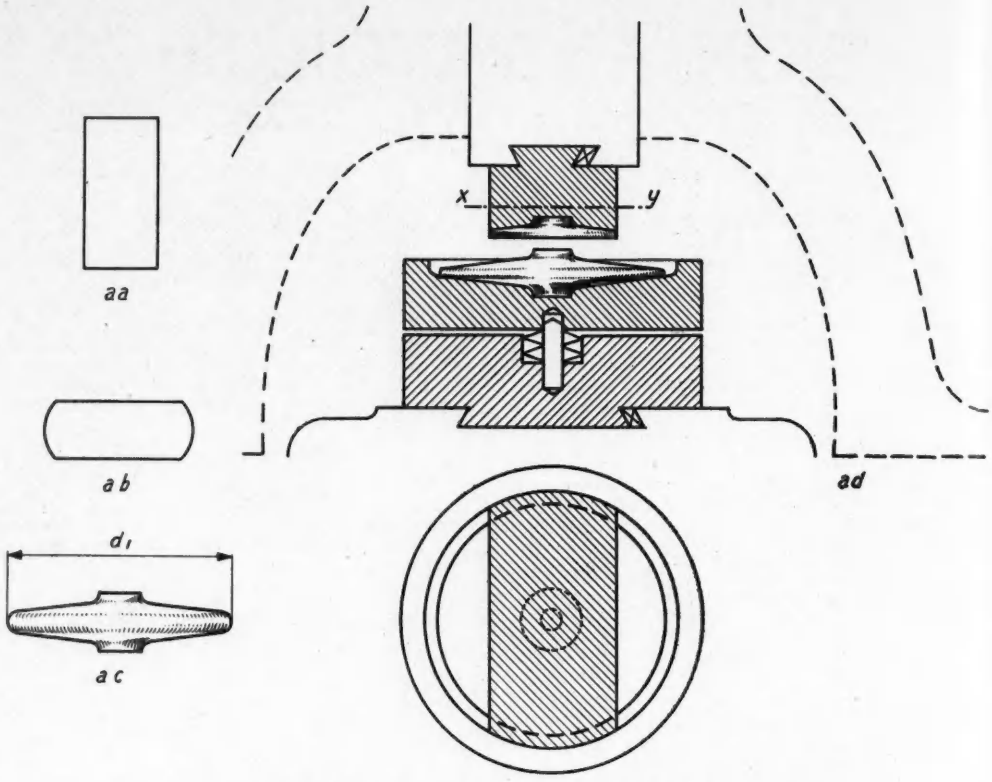

Fig. 11. **Hammer forging of disks of large diameter using "rotating anvil."**

wrinkles appear in the finished disk. Disks of aluminium or Almasil are best forged in a press, but duralumin bars cannot be deformed beyond a certain limit because cracks would then appear at the circumference of the disk. After a certain compression, the disks should be lightly forged from several sides so that their cylindrical form is changed. They can then be finished but this is very expensive on a press and is not so difficult for a forge hammer.

B. Rings. See Fig. 7.

C. Ribbed Disks. See Figs. 8 and 9.

D. Forgings with Heavy Bosses. (Fig. 10.)

These are generally forged under the power hammer. Arrangements of dies should obtain results like those shown in Fig. 10u and v, with the boss projecting upwards, because such arrangements are less difficult to forge. In a press material does not flow as easily, and not upwards, so that press forgings must be made with the bosses like that shown by the example in Fig. 10w.

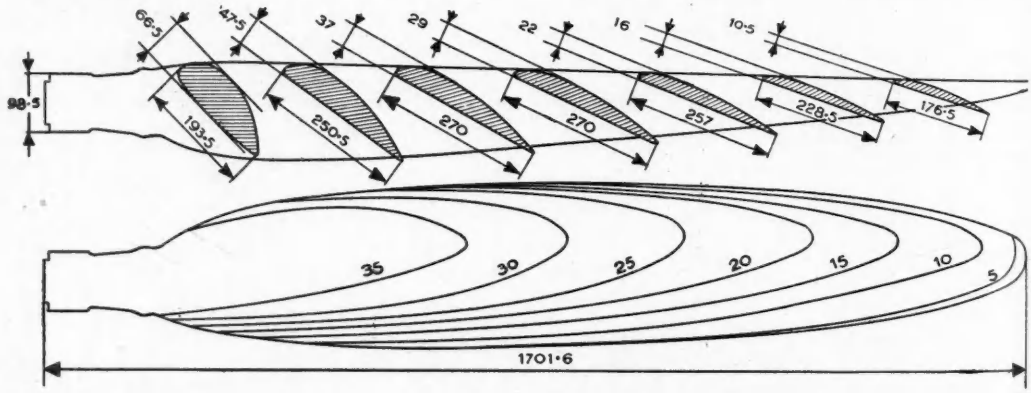

Fig. 12. **Lines of constant thickness of an airscrew blade.** (Blade twist developed into plane of paper; dimensions in mm).

E. Large Disks. (Fig. 11.)

Most presses or hammers are not powerful enough simultaneously to forge the whole of a disk surface. The billet (Fig. 11, aa) is, therefore, pre-forged into as large a disk as possible by using available hammers (Fig. 11, ac) and then finished by drop-forging on a "rotatable anvil" (Fig. 11, ad). The lower die is machined to support the whole of the disk and is rotatable about a centre pin, in a supporting block, from which it is lifted a little, when not under forging pressure, by Belleville spring washers. The upper die is reduced in width and strikes only a part of the disk at every hammer blow. As the lower die is slowly rotated through 180 degrees, the upper die progressively works on the whole surface of the disk.

F. Airscrew Blades. (Fig. 12.)

(1) *Hot Die Pressing*

The bar is first rough-forged, or rolled, and checked for cracks or other faults, which must be eliminated before pressing. The shape of the billet is designed so that the flash of the finished pressing shall be as thin as possible. The press has three hydraulic cylinders, each able to exert a force of 5,000 tons. The billet is heated to 480° C, placed in the lower die, which has been gas heated to 350° C, and compressed by one cylinder until the dies are $\frac{13}{16}$-in apart. The other two cylinders then continue the compression until a flash of $\frac{3}{8}$-in thickness has formed. The pressure is then released, the upper die lifted, and the dies are lubricated before the full force of the three cylinders is applied to the workpiece until it has deformed to the maximum possible extent. The flash is then $\frac{1}{16}$-in thick and a machining allowance of 0·08 to 0·10-in is left all round. The total time taken for this pressing is 65 seconds.

If the developed blade (Fig. 12) is subdivided into sections of constant thickness and the theoretical pressure on each section is calculated from the ratio of surface area to thickness, the pressure required for die pressing can be compared with Tresca's theoretical pressure for pressing between flat surfaces. In this particular case the theoretical pressure was 5,100 tons, or 8·2 tons per sq in of the pressing surface, whilst the actual die pressure was 15,000 tons or 23·8 tons per sq in. Similar tests and calculations have established the maximum pressures required for duralumin hot die pressings as follows :—

(a) About 20 tsi for flat die pressings with gates allowing an easy outlet for flash material ;

(b) 25 to 30 tsi for dies having wide and shallow flash gates, or causing heavy displacement of metal between the dies ;

(c) 40 tsi for die pressings with acute external angles;

(d) over 65 tsi for die pressings with heavy projections or deep recesses (e.g. pistons for aircraft engines).

(2) *Drop Forging Under Double-Acting Power Hammer*

Under a 12-ton double-acting power hammer, a pre-forged blade could be drop-forged in two heats, and in a total time of 65 seconds. In tests under a 17-ton hammer, drop forging was carried out in one heat with 16 hammer blows in a total time of 40 seconds. Machining allowances and flash thickness were the same as for the die pressing. During final tests under the 17-ton hammer, with specially polished dies, the flash was forged down to 0·16-in by 5 blows and to 0·14-in by another 8 blows. The final machining allowance was thus reduced by 0·02-in. In these tests, the forging temperature was 300° C, the dies were kept at only 80° C, and the flash was not trimmed in the same heat. Despite unfavourable temperature conditions, the 17-ton double-acting power hammer is thus able to drop-forge the blade in a shorter time and to closer finish dimensions than the 15,000-ton press can die-press the blade.

VI. CONCLUSIONS

Hydraulic presses are best for the forging of compact blocks where the necessary pressure per unit of surface area is fairly small. Medium-size presses can compress blocks of appreciable size ; larger presses can reduce forging time and the number of re-heats, and operations are shock-free. However, as the ingot spreads under compression and its height is reduced, the ratio D/h increases, the piece cools more rapidly, and the pressure required is correspondingly increased. Even large presses are, thus, soon limited by the dimensions of the pieces they can handle, although circumstances are even worse for die pressing. Whilst large presses are superseding giant power hammers, medium-sized power hammers are still superior for pre-forging, drop-forging to close dimensions, the economic forging of medium and small pieces, and for forgings with heavy projections when requiring large metal displacements in the die. Where a press cannot overcome the resistance to deformation of a workpiece, a hammer will be able to produce a slight deformation, and the total deformation theoretically obtainable depends on the number of hammer blows which the metal receives.

Follow-on Die with Separating Punch

By M. DAVID. (From *Werkstatt und Betrieb, Germany*, Vol. 81, No. 7, July, 1948, p. 196, 1 illustration).

WITH the usual type of follow-on dies containing a piercing punch, blanking punch and stop-pin, the strip must, after each stroke, be lifted over the stop-pin, and again positioned against the stop-pin from the back. This handling takes unnecessary time and correct positioning is not ensured, since thin sheets tend to bend and slip too far over the stop-pin, thus causing waste of material. Thick sheet may lift against the stop-pin, so that it does not lie flat on the die plate, thus leading to punch breakage. Side punches may eliminate the disadvantages referred to above, but require more material by punching out location strips at the side.

Another possibility of surmounting these disadvantages is afforded by the addition of a separating punch *a*, Fig. 1, which, with each stroke, cuts the neck of material between the blanks and opens a path for the stop-pin without the necessity of lifting the strip. The strip can then be pushed directly forward until the neck just formed by the blanking punch lies against the stop-pin. The advantages of this arrangement are obvious. The stop-pin is best arranged in the top plate in order to reduce the danger of cracking of the die plate during quench-hardening. The strip need not be lifted, and, therefore, the head space for the strip can be lower and the punch supports longer.

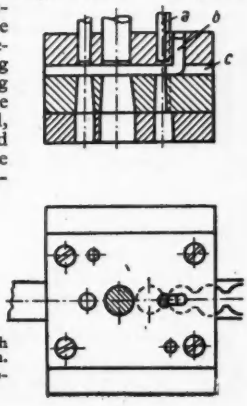

Fig. 1. **Follow-on die with additional separating punch.** *a* = Separating punch, *b* = stop-pin, *c* = strip guides.

The Practical Heat Treatment of High Speed Steel Cutting Tools

By W. E. BANCROFT and W. W. WIGHT. (From *Metal Progress, U.S.A.*, April, 1948, pp. 545-555, 11 illustrations.)

IN the last ten years a great many facts regarding the behaviour of high speed steel have been revealed by scientific investigation and research. Definite guiding principles and charts are now available which serve as a basis for designing heat treatments to produce any combination of properties within the physical limitations of high speed toolsteel.

For the purpose of this discussion, we list the six phases of heat treatment which can and should be controlled by the heat treater in order to obtain desired results consistently:

1. Austenitizing conditions—temperature and time at heat.
2. Rate of heating and cooling.
3. Temperature to which work is quenched before tempering.
4. Tempering.
5. Controlled use of isothermal transformation.
6. Surface condition.

The primary objective in hardening high speed steel tools is to develop the best possible combination of (a) hardness and wear resistance at room temperature; (b) resistance to softening at elevated temperature—that is, "hot hardness"—and (c) toughness, or resistance to shock without appreciable plastic deformation.

AUSTENITIZING CONDITIONS

It is well understood that, in general, high temperatures and long times will promote solution of carbides in the austenite, and enlarge the austenitic grains with consequent brittleness, and (on the other hand), that low temperatures and short times will produce fine grain and toughness, with low carbide solution and consequent low secondary hardness and low hot hardness.

Up to a certain temperature, holding time has little effect on grain size. There is, however, for each grade of high speed steel, a transition temperature above which grain size increases rapidly with any amount of holding time, as is shown in Fig. 1. Toolsteel manufacturers recommend austenitizing temperatures or temperature ranges for each grade they make. These recommended temperatures are intended to be safe, without causing excessive brittleness even with a little soaking time, and yet yield a reasonable amount of carbide solution and hot hardness. For general-purpose hardening, then, these recommended temperatures are the ones which should be used, provided they are properly defined and properly interpreted.

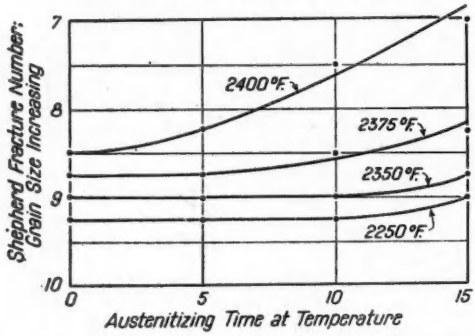

Fig. 1. **Austenitic grain size is relatively unaffected by time at heat until definite temperature is exceeded. (About 2375° F for this typical 18-4-1 steel.)**

It is important for the heat treater to ascertain what heating conditions are the basis for any given recommendation and make proper temperature correction for the type of equipment he is going to use.

The only general rule we know is that salt baths should be operated from 25 to 50° F lower than furnaces with a reducing-gas atmosphere, and furnaces with nearly neutral atmospheres should be operated about midway between these two extremes, in order to develop the same degree of carbide solution.

It is occasionally desirable to heat either higher or lower than normal in order to meet special requirements. Heavy-duty lathe and planer tools are one example of tools which may be deliberately overheated to get greater carbide solution and greater hardness—although with a considerable reduction in toughness. Lower than normal temperatures are recommended for delicate tools which are most apt to fail by breakage and which do not require the maximum of wear resistance. A low quenching temperature is the most effective means of producing maximum toughness without lowering the hardness below normal cutting levels.

None of the more or less standardized methods are satisfactory for evaluating toughness in parts hardened to cutting hardness which will break in a brittle manner. We believe that the most sensible way of measuring toughness in such parts is to see how much of a blow they will stand before breaking. Therefore, for our own testing work we have constructed a machine similar to the pendulum impact machines but designed to determine the maximum blow that a specimen will withstand before breaking. Essentially it consists of a pendulum with variable attached weights, a vice for holding the specimen and a quadrant scale graduated in centimetres of height.

In operation, the pendulum is drawn back to successively greater heights and allowed to fall against the specimen until it breaks. The shock resistance is then taken as the product of the height of the final blow and the weight, and is expressed in centimetre-grams (cm-g). It seems as though this procedure is more representative of service conditions and probably somewhat more sensitive than the standard impact test procedures.

The shock resistance obtained with this machine on a group of specimens quenched from temperatures between 2250 and 2350° F is shown in Fig. 2. In this experiment the tempering treatments were varied so as to produce a uniform hardness of Rockwell C-61 to 63, regardless of quenching temperature.

RATE OF HEATING AND COOLING

Having established the correct austenitizing conditions to use for a given job we may next consider the

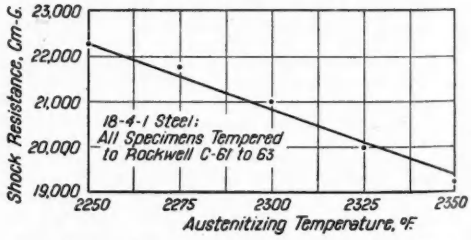

Fig. 2. **High speed steel of C-61 to 63 hardness is tougher as the austenitizing (quenching) temperature is lower. Note, though, that this is at the expense of wear resistance and hot hardness.**

most suitable methods of heating to that temperature and cooling from it. To a certain extent, of course, this may depend on the equipment available and on the type of work being hardened, but it seems probable that most tool rooms today are equipped with facilities for preheating and for hot quenching in a liquid bath at 1000 to 1200° F, as well as for oil quenching.

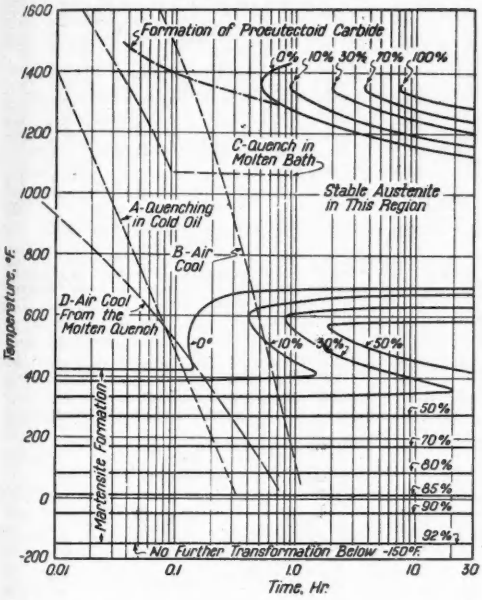

Fig. 3. **Transformation-time-temperature curves for 18-4-1 steel austenitized at 2350° F.**

In the commercial hardening of miscellaneous high speed steel tools, preheating either in one or two stages is desirable, first, because it reduces thermal shock which might cause distortion or cracking; second, because it helps to equalize the time at which both thin and thick sections reach the hardening temperature; and, in the third place, because it reduces the over-all time in the high-heat furnace, thus reducing the opportunity for surface changes and speeding up the whole hardening cycle.

Some operators prefer two pre-heating baths or furnaces, one at about 1200° F and the other at about 1500 to 1600° F, while others feel that one of large capacity operating at about 1550° F is adequate. Our own practice is to use two preheating salt baths which together have about four times the capacity of the high-heat bath. Both preheaters are operated at 1550° F for most work and, since we find that it takes about four times as long to bring a load of work up to 1550° F as it does to raise it from there on to the quenching temperature, we are able to maintain a steady flow of production without interruption between high-heat cycles. One precaution which should be mentioned is that, if the preheat temperature is too high (over about 1500° F) for some grades of high speed steel, it alone may cause a slight increase in grain size in the final condition.

The behaviour of high speed steel during cooling from the high-heat temperature is charted in the time-temperature-transformation curve (the "T.T.T." diagram) shown in Fig. 5. From this we learn these essential facts:

1. If small tools of high speed steel are quenched from the high heat into oil at room temperature (the approximate cooling curve *A* being as plotted in Fig. 3), all high-temperature reactions are by-passed and the transformation from austenite to martensite proceeds while cooling below about 450° F—exactly the same as in an ordinary alloy toolsteel during an oil quench. Of course, the comparatively rapid cooling in oil will cause non-uniform rates of transformation throughout the mass, and residual stresses will be set up which may or may not prove detrimental, depending on the shape and size of the tool.

2. If parts are cooled in still air all the way from the austenitizing temperature to room temperature (line *B* in Fig. 3) fairly high hardness may be expected in the as-cooled piece, since high-temperature transformation of austenite to softer products is very slow to start, and virtually all of the austenite will transform below 700° F, forming either bainite or martensite, both of which have high Rockwell hardness. However, air cooling of anything but very small, thin sections, which will cool rapidly, will permit some precipitation of carbides at temperatures above about 1300° F. This depletion of carbide from the solid solution, results in lower secondary hardness after the high draws, lower wear resistance, and lower hot hardness. Therefore, it is not desirable, in practice, to air cool anything but fairly thin sections.

3. Quenching from the high temperature in a molten bath between 1000 and 1200° F has several advantages: First, as shown by line *C* in Fig. 3, it cools the work through the high-temperature zones fast enough to prevent carbide precipitation; then, it equalizes the temperature throughout each portion in a temperature range where transformation to martensite does not occur and, if salt baths are used, it removes or dilutes the salt from the high-temperature bath which might be difficult to remove if allowed to solidify on the work.

4. Cooling in air from the hot quench to room temperature (curve *D* in Fig. 3) allows the austenite to transform slowly and uniformly throughout the mass while the piece is cooling below about 450° F.

5. Finally, the T.T.T. curve shows that, after cooling to room temperature by any method, some 15 per cent of the original austenite remains untransformed. This knowledge is of value in understanding the reactions during further cooling to subatmospheric temperatures (and also during conventional tempering operations).

For these various reasons the now commonly accepted practice of quenching in a hot bath and then air cooling to room temperature is considered sound and desirable from both a practical and theoretical standpoint. If salt baths are used for the quenching medium, some precautions will have to be taken to prevent its melting point from rising, as it is contaminated with high-heat salt carried over by the hot work. The bath should be held under 1200° F at all times—1100 to 1150° F being a practical working range. If lead baths are used to quench work out of an atmosphere furnace, maintenance of fluidity is no problem, and a working temperature of 1000 to 1100° F. is the general practice.

RELATIVE ADVANTAGES OF COOLING TO ROOM AND TO SUBZERO TEMPERATURES

The next of our factors which should be controlled is the temperature to which work is cooled before tempering. While by far the majority of high speed steel cutting tools are quenched to room temperature before tempering, there may be occasions where it is felt desirable either to interrupt the quench at some elevated temperature and temper immediately, or to continue cooling to far below zero. The first of these methods is utilized for those comparatively rare jobs where continuous cooling to room temperature may cause quench cracks.

The only facts which seem to be clearly established about subzero treatments are that if normally austenitized high speed steel of conventional composition is quenched continuously to — 100° F or lower, the transformation of austenite to martensite will continue until only about half as much austenite remains untransformed as would have been left had the cooling been stopped at room temperature. The horizontal lines in Fig. 3 representing martensite transformation illustrate this point — about 85 per cent is transformed upon reaching 70° F; only 92 per cent at — 150° F. Also it is known that if the cooling is interrupted at or near room temperature for any appreciable time, or if the steel is tempered before the subzero treatment, the austenite will have become so stabilized that no further transformation will occur during cooling to subzero temperatures.

Thus, it appears that the only way in which a subzero treatment is likely to be of benefit in normal hardening would be as a continuous extension of the quenching cycle. Even so, the refrigeration does not eliminate the necessity for double tempering at the usual high temperatures, and the physical properties obtained in the final condition seem to be no better than those after conventional quenching and tempering.

It has been suggested that a subzero treatment might improve the performance of tools which had been improperly heat treated—as, for instance, by undertempering, overtempering, overheating, or by arrested quenching above room temperature. However, in the authors' experience, many carefully conducted field tests of actual high speed steel cutting tools given a subzero treatment, either before or after tempering, or both, have failed to show any measurable superiority over others hardened by a normal quenching and tempering process.

The tempering operation is an essential and highly critical part of the complete hardening procedure. It is here that the final hardness, strength, toughness, and stability of the tool are produced (disregarding for the moment the effect of surface treatments).

Since the structure of as-quenched high speed consists of undissolved carbides, untransformed austenite, and untempered martensite, it is inherently weak, brittle, and unstable. In order to improve these conditions, the tempering operation should complete the transformation of the austenite as well as get all increments of the martensite in as well tempered and stress relieved a condition as possible, without lowering the hardness below a satisfactory level for cutting and wear resistance. There is, at present, considerable authentic information on the mechanism of tempering which serves to explain how this can best be accomplished. Without going into lengthy theoretical detail the essential things which the heat treater should understand are somewhat as follows:

1. The first tempering cycle, consisting of heating to a preselected temperature and holding for a definite time, tempers and stress relieves the original martensite and " conditions " the retained austenite so that most of it will transform.

2. The tempering and stress relieving of this original martensite is accomplished while heating to and holding at the tempering temperature.

3. Holding at the tempering temperature " conditions " the austenite so that most of it will transform to new martensite on continuous cooling to room temperature.

4. This formation of new martensite is accompanied by a volume change, and new internal stresses are set up which should be relieved by a second tempering cycle.

5. In order to bring about the complete transformation of all austenite present during the first tempering cycle, a definite minimum holding time at temperature is required, depending on the type of steel and the temperature used. Therefore, all initial tempering treatments should be regarded as time-temperature combinations. The lower the temperature, the longer time required. This is well shown in Fig. 4.

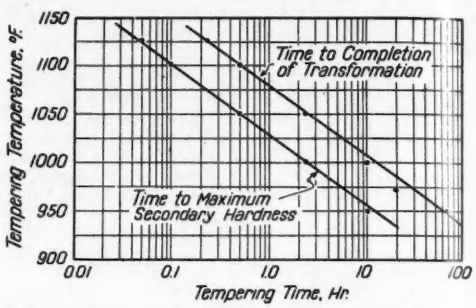

Fig. 4. **Tempering of high speed steel (averages for 18-4-1, 18-4-2, W-Mo and Mo-W types) is a time-temperature operation—low tempers require long times; high tempers need shorter times.**

6. The second tempering cycle is intended only to temper and stress relieve the martensite formed on cooling from the immediately preceding tempering operation, and is not so time-dependent as the first. The temperature should be about the same as the first cycle but 1 hour should be sufficient.

7. Since all high speed steels, when normally austenitized, exhibit the characteristic known as secondary hardening upon tempering, the heat treater has the choice of tempering so as to produce maximum secondary hardness, or a lesser degree, by tempering either under or over the temperature for maximum hardness.

8. If the steel is drawn at a temperature *under* that required for maximum hardness, the austenite will not completely transform upon cooling from any commercially feasible holding time, so that the steel will remain in an unstable microstructural condition due to the retained austenite. On the other hand, the toughness or shock resistance of such a piece may be high, so that there are occasions when this practice may be desirable.

9. If the tempering is done at temperatures *above* that required for maximum hardness, the austenite transformation will be practically complete in a short time and structural stability thus ensured, but hardness, strength, and toughness will all be lower than the optimum. Many believe that toughness or shock resistance is increased by overtempering, but careful study of all physical test data available fails to show any improvement in toughness until tempering temperatures over 1200° F have been reached, whereupon the hardness has been so lowered that good cutting properties have been lost. From Fig. 5 it can be seen that all three mechanical properties decrease along with hardness when the high speed is tempered at temperatures above that which produces maximum secondary hardness.

The effect of tempering temperature on the shock resistance, as measured by the authors' pendulum machine, is also shown in Fig. 6, and leads to the same conclusion.

10. For the reasons already given, double tempering is adequate, providing the first holding cycle is sufficient to cause complete transformation of the residual austenite. If, however, for any reason the first cycle is cut short, there will be some austenite left which will not transform during the second cycle, so that a third tempering cycle becomes necessary. As already mentioned, whenever quenching is arrested above room temperature, abnormal amounts of austenite are retained, and it has been shown that the first tempering cycle, no

matter how long its duration, will never completely transform all of this austenite. Under these conditions, three tempering cycles are always necessary.

11. It should be borne in mind that tempering time is always cumulative with respect to the " conditioning " of austenite. For example, four 1-hr draws will result in the same amount of transformation as one 4-hr draw at a given temperature. However, cycles should be so arranged that after the austenite transformation has been completed one more draw will be applied for stress relief.

ISOTHERMAL TREATMENT

Most of the commercial hardening cycles are designed to avoid as far as possible the transformation products which form above 400° F. The desired structure after quenching is martensite with the inevitable retained austenite; undesired are proeutectoid carbide, fine pearlite (primary troostite), and bainite. However, the isothermal transformation of austenite to bainite, in a manner comparable to the " austempering " process commercially applied to carbon and low-alloy steels, has been studied by several investigators.

The T.T.T. curves for high speed steel, Fig. 3, indicate that no transformation takes place upon holding for any reasonable time between 1150 and 700° F—even up to 30 hours in the interval between 1100 and 700° F. However, in the range between 600 and 400° F a transformation starts in a comparatively short time (8 min). Near 600° F this transformation goes to 50 per cent of completion in a little less than 2 hr; "primary bainite " is the transformation product. The austenite remaining becomes stabilized and little further transformation occurs either by continued holding or upon cooling to room temperature (an experimental fact that is not indicated on the T.T.T. diagram).

This residual austenite may be conditioned for further transformation by a normal tempering treatment; furthermore, the transformation to bainite will continue if cooling after tempering is again interrupted at the same level as before. This product of the second isothermal transformation has been designated as " secondary bainite."

Structurally, no difference appears to exist between primary and secondary bainite, when examined under the microscope, provided they transform at the same temperature.

Bainite, especially that formed in the lower temperature range, is but slightly softer than martensite, but—due to its formation at a higher temperature than martensite and the fact that its formation involves somewhat less volume change—the resultant structure contains considerably fewer internal stresses.

Much remains to be learned regarding the useful properties of this structure, and tests are being continued to determine its effect in various applications. However, the time cycles required to produce bainite are considerably longer than those usually employed in commercial practice, and outstanding improvement is, therefore, necessary to justify the increased time.

SURFACE TREATMENTS

One very common method of increasing abrasion resistance of high speed steel tools beyond that obtainable from regular hardening and tempering procedures is by " nitriding " in a molten cyanide bath. In practice, these baths are operated between 900 and 1100° F—generally at or below the tempering temperature at which the tools were drawn and at which no further softening would occur from the heating.

Nitrogen given up by the bath is absorbed by the tools, causing a surface layer of greatly increased hardness (although the actual hardness is difficult to measure). The depth of the case produced by most commercial cycles is 0·001 to 0·003 in. Well-substantiated reports of 100 per cent or more increase in tool life are not unusual. This may be attributed partly to increased wear resistance (due to higher hardness of the surface layers) and partly to the non-galling characteristics of this case which reduces the tendency of the cutting edges to pick up metal.

Like many other highly desirable conditions, however, a compromise must be made, since we obtain increased cutting efficiency at the expense of shock resistance or toughness. To avoid this, many variations of the cyanide treatment have been suggested, such as using shorter cycles, rapid cooling from the cyaniding temperature, and tempering in a neutral medium after the cyanide treatment. Data from some tests, using the pendulum tester, indicate that none of these methods have any appreciable effect in increasing toughness on high speed steel properly quenched and then tempered twice at 1050° F (ground before " nitriding ").

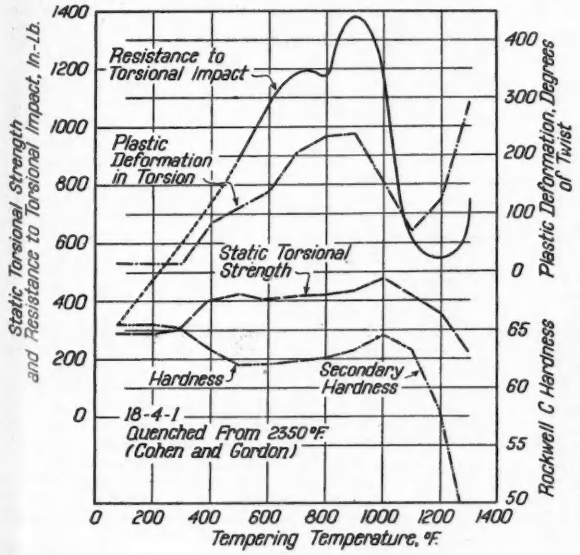
Static Torsional Strength and Resistance to Torsional Impact, In.-Lb.
Plastic Deformation, Degrees of Twist
Rockwell C Hardness
Resistance to Torsional Impact
Plastic Deformation in Torsion
Static Torsional Strength
Hardness
Secondary Hardness
18-4-1 Quenched From 2350°F. (Cohen and Gordon)
Tempering Temperature, °F.

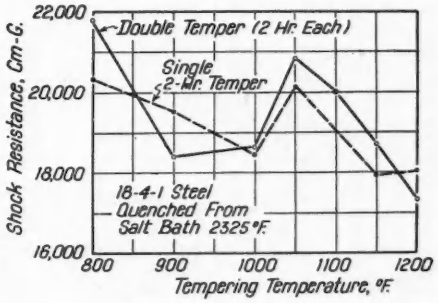
Shock Resistance, Cm.-G.
Double Temper (2 Hr. Each)
Single 2-Hr. Temper
18-4-1 Steel Quenched From Salt Bath 2325°F.
Tempering Temperature, °F.

Figs. 5. (Left) and 6. **Mechanical properties and especially toughness of properly quenched 18-4-1 high speed steel suffer when tempered above heat which develops maximum secondary hardness.**

Chromium plating, another widely used surface treatment for cutting tools, may increase surface hardness slightly, but is more generally believed to bring about improvement by reducing surface friction and tendency to "load." Heavy chromium plates tend to impair fatigue resistance and toughness of the tool; light deposits, however, have proven beneficial in many applications.

Other surface treatments are of the oxide type. They are produced by such methods wherein, by chemical action at low temperature (as in the formation of black oxide) or at elevated temperatures (as when using some tempering salts or steam-atmosphere tempering furnaces), a very adherent ferrous oxide is produced. The claim is made that the oxide reduces the tendency to pick up metal from the chip during cutting, and the less dense surface aids in retaining the cutting lubricant.

In connection with surface conditions, the layer produced by quench baths containing cyanide should be mentioned. This layer (being formed by the action of cyanide on steel at relatively high temperatures while the steel is in a fully austenitic condition) is high in carbon and, for purposes of this discussion, may be said to represent a carburized layer, generally 0·001 to 0·002-in in depth. This is extremely hard, and resists tempering up to 1150° F. When not removed by subsequent grinding and finishing operations, it impairs toughness to nearly the same degree as a "nitrided" case.

The present authors made a few tests to show the comparative shock resistance of specimens of 18-4-1 high speed steel which have been treated so as to have different types of surface layers. All specimens were tempered twice at 1050° F before testing. Results follow:

Treatment	Shock Resistance
Quenched in neutral salt, ground 0·004-in	21,175 cm-g
Same as above, then heated in cyanide bath at 1050° F for 30 min and air cooled	6,600
Ground before heat treatment, quenched in neutral salt	14,300
Ground before heat treatment, quenched in cyanide quenching salt	7,700

CONCLUSION

This discussion of the practical heat treatment of high speed cutting tools has been presented to show how any metallurgist trying to do the best possible job may re-examine his toolroom heat treatments. Frequently the information made available by research workers confirms the correctness of his methods which, as a matter of fact, might have been developed by trial and error procedure. At other times, it may reveal the possibilities of a hitherto neglected type of structure having properties quite different from those produced by conventional treatment.

In general, advanced practices have been altered but slightly, and recent changes are in the nature of refinements rather than radical departures from established practice. This is due, for the most part, to the above-mentioned fact that scientific work has confirmed the validity of standard practice. A conservative attitude by certain toolsteel users may, on the other hand, indicate a failure to appreciate the value of some recently developed theories.

Modern heat treatment of high speed steel cutting tools is based, then, both on past practical experience developed through trial-and-error procedures, and on scientific knowledge of the behaviour of the material as advanced by the research laboratories of our universities, steel manufacturers, and industrial plants. Obviously, the successful practice of known principles requires the ability to control intelligently the several factors which determine the final properties of the heat treated tools. The present authors hope that this presentation will enable other tool-steel users to make the best use of what is now known about that intricate but extraordinarily useful alloy—high speed steel.

Electro-Forming and Deposition brings New Latitude to the Designer

(From *INCO Magazine, U.S.A.*, Vol. 12, No. 1, 1948, pp. 12-13, 5 illustrations).

Two developments in nickel plating are now making it possible to turn out complicated shapes which have heretofore been impossible to produce on a production basis and to apply heavy electro-deposits of nickel on plastic bases. Both are being used in a number of different fields—from the forming of fountain pen caps and barrels to the electro-plating of plastic safety razor handles.

Chief advantage of the processes, developed by the Camin Laboratories Inc., N.Y., lies in the greater latitude they offer to the designer and engineer, both for such decorative items as fountain pen parts and for a variety of industrial items.

Formed shapes can be controlled within tolerances as small as plus or minus 2/10,000 of an inch. There is little limit to the complication in shapes which can be electro-formed. Rounds, squares, recesses, undercuts, and other variations can be combined in a single design. Where less complicated shapes are involved, the cost of electro-forming in some cases has been found to be approximately 25 per cent less than die casting or other types of forming, since tooling and die costs are eliminated. There are no stresses set up as is sometimes the case in die forming or similar types of fabrication, such as drawing.

Two types of mandrils are used for forming by Camin Laboratories. For relatively simple shapes not involving recesses, undercuts, and the like, a polished steel mandril is used. This forms the inside dimension of the shape to be formed, and upon it is built up the nickel plate to the thickness desired. When the shape has been completely formed, the mandril is easily withdrawn without damage to the plated structure. The steel mandrils are highly polished and impart a smooth, bright surface to the inside of the formed product. This has been found of particular value in specialized applications, such as for spindle sleeves which separate the hands of a watch, and wave guides for radar.

For complicated shapes, where undercuts or other surface variations prevent the withdrawal of the mandril, the latter is made from a low melting point alloy, such as Cerrobend which melts at 160 deg. F, or 52 deg. less than the boiling point of water, which is used to melt out the alloy. Incidentally, the alloy is recovered after melting out and can be used over and over again for making other mandrils.

While electro-deposits of metal have been applied to plastics in the past, it is believed that the Camin process is the first to apply, by means of automatic equipment, heavy and uniform deposits with excellent adhesion. In the plating operations, the plastic base is first given a minute film of pure silver and then sent to the automatic plating machine. Nickel is used almost exclusively in the Camin process not only because of its appearance and mechanical properties but also because of the established value of nickel as a base for the further application of chromium or precious metals.

New Materials, Processes and Equipment

NEW HEAT TRANSFER UNIT

Eastern Industries Incorporated, New Haven, Conn. has developed a new heavy duty heat transfer unit for cooling the magnetron power tube in an induction-heated oven. The unit is also suitable for cooling the tubes and condensers in television transmitters, short wave communication equipment, radar sets, and for general laboratory use.

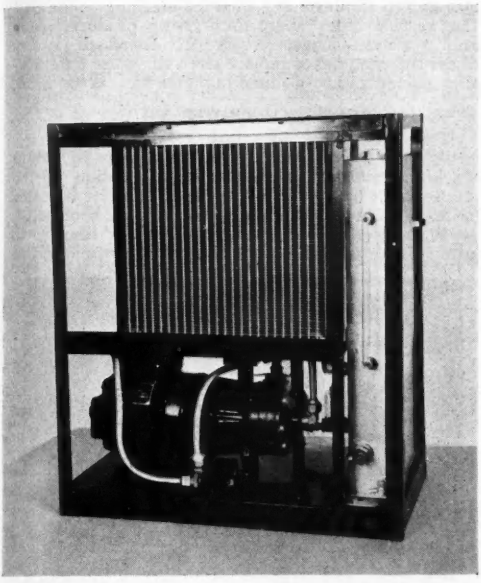

The heat generated by the magnetron tube is dissipated at the rate of 11,000 B.T.U.'s per hour, by circulating a cooling medium through the tube. The absorbed heat is then discharged into the air by means of a radiator and fan. This type of cooling ensures uniform temperature control and eliminates the inconvenience and expense of using tap water as a cooling agent.

HIGH PRODUCTION LAPPING MACHINE

Precision lapping under severe production schedules is now possible as a result of the development of the " Lapmaster " by the Crane Packing Company, Chicago 13. The new machine is applicable to production runs or individual jobs, and can be operated by unskilled workmen. Work handled in one operation may be of different sizes, shapes and heights. The new lapping machine embodies a continuously agitated compound tank, and alloy-iron lapping plate driven by a gear reduction motor, and combined work-holders and wear rings which are held in place by adjustable bars. The lapping cycle time is automatically controlled by a clock, which stops the lapping plate and closes the compound valve at the end of a predetermined period. Outstanding among many new features is the continuous self-conditioning of the lapping plate which affords controlled and continuous accuracy in flat, concave, and convex lapping up to ·000016 in.

After the work has been placed in the work holders, the machine is started by turning on switches to the

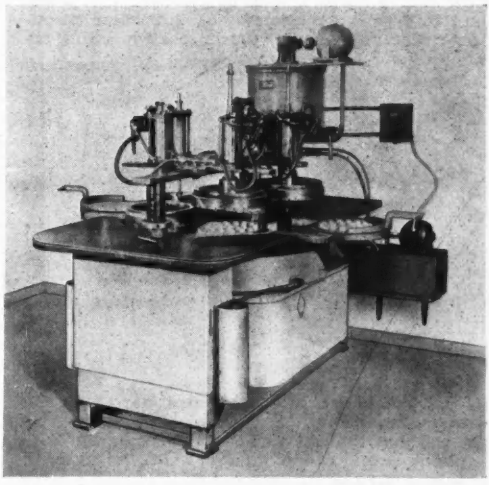

lapping plate motor and to the compound agitator. When the lapping plate motor is started, the solenoid compound valve opens, allowing the compound to run down the feed wire to the lapping plate, where it is evenly distributed to the surface by the rotation of the work holder. The wear rings and work holders rotate within their own orbit on the face of the lap. The lap rotates under the work, as do the wear rings. The work, in turn, is free to rotate on its own axis in the work holders. This free motion of the work generates a uniform abrading action which is absolutely essential in order to produce uniform concave, convex or flat lapping to close tolerances.

LIQUID WIRE STRIPPER

Stripping of electrical wires is speeded by the use of " Formula 21," developed by Aircraft-Marine Products, Inc., Harrisburg, Pa., for removing " Formex," " Formavar," enamel and similar wire insulating coatings. Its use is simple; merely dip wire in liquid and wipe off with rag or blow off with compressed air. No scraping, tools or special cleaning is required. This new product is non-corrosive, non-inflammable, and will not harm fabrics, wood, or metal. It is applicable for use in mass production as well as for repairs to motors, coils, relays, and similar electrically wired equipment.

CASE-HARDENING PASTE

A paste which does an excellent case-hardening job without special equipment, has been developed by Denfis Chemical Laboratories, Inc., Brooklyn 2, N.Y. A major advantage of this paste, which is called Carburit, is its ready use for selective hardening.

All that is necessary is to cover the section to be hardened with Carburit, and heat the work to about 1700° F. A case 0·010-in thick will form in 5 to 7 minutes and only 25 to 30 minutes are required for a 0·040-in case. After heating with Carburit in place, the work is cooled and reheated to 1500° F. Then the paste is knocked off and the work is quenched. The hardness produced in various irons and steels compares favourably with that produced by all other known methods.

NEW POCKET-SIZE SURFACE ROUGHNESS SCALES

A new pocket-size surface roughness comparator for sight and feel comparison with machined finishes has been announced by the General Electric Co., Schenectady, Special Products Division.

The new comparator is composed of two small metal rules 6 inches long and 1¼ inches wide. These illustrate degrees of roughness ranging from the smoothness of a bearing surface to the roughness of a flame cut.

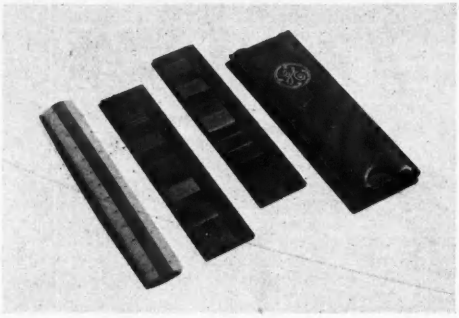

One side of each scale is divided into 12 surfaces, depicting a total of 24 different surfaces which are grouped into 10 degrees of surface roughness. Every degree is identified by a number which designates the nominal roughness in micro-inches.

DIE CASTING MACHINE

The world's largest standard die casting machine has just been introduced by the Kux Machine Co., Chicago.

Available in three different models, this machine has 800 tons locking pressure and will form castings in zinc weighing up to 30 lbs. and in aluminium weighing up to 10 lbs. Extremely high injection pressures are utilized reaching as much as 40,000 psi.

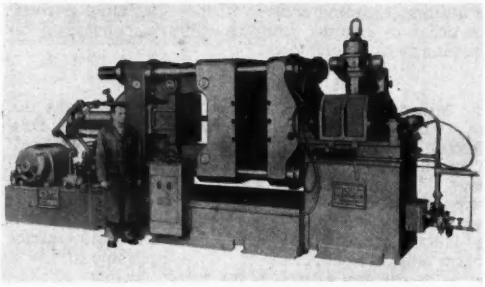

Having a die space of 40 × 25 inches between the tie bars and a 17½-in die separation, very large dies can be accommodated and castings having a deep draw are easily produced. The speed of operation is practically the same as on smaller machines, an average of 3 to 4 zinc casting cycles or 2 aluminium casting cycles per minute being possible.

Complete stroke control of the die opening and closing is built into the electrical circuit so that the die plates can be opened or closed by the amount desired or stopped in any position of the 17½-in total separation stroke.

EXTREME-PRESSURE LUBRICANT

Molykote, a new dry lubricant marketed by The Alpha Corporation, Greenwich, Conn., consists essentially of molybdenum disulphide powder, and has the appearance of graphite though it contains none. With light rubbing it adheres tenaciously to even the smoothest surfaces, and this property is a basis for its superiority. Numerous tests have shown its extremely low friction coefficient and a capacity to prevent galling, seizing or metal-to-metal contact at bearing pressures well over 10,000 psi, and at either high or low sliding velocities. Ten ounces will cover 500 sq. ft. of smooth metal surface with a tenacious, shiny coating. It is equally suitable for high, low, and room temperatures, and may be mixed to a paste with SAE 10 motor oil.

EMBOSSED ALUMINIUM

This new form of aluminium sheet developed by the Reynolds Metal Company, Louisville, Ky., has raised patterns which give it an unusually attractive appearance and so eliminate any need for finishing operations. The surface hides wear, thus giving products made from it a much longer service life. Increased rigidity allows this material to replace steel, thickness for thickness, making the use of aluminium even more economical.

NEW WORKSHOP VICE

The outstanding advantage of the Wearite vice, manufactured by Wright and Weaire Ltd., South Shields, Durham, lies in the foot operation of the release and grip control of the jaws. All the operator has to do is to open the jaws by depressing a foot pedal, insert the work and release the pedal for the jaws to grip. These movements, of course, leave the operator

with both hands free for the manipulation of the job itself. Angular adjustment of the work, to facilitate filing or other operations, is carried out without releasing the vice jaws. The lever seen at the right hand side of the vice base is pulled to release the main vice arm which works on a ball and socket mounting. Accurate adjustment can then be made to any required angle and the vice instantly locked by means of the lever. The vice can also be used as a jig when flow work of an awkward nature is the problem.

CLASSIFIED ABSTRACTS

Numerous important abstracts which, for lack of space, cannot be published in our main editorial columns, are regularly included in condensed form in this section. Subscribers may obtain photostat copies of all original articles at cost.

ELECTRONICS

An Electronic Switch with Variable Commutating Frequency

By E. E. CARPENTIER. (From *Philips Technical Review, Holland*, Vol. 9, No. 11, pp. 340-346, 14 illustrations.)

A DESCRIPTION is given of a new construction of an electronic switch for the simultaneous production of two oscillograms. Various steps have been taken to avoid disturbing peaks in the output voltage. The normal oscillograph amplifier, which led to distortion of the commutating voltage, is no longer used (except as pre-amplifier for one of the voltages to be imaged). As a result, it has been possible to raise the commutating frequency to 40,000 c/s, thereby improving the clearness of the details in the oscillograms. Moreover, this frequency is continuously variable, to 2 c/s downwards, which in certain cases is an advantage. The input may be asymmetrical or symmetrical as desired, the latter being useful, *inter alia*, when it is desired to produce more than two oscillograms simultaneously with the aid of electronic switches in cascade.

ELECTROPLATING

Electrodeposition of Gamma Manganese

By D. SCHLAIN and J. D. PRATER. (From *Journal of The Electrochemical Society, U.S.A.*, Vol. 94, No. 2, August, 1948, pp. 58-73, 6 illustrations.)

PROCEDURES are given by which electrolytic manganese can consistently be deposited in the flexible gamma form rather than the usual brittle alpha form. With electrolytes containing manganese and ammonium sulphates and free of sulphur dioxide or colloidal sulphur, excellent deposits were obtained on copper cathodes at current efficiencies of 62 to 72 per cent; deposits on stainless steel cathodes were much poorer. The use of colourless ammonium sulphide for purification did not interfere with the deposition of gamma manganese, but the use of yellow ammonium sulphide, unless followed by a further purification step (presumably to remove colloidal sulphur), resulted in only slightly flexible deposits consisting of gamma manganese containing some alpha. Electrolytes containing sulphur dioxide yielded only alpha manganese. Gamma manganese deposits were used successfully as starting sheets for the deposition of alpha manganese.

IRON AND STEEL

Prevention of Mechanical Failures in Steel Plant Equipment

By O. J. HORGER and G. A. STUMPF. (From *Iron and Steel Engineer, U.S.A.*, Vol. 25, No. 5, May, 1948, pp. 69-76, 22 illustrations.)

THIS paper discusses many specific cases of failures which have occurred in various machinery parts used in steel plant equipment. Both plant maintenance and operating men will be interested in the economical means employed to correct these failures which constitute an expensive item in annual operations.

Many of the failures discussed are common to the industry and accepted as something which always develops in plant operation. Yet definite improvement in life of these parts was obtained by concentrated effort in the application of modern technological practices.

Failures due to both fatigue fracture and wear are presented. In most cases no radical design changes were required but improvement in life obtained by either local changes in design, proper type of steel and heat treatment, and/or placing favourable residual compressive stresses in the surface layers by means of surface cold working the region where fatigue failure occurred.

Actual cases of failures and corrective steps taken are outlined.

METALLURGICAL ENGINEERING

Electrometric Study of the Behaviour of Stainless Steels in Acids

By M. L. GUITTON. (From *Revue de Metallurgie, France*, Vol. 44, Nos. 11 and 12, November-December, 1947, pp. 330-348, 20 illustrations.)

THIS article gives a detailed account of tests of the behaviour of a chrome-manganese stainless steel in oxalic acid (18 per cent chromium, 10 per cent manganese, 5 per cent solution of oxalic acid at 30° C). It is considered that the study of passivity of stainless steels is more worthwhile than the study of corrosion, from a practical point of view, as their most extensive uses are in the decorative trades, food industries and chemical industries, where they are largely in a passive state.

The results of tests are given as follows :—

Sand-blasted test pieces in still solution; the same tests in agitated solution; and the same tests with controlled aeration (oxygenated, de-oxygenated by nitrogen, de-oxygenated by boiling).

Polished test pieces (emery paper 000): brushed (metal brush, dry and wet); not de-scaled; acid de-scaled.

Potential-time graphs for immersion periods up to 1,000 hours show that the principal factor in the variation of results is the degree of aeration of the solutions at a certain critical phase of immersion, and more precisely, with the material used, the existence of communication between the acid flasks and the air.

The potential curves show a succession of many levels of potential with fairly rapid passage from one to another. With sand-blasted test pieces, these are :—

1. A first stage, electro-negative, with visible corrosion.
2. A second stage, still electro-negative, but 100 millivolts higher than stage 1: transition level, unstable, with very slow corrosion, during which the dissolved oxygen acts.
3. A third stage, electro-positive and stable.

Test-pieces stay for 10 minutes in stage 1, several hours in stage 2, and then, according to whether there is communication with the atmosphere or not, rise to stage 3 or fall back to stage 1. There is definite passivation in the first case, definite corrosion in the second.

There is always final passivation with elimination of the transitional stage in those cases where the solution is agitated. The essential fact is the possibility of passivation taking birth in the acid medium itself. The acquired passivity requires the presence of oxygen and a certain time for its formation.

A remarkable phenomenon is that of the sensitization of active test pieces by preliminary acid etch. Lightly etched in HCl, sand-blasted test pieces im-

TESTAL

Aluminium Alloys

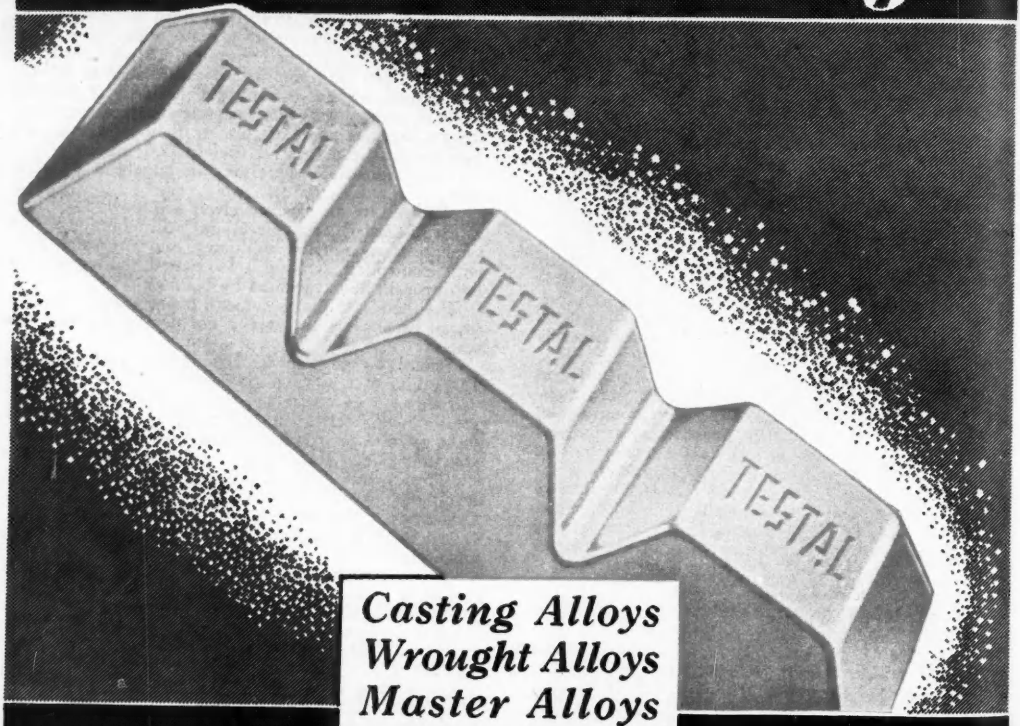

Casting Alloys
Wrought Alloys
Master Alloys

B·K·L·ALLOYS LIMITED

FACTORY CENTRE · KINGS NORTON · BIRMINGHAM 30

TEL·KIN 1162/5

mersed in oxalic acid take passivity very quickly with no transitional electro-negative phase. This, however, is always accompanied by a certain corrosion, so that it is only possible to obtain passivity without corrosion in an oxalic acid medium by preliminary passivation in moist air or by nitric acid.

It is not always easy to distinguish acquired passivity from original passivity. They are not of the same nature and, in many cases, there is a passage from one to the other in the acid, shown by a more or less sharp depression in the potential curves.

The potential always shows the actual speed of dissolution of the test piece, but does not generally allow of foreseeing the final condition of the metal. Only an electropositive potential acquired in the acid gives definite proof that the test piece will never be affected by the acid.

METALS CORROSION

Corrosion Conditions in Exhaust Pipes of I.C. Engines

By G. SCHIKORR. (From *Metalloberfläche, Germany*, Vol. 2, No. 4, April, 1948, pp. 73-79, 4 illustrations.)

FREE oxygen, steam and carbon dioxide in combustion gases may lead to chemical attack on iron. Since, however, the speed of attack is highly important, the impurities in the petrol which destroy, or prevent the formation of, a protective layer on the pipe material constitute the main danger. Oxides of sulphur, even in small percentages, are especially dangerous; they attack iron directly and the iron sulphide so formed is easily oxidised and prevents formation of a protective layer. This reaction is of a pronounced character above 200° C, but even below the dew point a strong attack by sulphuric acid may destroy the iron. During normal running of a car, the temperature probably does not fall below the dew point, but this danger is very real in delivery vans running only for short periods, and this also applies when combustion gases are used to heat the interior of the car. Death by CO poisoning due to corrosion of the heat exchanger actually led to the investigation described. Cylinder and exhaust corrosion can occur during intermittent running and during longer standing periods, when sulphuric acid condenses on iron walls. A humidity of 85 per cent is sufficient for the attack.

A normal 6-cylinder car engine was used for the tests described, and cast iron and copper test pieces were arranged at different points of the exhaust pipe where the temperatures during running reached about 400° C (engine itself and exhaust conditions near the engine), 180° C (conditions at exhaust outlet during normal running), and 70° C respectively (special conditions at temperatures below dew point). The temperatures, petrol consumption, sulphur contents of combustion gases, and the loss of weight due to corrosion during a certain time were measured. Results showed that with a daily running period of 5 hours and a daily consumption of 3 gallons of commercial petrol with 0·1 per cent sulphur content, cast iron at 400° C corroded fairly quickly during the first day, but later withstood attack fairly well, decreasing only by 0·0025-in wall thickness per year. At 180° C, the attack was negligible, but at 70° C it was considerable and could reach values up to 0·056-in per year. Copper corrodes considerably at 400° C up to 0·04-in per year, and corrosion is not slowed down by formation of a protective layer. Corrosion of copper at 180° C was 0·0012-in, and at 70° C was 0·0032-in wall thickness per year.

Results clearly show the causes of corrosion of heat exchangers for cars. It is to be expected that results for steel will be similar to those obtained on cast iron. Accidents due to corrosion could be avoided (a) if the temperature in the heat exchanger was always kept well above the dew point; (b) if the heat exchanger was so designed that exhaust gases could not reach the interior of the car, even if pipe walls were destroyed by corrosion; or (c) if materials of better corrosion resistance at temperatures below the dew point were chosen. Copper tubes of 0·08-in wall thickness or leaded cast iron would be satisfactory at low temperatures but unsuitable for high temperatures. Copper for the low-temperature parts and steel for parts running at higher temperatures may be satisfactory, but the danger of corrosion during intermittent running and longer periods of standing must be watched. Chromium-plated tubes may offer the best solution for all temperatures.

WELDING

Designing for Welding

By J. MIKULAK. (From *Machine Design, U.S.A.*, Vol. 20, No. 9, September, 1948, pp. 147-152, 10 illustrations.)

THE following rules for design are given, which are explained in detail and illustrated by examples:—

(1) Eliminate welding where possible and use welding technique and equipment where this produces the most economical result. The reason for this rule is the comparatively high cost of the welding process, e.g., wherever possible, bending or pressing should be done with a view to minimum cost and to better set-up without resorting to straightening. It should also be borne in mind that the total welding cost depends on three factors: (1) preparation; (2) welding; (3) finishing.

(2) Use materials of maximum weldability, such as open-hearth steel. Ductility of the metals being welded is an important factor, while brittle material requires special care.

(3) Produce designs where good set-up is easily obtained and where, at the same time, they will not require an excessive amount of welding. The effect of poor set-up upon cost is, for instance, such that welding speed is reduced 65 per cent when welding on ¼-inch material with a gap equal to the thickness of the material. Considerable latitude in tolerances on the final product is possible in the welding operation itself by standardized procedures and by the use of proper welding jigs.

(4) Use as few elements as possible to compose the weld consistent with quantity being produced.

(5) Design so that as little handling as possible is necessary during fabrication.

(6) Eliminate as much direct labour as possible in producing the weld.

(7) Eliminate, to the greatest possible extent, machining and straightening operations on the final weld.

(8) Design joint so that stresses are well balanced. When static loads are anticipated, complete penetration may not be required with heavy plate. However, an insufficient amount of welding will produce not a single mass, but rather a complexity of several masses.

(9) Design so that welding is uniform about the neutral axis of the structure as well as that of each joint. Residual stresses in welds must in many cases be minimised, as they easily originate when distortion is kept low. It is frequently remarked that "the weld is stronger than the parent plate," but this does not always prove to be true and, generally, inadequate provisions for taking care of residual stresses account for its undoing.

(10) Study each point from a metallurgical and performance standpoint.

(11) Study the design to determine if it can be readily handled on equipment to be used by the shop organisation.

PACING PROGRESS

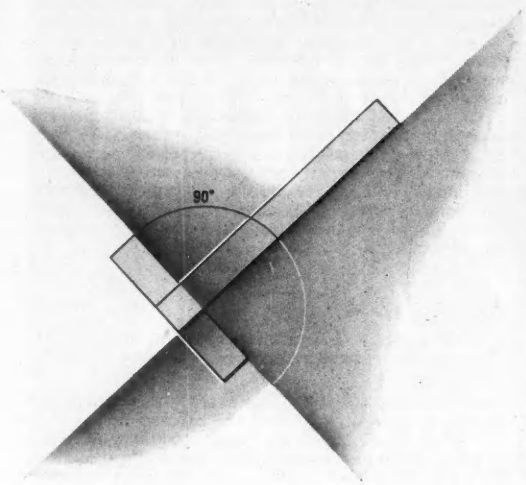

Right to a T

Still an apt expression for things that fit exactly, even though the fitter now has other instruments in addition to his T-square, to suit the ultra-close tolerances worked to by Kearns machines. From the small S type to the 45-ton No. 6; whether on surfacing, boring or other of the many operations they variously perform (such as milling, drilling, tapping, turning), every member of the comprehensive range delivers work that is right to a T.

KEARNS FOR BORERS

H. W. KEARNS & COMPANY LTD.
BROADHEATH *near* MANCHESTER
Hopwood

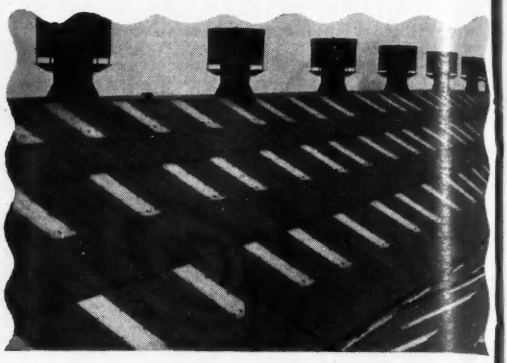

Corrugated 'PERSPEX'
acrylic sheet
for roof lighting

Corrugated 'Perspex' acrylic sheet can be fixed as easily as normal corrugated sheet, using ordinary hook bolts and washers. Made in 9 different profiles, and available in lengths from 3 feet to 7 feet in intervals of 6 inches.

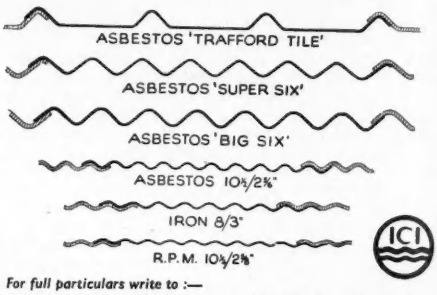

For full particulars write to :—
IMPERIAL CHEMICAL INDUSTRIES LIMITED,
LONDON, S.W.1

C.P.11

NEWS OF THE MONTH

PERSONAL

Mr. D. G. W. Acworth, M.I.E.E., has been appointed manager of the export department of the General Electric Co. Ltd., in succession to **Mr. H. W. Adams** who has retired.

Mr. J. E. Bennett has been elected chairman of Crane Ltd., 45 Leman Street, London, E.1. **Mr. R. E. Dunnett** has been appointed managing director of the company.

Mr. T. H. Y. Bonsey, A.M.I.E.E., has been appointed sales manager, and **Mr. C. H. E. Ridpath, A.M.I.E.E.,** deputy sales manager of the Aluminium Wire and Cable Co. Ltd., 10 Buckingham Place, London, S.W.1.

Mr. N. C. Cain has been appointed civil engineer, **Mr. W. Archibald,** mechanical engineer, and **Mr. W. S. Marshall,** railway operating superintendent to the Ulster Transport Authority.

Dr. Bruce Chalmers, Ph.D. (Lond.), D.Sc. (Lond.), F.Inst.P., F.I.M., has resigned his position as Head of the Metallurgy Division of the Atomic Energy Research Establishment, to take up the post of Professor of Physical Metallurgy at the University of Toronto, Canada.

Mr. C. H. Chaplain has been appointed manager of the publicity department of The British Thomson-Houston Co., Ltd. to succeed **Mr. H. A. Price-Hughes, A.M.I.E.E.,** who retired after 44 years' service with the Company.

Sir Eyre Gordon, C.S.I., C.I.E., has been appointed chairman of the Northern Ireland Joint Electricity Committee.

Mr. S. B. Hainsworth, managing director of J. H. Fenner & Co. Ltd., Winewall Mill, Colne, Lancs., has moved his headquarters to the new factory of the Company at Marfleet, Hull.

Colonel C. F. Hitchins, D.S.O., M.I.Mech.E., M.I.N.A., has been elected chairman of the Pearson & Knowles Coal and Iron Co., Ltd.

Mr. L. B. Hutchinson has been appointed a deputy secretary in the Ministry of Supply.

Mr. Basil R. Jackson has been elected a director of the Anglo-Iranian Oil Co., Ltd.

Mr. Brinley Jones, B.Met., senior metallurgist of the English Steel Corporation Ltd., Vickers Works, Sheffield, joined the Climax Molybdenum Company of Europe Ltd. as manager.

Mr. J. W. Laing has been appointed chief engineer of the Witton Engineering Works of the General Electric Co. Ltd.

Sir Robert Letch, M.Inst.T., has been elected vice-president of the Institute of Transport, 80 Portland Place, London, W.1.

Mr. J. A. C. Manson, F.R.Ae.S., has joined the Fairey Aviation Co., Ltd., Hayes, Middx., as personal assistant to the general manager.

Mr. W. Maxfield, Principal of the Industrial Capacity Exchange, 21 Clarendon Street, London, S.W.1, resigned his secretaryship of the Sheet Metal Industries Association to devote all his time to the Exchange.

Mr. A. E. McCormack, A.M.I.E.E., has joined Johnson & Phillips Ltd., Charlton, London, S.E.7, as a senior sales engineer.

Sir Robert Robinson, F.R.S., President of the Royal Society, and **Mr. W. L. Tregoning,** industrial adviser to the Finance Corporation for Industry Ltd., have both joined the board of Petrochemicals Ltd. Sir Robert Robinson has also joined the board of Petrocarbon Ltd., an associated company.

Mr. W. E. Stanley has been appointed a director of Darwins Ltd., Sheffield.

Dr. D. T. A. Townend, director-general of the British Coal Utilisation Research Association, has been installed as President of the Institute of Fuel.

Mr. E. S. Waddington, M.S.E., M.Inst.W., A.M.I.E.(s.a.), Assoc.I.E.E., of the Industrial Department of Philips Electrical Ltd., has been elected vice-chairman of the Finance Committee of the Institute of Welding and vice-chairman of the BEAMA Resistance Welding Machine section.

The Hon. J. Kenneth Weir, C.B.E., has been elected a director of the Dunlop Rubber Co. Ltd. **Mr. J. M. Billane** has been appointed the firm's overseas sales manager.

Mr. A. G. K. Williams has been appointed manager of the Cardiff office of George Ellison Ltd., in succession to Mr. Gwynne Lewis.

Mr. A. H. A. Wynn, M.A. (Cantab.), formerly research engineer to A. C. Cossor Ltd., has been appointed director of the Safety in Mines Research and Testing Stations of the Ministry of Fuel and Power at Sheffield and Buxton.

BUSINESS NOTES

Welding Rods Ltd. has removed the head office of the company to 76 Attercliffe Road, Sheffield 4; Telephone: Sheffield 24231.

Petbow Ltd. has opened a new factory at Richborough Works, Sandwich, Kent. For the time being, the company's head office will remain at Balmoral Road, Watford, Herts.

Burton, Griffiths & Co. Ltd. have removed their Small Tool Division from Mackadown Lane, Marston Green, Birmingham, to Montgomery Street, Sparkbrook, Birmingham 11.

Aveling-Barford Ltd., Invicta Works, Grantham, have removed their London office to Morris House, 1/5 Jermyn Street, London, S.W.1. **Mr. C. G. Miller, M.I.Mech.E.,** is manager in charge of the London office.

The Directorate of Paint Materials of the Board of Trade has moved to Horseferry House, Horseferry Road, London, S.W.1. Telephone: VICtoria 6800.

BRITISH STANDARDS

(Copies of British Standards may be obtained from the British Standards Institution, 24 Victoria Street, London, S.W.1.)

Steel Plate, Sheet and Strip. Now that the revised B.S. 970 has been issued providing a comprehensive schedule of wrought steels for general use in the engineering industries, B.S. 1449 has been prepared to provide a similar comprehensive schedule covering steels which are commonly supplied in the form of plate, sheet and strip. This British Standard is an extension to, and should be regarded as a companion to, B.S. 970.

The first section, covering general clauses, includes details of manufacture, methods of testing, finish and tolerances on dimensions, and section 2 gives for each steel the chemical composition and the mechanical properties in the form of plate, sheet and strip, as applicable. Price 2/6.

Long Period High Sensitivity, Tensile Creep Testing. B.S. No. A.23: 1948 covers the essential requirements for testing equipment and method of test to cover tensile creep (total plastic) strains down to 0.001 (0.1 per cent) and in periods up to 10,000 hours. It is applicable to standard tests on bars, plates, sections, sheets, and cast or forged parts of sufficient size.

Details are given in sections 1 and 2 of the recommended test specimen and requirements are stated for the testing machine, thermocouples, temperature indicators and control, and extensometer. Section 3 describes the test method and includes details of the preparation of the specimen, the checking of the instruments and the presentation of results. Price 1/-.

Graphical Symbols for Telecommunications. It is of great importance that the symbols used in diagrams, plans, etc., relating to all branches of Telecommunication as used by Telecommunication Authorities, the Services, Manufacturers of Apparatus and in the teaching profession should be as far as possible the same.

This standard has been considerably extended since the last

A GUARANTEE OF
Money Saving
For protective purposes, or to resist wear and corrosion on new jobs, or for building up worn machine-shop parts and the salvage of machine-shop errors, specify the Brailey process—" a guarantee of money saving ! "
BRAILEY

BRAILEY ELECTROPLATERS LTD.

CHAPEL STREET · SALFORD 3, LANCS.

B26

Our technical representatives will gladly advise you on the varying types of the Weston Seals. These include our Gitseals and Weston Oil Retainers fitted with best quality chrome leather inserts, also the Weston Synthetic Rubber Oilseals all precision made to give the lightest possible contact consistent with efficient sealing.

WESTON
OIL SEALS

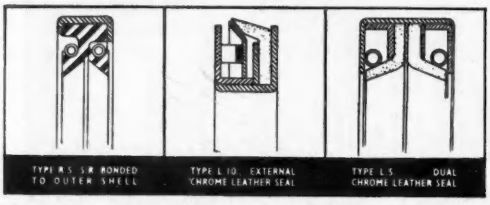

CHARLES WESTON & CO. LTD., IRWELL BANK WORKS, DOUGLAS GREEN, PENDLETON, SALFORD, 6.
PHONE: PENDLETON 2857-8-9. BIRMINGHAM, MIDLAND 6952. LONDON, HOLBORN 0414

Smee's W 58

Manufacturers

whose products are subject to VIBRATION are today safeguarding their REPUTATION and GOODWILL by fitting . . .

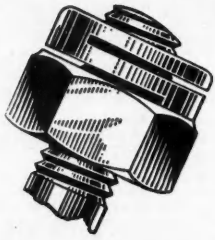

PHILIDAS

VIBRATION-PROOF SELF-LOCKING NUTS

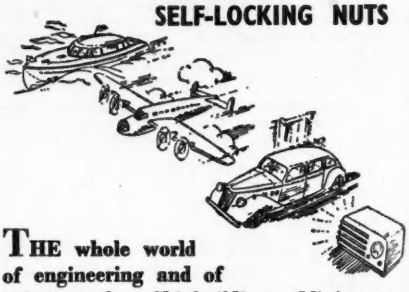

THE whole world of engineering and of industry—from Shipbuilding to Miniature Radio — is proving by its own Tests and Time Study Investigations the very real ECONOMY and EFFICIENCY of PHILIDAS Self-Locking Nuts — The nuts with a "Steadfast" Purpose.

We will gladly send literature and samples for test. The Philidas Technical Research Dept. is at your Service.

PHILIDAS LTD.
Bath Road, Harmondsworth, Middlesex
Telephone: West Drayton 3001 (3 lines)

edition to keep pace with recent developments and covers telecommunication in general, telephony, telegraphy, and radio communication in considerable detail.

Guiding principles to be observed in using the symbols in preparation of diagrams are also suggested. A series of detailed diagrams exemplifying the use of the symbols is also included. In general, the symbols are in accord with those standardized by the International Electrotechnical Commission. Among the subjects dealt with for the first time in this edition is carrier communication and co-axial cables. Price 10/6.

INSTITUTION MEETINGS

The Institution of Mechanical Engineers.

MEETINGS are held at the Institution, Storey's Gate, St. James's Park, London, S.W.1, at 6 p.m.

Jan. 7. Informal Meeting: "Rotary Motion" to be introduced by W. Abbott, O.B.E., Ph.D., B.Sc. (Eng.), M.I.Mech.E.

Jan. 11. Automobile Division General Meeting: "Basic Problem in the Engineering of a Modern All-Metal Motor Body," by E. S. White.

Jan. 14. Applied Mechanics Group: "Bending Stresses and Load Distribution in Screw Threads," by D. G. Sopwith, B.Sc.Tech., Wh.Sc., A.M.I.Mech.E., and "Tensile Fillet Stresses in Loaded Projections," by R. B. Heywood, B.Sc., A.M.I.Mech.E.

Jan. 21. Thomas Lowe Gray Lecture: "Marine Engineering in the Royal Navy," by Eng. Vice-Admiral Sir John Kingcome, K.C.B., M.I.Mech.E.

Jan. 28. "The Application of Free Jets to the Mixing of Fluids in Bulk," by H. Fossett, M.I.Mech.E., and L. E. Prosser, B.Sc. (Eng.), A.M.I.Mech.E., and "Investigations into Cyclone Dust Collectors," by Professor A. J. ter Linden.

The Institute of Marine Engineers.

Meetings will be held at the Institute, 85 The Minories, London, E.C.3, at 5.30 p.m.

Jan. 11. "Methods of Non-Destructive Testing of Large Marine Forgings and Castings," by J. Rhodes, B.Sc., T. H. Arnold, and J. R. Rait, D.Sc., Ph.D.

Feb. 8. "Corrosion of Turbine Journals," by S. E. Bowrey, R.N.S.S.

Mar. 8. "Trends in the Development in Marine Reduction Gearing," by A. W. Davis.

Apr. 12. "The Geared Diesel Machinery of the Liner 'Willem Ruys,'" by D. Ruys.

Society of Instrument Technology—Midland Section.

Meetings will be held at the Arden Hotel, New Street, Birmingham, at 7 p.m.

Feb. 18. "Some Instruments for Iron Testing," by N. F. Astbury, M.A., F.Inst.P., A.M.I.E.E., F.R.S.A., Director of Research, Guest, Keen & Nettlefolds Group of Companies.

Mar. 18. "The Microscope in Industry," by W. Wilson, D.Sc., B.Eng., F.Inst.P., M.I.E.E., of the General Electric Co., Ltd.

BOOKS

"Electrical Devices." By H. A. Miller. Publishers: Sir Isaac Pitman & Sons, Ltd., London. 1st Edition, 100 pages, 71 figs. Price 12/6 net.

This book summarises some of the electronic devices in common use in electrical, radio, and illuminating engineering, as well as such used in the home. Two types of readers have been borne in mind: the student and the electrical engineer not primarily concerned with electronics. A successful attempt to fill the gap between elementary theory and technical specialization.

"Photoelectric Cells in Industry." By R. C. Walker, B.Sc. Published by Sir Isaac Pitman & Sons, Ltd., London. 1st Edition, 1948, 500 pages. Price 40/- net.

No better title could have been given to this book describing photo-electric industrial equipment that are being or have been employed in industry. Such a representative selection of the industrial uses of light-sensitive cells of the emission and rectifier types is of great value to practical men whose purpose is to employ electrons rather than theorize about their internal affairs. So much as is given of the theory of operation of these services is lucid and readable. Considering the remarkable development of the photo-electric cell during the last few years and its growing number of applications, the present book is recommended not only to electrical engineers but to control engineers, safety engineers, designers of special and automatic machinery and all others concerned with or interested in industrial development.

"Production Engineering: Practical Method of Production Planning and Control." By J. S. Murphy. Published by The Louis Cassier Co., Ltd., London. 226 pages. Price 12/6 net.

This book is intended for students of production engineering and young planning engineers, to give an insight into the various systems of production planning and control. Moreover, as methods and systems vary so much in different organisations, there is also in the book much of interest and benefit to experienced production engineers, who now have an opportunity to compare the methods of others with their own.

Contents include: Planning a Production Programme—Design for Production—Drawing Office Organisation—Process Layout—Manufacturing Processes and Methods—Jigs, Tools and Fixtures—Workshop Layout and Organisation—Production Control—Time and Motion Study—Estimating and Costing.

THE NEW HOOVER FACTORY AT MERTHYR TYDFIL

Hoover Limited have opened their new factory at Merthyr Tydfil on the 12th October. The opening ceremony was attended by the Rt. Hon. George Isaacs, Minister of Labour, Col. Sir Gerald Bruce, Lord Lieutenant of Glamorgan, Sir Frederick Bain, Chairman of the Federation of British Industries, Mr. C. B. Colston, Chairman and Managing Director of Hoover Limited, and four hundred guests, including representatives and friends of the Hoover organization from all over the world and representatives of the press.

The Minister of Labour has mentioned in his speech that whilst the firm's peace-time industrial activities are well known to all, it is less well known that Hoover Limited ran 17 factories during the war, and turned out a great variety of equipment for aircraft and armoured fighting vehicles. These activities were of the greatest possible value to the country. Mr. Isaacs qualified the fact that Hoovers established the new factory in the South Wales Development Area as a service to the Nation and to South Wales in particular. "Success to this new venture"—he said—"will bring happiness and prosperity where despair and poverty previously held sway." Mr. Isaacs also stressed the firm's excellent industrial relations and the important place given to Joint Consultation.

Mr. C. B. Colston, Chairman and Managing Director of the Company, who was appointed Regional Controller of the London and South-Eastern Region of the Ministry of Production and Chairman of the Regional Board, and in recognition of his services was subsequently awarded the C.B.E., introduced to the guests the directors and executives of Hoover Limited and Mr. George Gibson, the inventor of the new electric washing machine, which has gone into production in the new factory after three years of research and development work.

Outstanding feature of the neatly-designed Hoover electric washing machine, is a "pulsator" placed flush inside the stainless steel container so that there is no frictional contact with the washing.

The entirely modern new factory which has been specially built for the production of the Hoover washing machine, occupies an area of nearly 90,000 sq. feet. It employs already more than 700 workers, 8 per cent of whom are partially disabled ex-miners. Plans of expansions provide for doubling the number of workers by the middle of next year.

Classified Advertisements.

The Rate for all classified advertisements is 6d. per word; in bold print 9d. per word; minimum order 6s. Box number advertisements 1s. extra. Instructions together with remittance must be received not later than the 3rd of each month for advertisements to appear in the same month's issue.

SITUATIONS VACANT

£50 FOR ONE JOB. Scale Model Making Pays! We supply Plans, Instructions, and sell your work. Addressed envelope—B12, Biltex, 6, Silver Crescent, London, W.4.

WORK WANTED

URGENT PRIORITY CASTINGS.—Well-equipped, old established Foundry has small part of its capacity immediately available for British engineering firms making for export or other high priorities. Precision aluminium gravity die castings; zinc pressure die castings.—Write or 'phone **Thos. Ashworth & Co., Ltd.** (Dept. A/15/11), Vulcan Works, Burnley, Lancs. (Burnley 3505).

MACHINERY, ETC., FOR SALE

MOISTURE TEST—3 MINUTES! Exact percentage of moisture in foundry sand determined in three minutes by **"Speedy" Moisture Tester.** Portable; non-electric; simple for use by unskilled labour; inexpensive. Over 3,000 in use in Foundries and many other industries.—Write for fully descriptive illustrated Brochure to **Thos. Ashworth & Co., Ltd.** (Dept. ED/7), Burnley, Lancs. Agencies open.

NISSEN TYPE HUTS, ex-Government stock, reconditioned and supplied ready for erection. All sizes in 6 ft. multiples. 36 ft. by 16 ft., £80 & £65; 24 ft. by 16 ft., £56 & £46; 72 ft. by 16 ft., £148 & £118; delivered U.K. Plasterboard huts and other buildings. Some 24 ft. span Nissens.—Write, call or telephone, **Universal Supplies (Belvedere) Ltd.,** Dept. 50, Crabtree Manorway, Belvedere, Kent. Telephone No. ERITH 2948.

FIDELITY INSTRUMENT CO.

Specialists in precision optical work. Experimental, prototype, and limited production. Design work on optical systems.

284, Western Road, London, S.W.19.

Tel.: MITCHAM 2241.

SPECIAL PURPOSE MACHINES

DESIGNED AND BUILT TO CUSTOMERS' REQUIREMENTS

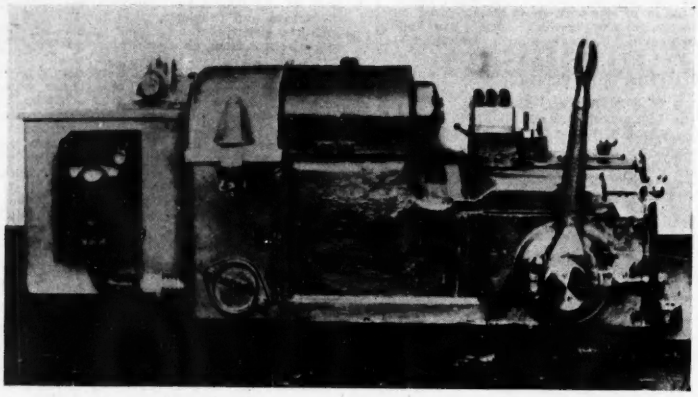

Hand Operated Button Turning Machine, individually motorised with pick off pulleys giving speeds from 3,000 to 4,500 R.P.M. Case hardened alloy steel spindle mounted on Hoffmann Angular Contact Bearings. Fully utilizes advantage of Tungsten Carbide Cutting Tools. One operator can handle 14 gross of buttons per hour.

GEO. H. WHITEHOUSE & SON LTD

THE ENGINEERS

GREAT BRIDGE - STAFFS. TELEPHONE: 1145-6

DROP FORGED FROM CHROME STEEL
DROPSTAMCO
Double Bi-Hex Ring Spanners and 15° Double Open-ended Spanners, Drop Forged from Chrome Steel.
Engineers' 6" Combination Pliers and other Hot Steel Drop Forgings for the Motor, Hand Tool and Engineering Trades, from 2 oz. to 7 lb.
Telephone: EAST 2001/2
TELEGRAMS: DROPSTAMCO B'HAM
CHROME SPANNERS & FORGED STEEL PLIERS
DROP STAMPING CO. LTD.
BIRCH ROAD WITTON BIRMINGHAM ENG.

LATEST INDUSTRIAL LITERATURE

1. Induction Melting. Nicely produced brochure briefly explaining the principle of high frequency heating and its application to melting processes. The brochure contains illustrated description of H.F. melting furnaces for ferrous and non-ferrous metals and alloys, with performance data of standard equipment. Two pages are devoted to laboratory and small scale production melting furnaces.

2. Nickel Alloy Steels for Machine Tools. This excellent little 24-page booklet is intended for the designer of machine tools for whom the right choice of steel for the various components is of paramount importance. The booklet contains a great wealth of data on the chemical composition, mechanical and fabricating properties, heat treatment, etc., of a variety of alloy steels commonly employed in machine tool construction. Diagrams and tables are given in excellent fashion so as to provide easy reference for the user.

3. Automatic Process and Temperature Control by Magnetic Valves. Information sheets describing and illustrating equipment for the control of low, medium and high pressure hot water, saturated steam, coke oven gas, oil, compressed air and all fluids and other gases, normally passed through pipes. The wide field of applications include heating of buildings and factories; air conditioning and refrigeration installations; oil, gas and compressed air installations; humidification; pasteurizing; domestic hot and cold water service; and safety precautions.

4. New Decorative and Protective Coating for Metal and Plastic Surfaces. Folder on a new range of coatings which has been developed after much research to achieve some important advantages over other coatings for metal and plastics. Shorter stoving period at lower temperature, exceptional durability and resistance to stresses and strains which cause ordinary finishes to deteriorate, are some of the advantages claimed for the new finish. Colour chart for 22 colours plus black and white, including pastel shades, is an additional feature of the folder.

5. Brake Linings and Clutch Linings. This 48-page booklet can be regarded as a technical treatise on the subject of brake and clutch problems. It explains in simple language, accompanied by good illustrations, the developments which have led to the modern designs of brakes and clutches and to the present qualities of friction products. Design engineers and others employed in the automotive industries will find it an interesting and useful booklet.

6. Roller Mill and Mechanical Air Separator for Laboratories. Illustrated brochure showing the construction of, and describing a compact unit pulverizer specially designed for grinding small lots of materials from a few ounces to several pounds at a time. The machine can be taken apart easily for cleaning or changing screens. Included in the brochure is illustrated description of a small capacity mechanical air classifier for the separation of fine particle size products.

7. Absolute Rust Prevention by Unique Paint. Tests carried out over a number of years have established that chromate pigments have the power of inhibiting corrosion and rendering metal passive. Based on these findings, new primer and finishing paints have been developed which give a higher degree of protection than ordinary metal paints. In a folder devoted to the new paints it is also claimed that they are more economical than any known type of metal protective paint.

8. Electric Metal Band-Sawing Machine. Interesting, well-illustrated brochure with description of a portable and self-contained band-sawing machine of the latest design. Built on true machine tool principles, the machine incorporates the most recent advances in design and metallurgy. Some of the unique advantages obtainable with the machine:—Straight cutting which eliminates squaring operations and thus saves time and material; Accuracy of cut; Continuous cutting action which greatly reduces cutting time; Electric drive; Chip remover; Automatic stop switch and Saw feed. General recommendations and tables of materials, speeds, etc., complete the clear and concise description of the machine.

9. Power Factor Improvement by Self Starting Synchronous Motors. This well designed 16-page brochure provides much interesting and useful information on self starting synchronous motors which improve the power factor while at the same time doing useful work, such as driving air compressors, textile machinery, line shafting, fans, pumps, blowers and similar drives where no speed regulation is required. Design and construction features are described and illustrated with numerous photographs, and the advantage attending the installation of such motors is graphically illustrated.

10. Remote Indication and Centralised Control. 20-page brochure dealing with Instrumentation in Industry. The principle of remote control is illustrated diagrammatically for a variety of industrial applications. Excellent photographs show many instruments and apparatus used in waterworks, drainage, docks and harbours, steelworks and in electricity supply undertakings. The last two pages of the brochure are devoted to illustrating position controllers.

11. Gears and Gear Units. Engineers employed in the automotive industries will be interested to have a copy of this excellently reproduced 40-page brochure. It contains full-page photographic presentation and description of Automobile and commercial vehicle gear boxes; Steering units; Marine units; Locomotive units; Railcar units; Tramcar units; Worm gears; Differential units; Bevel gears; Combined drives; Gear box gears and Transmission components. In each of these brief chapters latest developments are briefly surveyed.

12. Five-Language Machinery Catalogue. This catalogue whilst prominently displaying photographic reproductions of various machines and equipment, has the unique feature of publishing brief descriptions in English, Spanish, Portuguese, French and Dutch. Special sections deal with a Universal woodworking machine; Bandsaws including Filing and Jigsawing machines; Electric cranes including Mechanical cupola charging plants; Transmission Appliances; Lathes for maintenance and production work and for special purposes; Guillotine Shearing machines; Multiple punching machines; Motor driven machines for bending and straightening and for punching beams, steel rails, channels, angles, etc., and Plate bending rolls.

13. Fabrication in Steel. This 12-page brochure wishes to demonstrate that to the discerning engineer a photograph with descriptive title and a brief caption conveys as much, if not more, than many a lengthy written description. The photographs depict fabricated equipment mainly for the chemical, oil and allied industries.

14. Screening. 24-page brochure, printed on heavy art paper, with excellent illustrations describing modern screening equipment for both fine and coarse screening. Design features and applications are clearly explained.

15. Guillotine Shearing Machines. 24-page booklet showing and describing a complete range of guillotine shears designed to cut, quickly and accurately, mild steel sheet or plate up to ¼-in. thick. By a small adjustment to the cutting angle of the blades, plastic, rubber, fibre and similar materials can be cut or trimmed. Included in the booklet is the description of a portable universal double end punching, shearing, section cropping and notching machine.

16. Steel Castings and Gears. This 64-page book is divided into two main sections. The first section deals with the production of steel castings. It describes and illustrates a modern foundry, shows casting operations and a number of photographs of cast steel for specific applications; testing apparatus and other laboratory equipment used for analysis and testing are also shown. The second part of the book is devoted to Gears, especially to heavy gears and gear units. Here again, machinery as well as typical gears and gear drives are shown in numerous excellent photographic illustrations. 24 pages of the book are devoted to selected technical data to give the greatest possible assistance to gear users in achieving the most efficient and economical designs.

17. "Easyset" Tee Square. Folder on a precision drawing instrument designed to ensure extremely accurate draughtsmanship with greater ease.

18. Manufacturing Milling Machines. Illustrated folder with specifications of 24-in., 36-in., 48-in. and 54-in. Unit Construction Automatic Manufacturing Milling Machines with detailed specifications for both single and duplex machines in inches and millimetres.

19. Acoustic Strain Gauge. After dealing briefly with the principle of strain and its measurement and, particularly, with the principle on which the acoustic strain gauge is operating, this folder gives an illustrated description of a portable strain gauge of latest design. Specification of the battery operated equipment is given in full detail.

20. Electric Storage Batteries. 16-page booklet showing various applications of traction batteries, including some rather unique applications. The booklet also illustrates the use of Marine type batteries for emergency lighting on liners, and Diesel engine starting batteries as fitted on main-line Diesel-electric locomotives.

MAIL THIS COUPON TODAY

THE ENGINEERS' DIGEST,
120, Wigmore Street, London, W.1.

Date.....

Please send free and without obligation the literature indicated by the following circled numbers :

1	2	3	4	5	6	7	8	9	10
11	12	13	14	15	16	17	18	19	20

Name .....

Position .....

Company.....

Address .....

PRECISION MACHINING
in Repetition Quantities for
All Classes of Light Engineering

We can offer the facilities of a well equipped Modern Engineering Plant comprising :—

- AUTOMATIC MACHINES
- CAPSTAN AND CENTRE LATHES
- GRINDING MACHINES, ETC.
- CASE HARDENING AND HEAT TREATMENT
- PRECISION THREAD ROLLING IN ANY METAL

and which is at your service for the production of high class quality components with accuracy and finish.

A.I.D. approved.

The...

HANWELL ENGINEERING COMPANY LIMITED

Established 1925 — COUNTESS ROAD NORTHAMPTON — Phone: 3766-3767

"SENIOR"

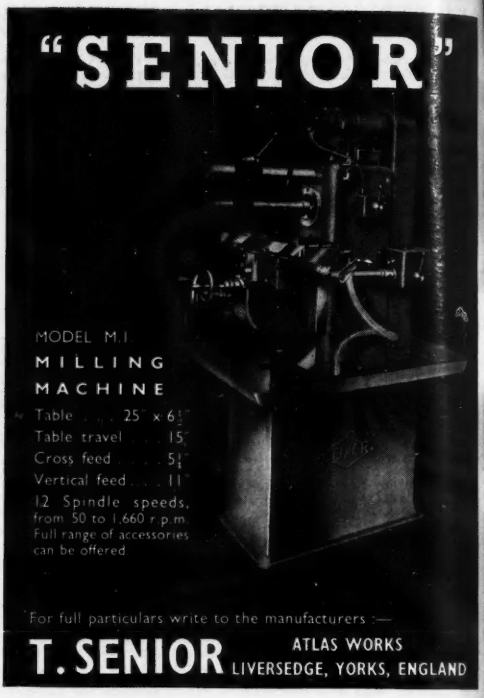
MODEL M.1
MILLING
MACHINE
Table ... 25" x 6½"
Table travel ... 15"
Cross feed ... 5¼"
Vertical feed ... 11"
12 Spindle speeds, from 50 to 1,660 r.p.m.
Full range of accessories can be offered

For full particulars write to the manufacturers :—

T. SENIOR ATLAS WORKS LIVERSEDGE, YORKS, ENGLAND

Made from tough steel and scientifically designed for continuous hard service to ensure long, smooth running. Also **'BAT' CARDED BELT HOOKS** for light, fast drives. Sold by Mill Furnishers and Hardwaremen everywhere. Send for samples and prices to the Sole Manufacturers:

AUTOMAT'C PRESSINGS LTD. Blackheath, Birmingham.
'Phone: Blackheath 1041.

"ORME" Series

- ★ DRAWING INSTRUMENTS
- ★ DRAWING OFFICE EQUIPMENT
- ★ PHOTO PAPERS & CLOTHS
- ★ DRAWING BOARDS & TEE SQUARES
- ★ PLAN FILING CABINETS
- ★ DRAWING & DETAIL PAPERS
- ★ PENCILS · RUBBERS · DRAWING INKS & OFFICE SUNDRIES

Photo Printing of every description.

Photographic Reproductions of Original Plans, Documents, Maps, etc. Size for size, Reductions and Enlargements.

Tracing Work of all types undertaken. Service and best workmanship assured.

LOMAS & BAYNES LTD.
ORME BUILDINGS,
14 THE PARSONAGE,
MANCHESTER 3.

'Phones : BLA 7150 & 3198.
Telegrams : "LOMBAYN, MANCHESTER."